Biomed Tech 2013; 58 (Suppl. 1) © 2013 by Walter de Gruyter · Berlin · Boston. DOI 10.1515/bmt-2013-4426

CURRENT DEVELOPMENTS IN AUTOMATIC DRUG DELIVERY IN ANESTHESIA

Simanski O[1], Sievert A[1,2], Janda M[3], Bajorat J[3]

[1]Automation and Mechatronics Group, Hochschule Wismar - University of Applied Sciences: Technology Business and Design, Wismar, Germany
[2]Institute of Automation, University of Rostock, Rostock, Germany
[3]Clinic of Anaesthesiology and Intensive Care, University of Rostock, Rostock, Germany

olaf.simanski@hs-wismar.de

Abstract: *The main objectives during general anaesthesia are adequate level of hypnosis, analgesia, relaxation, and stable vital functions. During the last 20 years many controllers for the automatic drug delivery in anaesthesia were developed. Our group also developed controllers for the neuromuscular blockade, the depth of hypnosis and the analgesia. In order to administer the medication as needed, a model-based control design or a model-based control is a goal worth striving for. The controller designed in our group and first results of the studies are presented and evaluated briefly.*

Keywords: *automation in anaesthesia, automatic drug delivery*

Introduction

In clinical practice anaesthesiologists have to observe and control a huge amount of hemodynamic and respiratory variables as well as clinical signs for adequate hypnosis and analgesia. In neuro-, thoracic- and abdominal surgery a continuous neuromuscular block is needed to guarantee optimal surgical conditions. A neuromuscular blocking drug is administered in order to prevent reflex muscle movement.
New short-acting drugs are introduced over the last years. This makes a continuous mode for drug application possible and implies the use of automatic control.
For the design of a closed-loop control system a measurable control value and remote controllable infusion pumps are needed.

Measurement and Modelling

For the determination of the degree of neuromuscular blockade is the muscle response recorded. The evoked muscle response after supramaximal stimulation of a motoric nerve (e.g. ulnaris nerve - adductor pollicis muscle) can be registered by electromyography (EMG) or acceleromyography (AMG). A frequently used device is the "NMT-module" (Fa. General Electric) [1].
Measuring depth of hypnosis is often discussed and no final answer can be given. Different algorithms are known for estimation the depth of hypnosis from the raw EEG.
The bispectral index (BIS) becomes very popular in the last years and has been validated in large studies. The algorithm combines the power spectrum and bispectrum with a burst suppression analysis. The BIS describes a complex EEG pattern within a simple variable. The BIS-monitor (Fa. Aspect Medical) reflects the state of hypnosis with help of an index between 0-100, where 0 represents an isoelectrical EEG.
The main problem of measuring the analgesia level is the loss of parameters, which describe the current status. A rather new commercial device called A.N.I.-Monitor (Fa. MetroDoloris) uses a wavelet transformation of the ECG to gather information about the parasympathetic tone. The A.N.I.-Monitor outputs a simple numeric value with a scale from 0 - 100 to describe the state of analgesia calculated from the hearth rate variability (HRV) [2]. More popular is the use of direct HRV parameters to detect the analgesia level [4].
For the controller design it's desirable to use a model description that explains the interaction between the drug infusion and the measurable effect. The most popular kind to model the drug distribution and elimination are pharmacokinetic-pharmacodynamic (PKPD) models.
Pharmacokinetics describes the dynamic process of drug distribution in the body from the infusion to the concentration in the blood and pharmacodynamics describes the interaction from the blood concentration and the measureable effect [3]. Figure 1 shows the general structure of the PKPD model description.

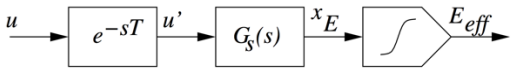

Figure 1: Structure of the simple drug interaction model in Wiener structure, with u as infusion rate, e^{-sT} as delay time for the drug transport, G(s) as transfer function of the PKPD model and E_{eff} as measurable effect after the static nonlinearity.

Depending on the used drug G(s) is a third order model for the neuromuscular blocking drug or a fourth order model for the hypnotic drug Propofol.
Figure 2 shows the schematic description of the developed control system. An adaptive generalized predictive controller (aGPC) was developed for the control of the neuromuscular blockade [5]. Because of the nonlinear behaviour of the measurement of the depth of hypnosis a simple fuzzy controller as nonlinear controller was integrated. For the design of the fuzzy PD+I controller a standard implementation of the integral (I) part was used. The rules for the proportional-

differential (PD) part were designed with the help of the expert knowledge of our anaesthesiologists. A rule-based expert-fuzzy system controls the level of analgesia [4]. It was designed to reflect the decision-making process of anaesthetists regarding the change of infusion rate.

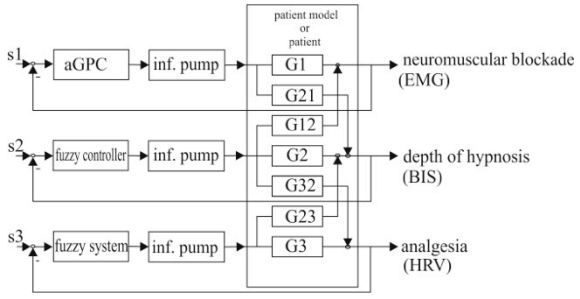

Figure 2: Implementation of the control system at the Control Application Centre at the University of Rostock, with set points s_x and transfer functions G_x and G_{xy}.

Results and Discussion

During the last years different multiple-input multiple-output (MIMO) studies were done [4,5]. Exemplary results show Figure 3 and Figure 4. Figure 3 illustrates one example of a MIMO control of neuromuscular blockade and depth of hypnosis.

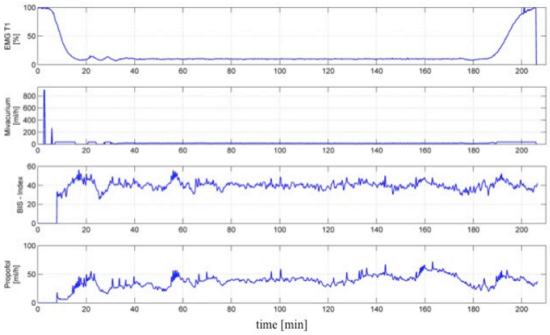

Figure 3: MIMO control study of neuromuscular blockade (NMB) and depth of hypnosis. 1.-plot: NMB-level T1; 2.-plot: drug infusion rate of Mivacurium; 3.-plot: BIS-Index and the last one shows the drug infusion rate of Propofol.

The MIMO control of the depth of hypnosis and the analgesia were also successfully validated. Figure 4 shows an example. The results of both studies were with good performance. These MIMO control system was designed as a decentralized MIMO system. The cross reactions between hypnotic and analgesic drug were interpreted as disturbances. Figure 5 shows a way in which the interaction between hypnotic and analgesic drugs can be modelled. Both drugs can be described with a separate PK model and a common PD model that reflected the interaction of both drugs.

The results of both MIMO control studies show the potential of automatic drug delivery systems to assist the medical staff in the daily work. In near future the control systems should be validated in bigger studies to promote the idea and the development.

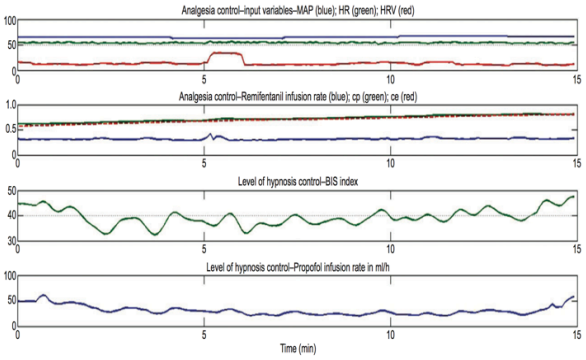

Figure 4; Results of the MIMO study of analgesia and depth of hypnosis. 1.-plot: analgesia parameter, arterial blood pressure (MAP, on the top), heart rate (HR, in the middle), heart rate variability (HRV, on the bottom); 2.-plot: drug infusion rate of Remifentanil (on the top the concentration in blood, on the bottom the rate); 3.-plot: depth of hypnosis level and the last one shows the drug infusion rate of Propofol.

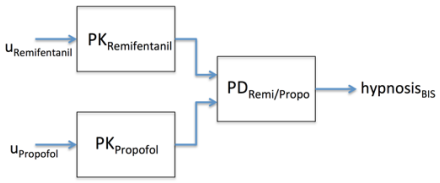

Figure 5: Modelling of the Remifentanil-Propofol interaction regarding to the level of hypnosis.

Bibliography

[1] K. Stadler, "Modeling and control in anesthesia from design to validation." Ph.D. dissertation, ETH Zürich, Institut für Automatik Publikation No.23., 2003.

[2] R. Logier, M. Jeanne, J. De Jonckheere, A. Dassonneville, M. Delecroix, and B. Tavernier, "Physiodoloris: a monitoring device for analgesia / nociception balance evaluation using heart rate variability analysis," in Engineering in Medicine and Biology Society (EMBC), 2010 Annual International Conference of the IEEE, 2010, pp. 1194–1197.

[3] G. T. Tucker, "Pharmacokinetic and pharmacodynamic models," Advances in Pain Research and Therapy, vol. 14, no. 4, pp. 181–201, 1990.

[4] M. Janda, A. Schubert, J. Bajorat, R. Hofmockel, GFE. Nöldge-Schomburg, B. P. Lampe, O. Simanski: Design and implementation of a control system reflecting the level of analgesia during general anesthesia. *Biomedizinische Technik/Biomedical Engineering* 1/2013 pp. 1-12;

[5] M. Janda, O. Simanski, J. Bajorat, B. Pohl, G.F.E Noeldge-Schomburg, R. Hofmockel: Clinical evaluation of a simultaneous closed-loop anaesthesia control system for depth of anaesthesia and neuromuscular blockade Anaesthesia, 2011, doi:10.1111/j.1365-2044.2011.06875.x

Biomed Tech 2013; 58 (Suppl. 1) © 2013 by Walter de Gruyter · Berlin · Boston. DOI 10.1515/bmt-2013-4427

ULTRASOUND SENSORY FOR MONITORING MECHANICAL STRESS ON RISK STRUCTURES IN SURGICAL TRAINING SYSTEMS

Tobias Pilic[1,2], Matthias Müller[1,2], Ben Andrack[1,2], Werner Korb[1,2] and Matthias Sturm[1]

[1]Faculty Electrical Engineering & Information Technology, Leipzig University of Applied Sciences, Germany
[2]Innovative Surgical Training Technologies (ISTT), Germany

tobias.pilic@stud.htwk-leipzig.de

Abstract: *This work presents an approach for measuring the results of mechanical stress in surgical training systems made of realistic artificial tissues. The measurement system is based on ultrasound sensory and is able to monitor deformations of structures. During the trained surgery, it is used to recognize deformations, tensions and damages of risk structures. The system was evaluated in a simulator for training discectomy of the lumbar spine. Within this simulator the system monitored the mechanical stress on the nerve roots. Evaluation results show that this kind of sensory could greatly enhance the feedback on the training performance of young surgeons.*

Keywords: *Training, Simulator, Surgery, Discectomy, Ultrasound*

Introduction

Nowadays young surgeons acquire most of their skills directly from more experienced surgeons. Busy clinical practice, however, leaves little time for this type of training in the OR. the question arises whether the current training principles remain applicable in the future. Innovative training concepts based on surgical simulators may be an alternative for improving the quality of medical education.

In the past, many simulators were based on virtual reality [1]. But due to limiting aspects in realism and haptics, they are not widely accepted by clinical doctors. Therefore, the current research focuses also on patient-based models consisting of synthetic and biological materials. These models provide training with actual instruments using a more realistic workflow. In contrast to classical education, it is possible to collect model comparison values assessing the quality of the intervention using sensors in the model. Thus, it is possible to provide young surgeons with objective feedback.

The basis of the work presented here is a simulator for the training of discectomy (removal of herniated discs) of the lumbar spine. It was developed as part of a two-year research project. For this simulator, an ultrasound sensor to determine the compression of nerve roots has been developed and validated. The prototype system sends a continuous ultrasound signal into one end of the tubular, air-filled nerve root model. An ultrasound receiver on the other end measures the signal. By evaluating the amplitude of the signal, a conclusion about the compression and the change in diameter can be drawn. Further statements such as the position of the compression or general traction stress on the root are not possible with this simple principle of measurement. In addition, the system must be extensively calibrated before each use and does not provide for high reproducibility. Therefore, the measurement system is upgraded in the course of this work to the pulse-echo method.

Methods

The basic idea of the pulse-echo-method is to induce a short ultrasound pulse lengthwise into the nerve root. The longitudinal wave travels along that root. It is partially reflected and transmitted at a narrowed location (Fig. 1). This is caused by the cross-sectional variation at that point.

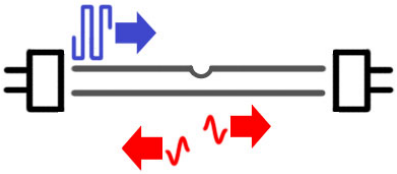

Figure 1: **Illustration of the Pulse-Echo-Method.** The initial pulse (shown in blue) is coupled into the nerve root and travels longitudinally. The diameter is changed suddenly at the point deformation. This is induced by externally applied pressure due to the operative procedure. Because of the altered acoustic impedance, the wave is split into a reflection and a transmission part.

The reflected pulse inherits an amount of energy directly related to the change in diameter, hence, it is a measure of the deformation. Furthermore, it is possible to calculate the exact position of the deformation by measuring the time between sending and receiving, using the temperature-dependant sonic speed and simple kinetics.

The architecture (Fig. 2) is comparable to common sonographic devices. Theoretically, one ultrasound capsule should be sufficient for both, transmission and reception. The H-bridge manages the connection to the corresponding circuit. The goal is to use the transmitter in the very moment of transmitting and the receiver in the very moment of receiving a reflected pulse without affecting each other. Hence, one ultrasound transducer is sufficient as sensor and actor. As an extension, a second ultrasound transducer was added at the opposite site of the root model. This enables us to measure the transmitted pulse and draw additional conclusions. For example we are able to measure the longitudinal tension of the nerve root an we can detect damages in

the outer skin of the root caused by the surgery. It also simplifies the automatic calibration of the measurement system.

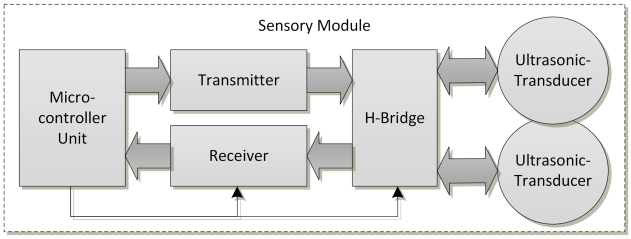

Figure 2: **System Architecture.** The control of the analogue circuitry and the analysis of the measured data is done by a Cortex-M4 microcontroller with DSP functionality. A standardized bus-system enables the readout of the collected data for further use.

The H-bridge consists of several analogue switches and is controlled by a microcontroller-unit. That unit also defines the critical time basis for the pulse-echo-method. Amplifier stages are facilitated to implement the transmitter and receiver. The gain of the receiver is programmable. An equal effect is achieved within the transmitter by using different amplitudes for the signal generated by the DAC (Digital-Analogue-Converter) of the microcontroller. One temperature sensor is the basis for calculating the sonic speed.

Results

The experiments undertaken with the prototype system generated promising results. One period of a pulse-echo-waveform is presented in Fig. 3.

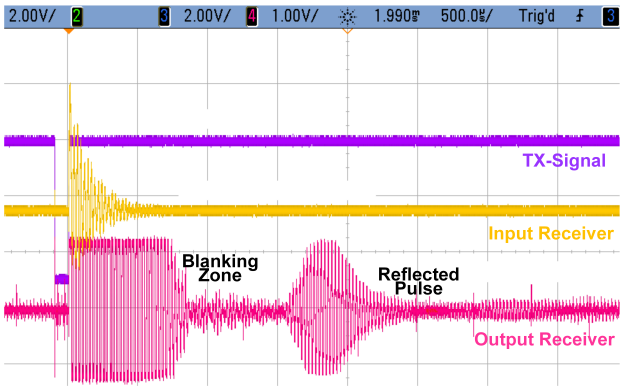

Figure 3: **Measured Results.** The timebase is provided by the TX-Signal (in purple). One can see the strongly prolonged transmission pulse and the reflection from the compression at the output of the receiver (in pink).

It is possible to identify the received pulse inside the waveform (in red). There is a non-linear relationship between that pulse and the total amount of cross-sectional reduction. Further measurements and simulations must identify that relationship according to the surgical application. This is necessary to enable the software for interpreting the measured waveforms automatically. The time deviation between transmitted and reflected pulse is directly related to the location of the deformation.

One drawback of the system is the prolonged waveform after switching between transmission and reception. This so called *Blanking Zone* is the result of the post-pulse oscillation of the ultrasound transducer and the excitation of that transducer through reflected parts of the transmitted signal through the casing. It is not possible to receive and interpret any kind of reflected signals in this time. The problem is amplified by the use of bigger and cheaper ultrasound capsules (usually with a frequency of 40 kHz). Those require a coupling with a higher cross-sectional change. The change is caused by the transition of the 16 mm transducer to the diameter of 6 mm at the nerve root model. The occurring reflection effect widens the *Blanking Zone*. Hence, the range in which deformations can be detected is even more restricted.

Requirements concerning the electronic circuit itself were high as well. As Noise and disturbances caused by the high-frequency controller and the high amplitude of the transmission can easily lead to crosstalk into the high-gain receiver.

Discussion

The measurement method has proven to be an efficient and universal system for detecting deformations in artificial tissue structures. Evaluations during a previous project [2] confirmed both, the usability of the sensor data for training, as well as a strong demand from physicians for an objective training feedback. The next generation of the discectomy generator presented here is being developed for production. Future scientific work will focus on the usage of the collected sensor data as different scenarios are imageable. They range from active acoustic or visual feedback during training to the combination with video recordings for subsequent training evaluation. Other work will try to determine whether it is possible to recognize the current status of the training operation from certain events within the sensor data. This would be an important step in order to actively and automatically control certain situations within the Situs. It might even be possible to train without intensive supervision by an experienced surgeon.

Bibliography

[1] R. Satava, “Historical review of surgical simulation—a personal perspective,” *World Journal of Surgery*, vol. 32, no. 2, pp. 141–148, 2008.

[2] B. Andrack, T. Byrnes, V. L. E. Bernal, G. Bausch, and W. Korb, “Use of a surgeon as a validation instrument in a high-fidelity simulation environment,” in *2012 Symposium on Human Factors and Ergonomics in Health Care: Bridging the Gap*, (Baltimore), pp. 197–201, 2012.

Biomed Tech 2013; 58 (Suppl. 1) © 2013 by Walter de Gruyter · Berlin · Boston. DOI 10.1515/bmt-2013-4428

CLOSED LOOP CONTROL OF SPONTANEOUS BREATHING DURING LONG TERM SEDATION

Marian Walter[1], Timo Tigges[1], Ralf Bensberg[2] and Steffen Leonhardt[1]

[1]Lehrstuhl für Medizinische Informationstechnik, RWTH Aachen, Deutschland

[2]Klinik für Anästhesiologie, Universitätsklinikum Aachen, Deutschland

walter@hia.rwth-aachen.de

Abstract: *This article presents a controller design for administration of Remifentanyl to control spontaneous breathing. Using established physiological models a reduced order model is derived and used for control design. Controllers were evaluated in-silico and finally in first in-vivo trials.*

Keywords: *Control, Spontaneous Breathing, Remifentanyl*

Introduction

Spontaneous breathing is a key element in modern long term ventilator therapy. It has a proven positive effect on treatment outcome, reduces possibility of lung atelectasis and muscular atrophy and supports weaning from ventilation. In clinical routine ventilated patients are typically anaesthesized by a combination of a hypnotic and an opioid drug. Both lead to a depression of the spontaneous ventilation. If one wants to maintain spontaneous breathing during anaesthesia, a fine balance of drug dosage has to be found, which has to be adapted to increasing dose tolerance and changes in patient status and ventilatory drive.
In order to support clinical staff in maintaining optimal therapy and safe adherence to dosage limits, closed loop control of dosage application may be helpful. Especially, when spontaneous breathing is controlled within complex and automated treatment procedures (e.g. automated ARDS-Net) or in combination with extracorporeal lung support.

Methods

Model of the control plant: A lot of authors have developed models of the respiratory system in the past decades. Starting from first models in the 40s, most modern approaches base on the model introduced by Grodins [1]. The model used in our work is based on Ursinos extension of Grodins model [2], but we adapted some parameters to optimize model fit to our data. The second important model part relates to the pharmacological model, which covers pharmacokinetics [3] and pharmacodynamics [4]. The overall model structure can be seen in figure 1.
In general, this complex and interconnected model results in a model order of 15th grade with several nonlinearites, which is not suited for most algorithms for designing controllers. Thus we performed a model reduction procedure. Most dynamical processes can be described by a lower order system sufficiently. Choosing a Hammerstein structure, we concentrated the nonlinear behaviour in one static nonlinearity.

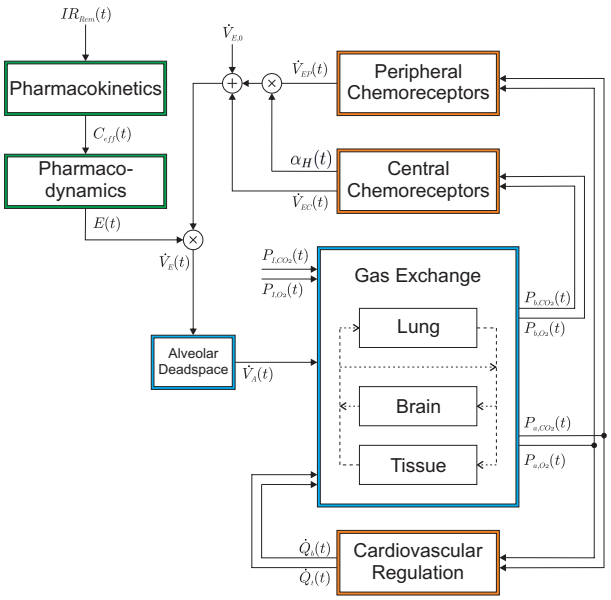

Figure 1: Model block diagram *virtual patient*. Adapted from literature [5, 4]

The static nonlinearity was determined by calculating the static operating points in the range of typical input values. The final model order of 2nd order resulted from evaluating "Akaike's final prediction error" while determining the model parameters from a system identification with an APRBS signal. Figure 2 shows a typical comparison of the full model with the reduced model. The basic process characteristic is covered well, but differences mainly coming from the simplification of the nonlinearities can be seen. On the other hand we expect these differences to be small compared to inter-individual variations of parameters in the real application.

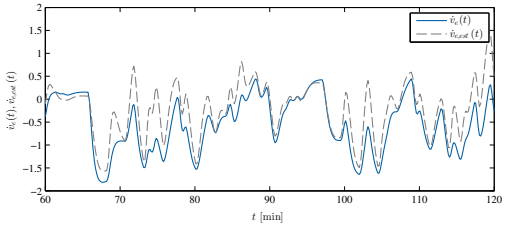

Figure 2: Comparison of the complex ($\dot{v}_{e,sim}(t)$) and the reduced order model ($\dot{v}_{e,est}(t)$)

Controller Design: Two different control structures were implemented. At first we started designing a conventional PID controller and subsequently designed a model based predictive controller (MPC). The MPC is expected to have benefits when applied to slow processes with large time lag. Both controllers were designed first compensating the static nonlinearity with an inverse characteristic. Thus design methods for linear processes could be applied for the controller design.
PID parameters were numerically optimized regarding control settling time, overshoot and disturbance rejection in the presence of significantly noisy measurements. In the end this resulted in a relatively small D component, leaving a quasi PI controller.
The model predictive controller (MPC) consists of an algorithm wich calculates an optimal input trajectory based on the system states in each sample step. System states were calculated using a Kalman filter. The control structure implemented followed the methodology described in [6]. Again, the choice of control design parameters was optimized following the same criteria as in the PID case.

Results

We used the complex simulation model for controller evaluation. Both controller showed a similar performance.

	T_{set}	e_{max}	IAE	$T_{set,dist}$
PID	15.33 sec	1.03%	649.93	9.83 sec
MPC	14.67 sec	4.42%	476.5	14 sec

A second criteria of control performance is robustness against changes in process parameters. Figure 3 shows an exemplary step response to changes in reference value and disturbance at a 50% changed drug sensitivity.

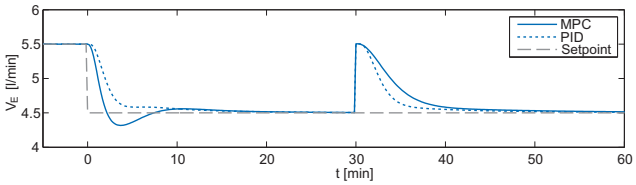

Figure 3: Simulation result for 50% increased Remifentanil-sensitivity

The designed controllers were evaluated in a first animal trial. Figure 4 shows a typical resulting control performance of the MPC. On the one hand, one can see, that spontaneous breathing can be adjusted according to the setpoint. On the other hand, the significant time variance of the process can be observed. In the beginning, the dose of Remifentanyl is sufficent to maintain sedation. At the end of the experiment, the very same dose of Remifentanyl leads to an unsufficient sedation indicated by the exponential rise in minute ventilation and muscle activity, so the control had to be stopped and a bolus of propofol was administered. This indicates that special safety procedures for dosage at the set point boundaries have to be implemented in order to react fast to such unexpected events.

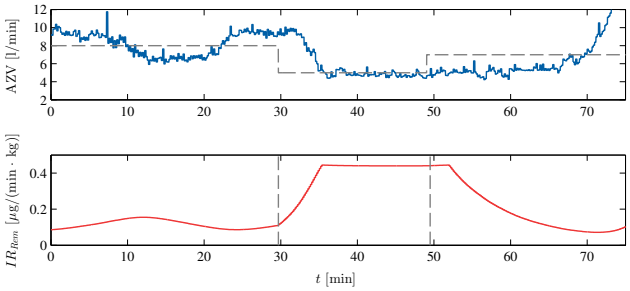

Figure 4: MPC-control of minute ventilation during an animal trial

Discussion

We could show, that an algorithm for control of spontaneous breathing can be derived from the models presented in the literature. However control performance in animal experiments was only partly convincing. The PID controler did not perform well, as system changes and disturbances were too significant for the controller to reach a stationary control target. A lot of the problems result from the pigs, which we used as an animal model. During the trials we found, that regulation of spontaneous breathing is much more delicate compared to human subjects, especially the respective influence of Remifentanyl and Propofol. Future work will concentrate on a multivariable control approach, where Propofol is included in the controller as well.

Bibliography

[1] F. S. Grodins, J. Buell, and A. J. Bart, "Mathematical analysis and digital simulation of the respiratory control system," *J Appl Physiol*, vol. 22, no. 2, pp. 260–276, 1967.

[2] M. Ursino, E. Magosso, and G. Avanzolini, "An integrated model of the human ventilatory control system: the response to hypercapnia," *Clinical physiology*, vol. 21, no. 4, pp. 447 – 464, 2001.

[3] C. F. Minto, T. W. Schnider, T. D. Egan, E. Youngs, H. J. M. Lemmens, P. L. Gambus, V. Billard, J. F. Hoke, K. H. P. Moore, D. J. Hermann, K. T. Muir, J. W. Mandema, and S. L. Shafer, "Influence of age and gender on the pharmacokinetics and pharmacodynamics of remifentanil: I. model development," *Anesthesiology*, vol. 86, no. 1, pp. 10–23, 1997.

[4] A. L. Caruso, *Personalized drug dosing through modeling and feedback*. PhD thesis, ETH Zürich, 2009.

[5] E. Magosso, M. Ursino, and J. van Oostrom, "Opioid-induced respiratory depression: a mathematical model for fentanyl," *IEEE transactions on bio-medical engineering*, vol. 51, pp. 1115 – 1128, 2004.

[6] J. M. Maciejowski, *Predictive control with constraints*. Prentice Hall, 2002.

Biomed Tech 2013; 58 (Suppl. 1) © 2013 by Walter de Gruyter · Berlin · Boston. DOI 10.1515/bmt-2013-4429

Novel cap system with active actuators for rapid dry electroencephalography

Fiedler P[1], Griebel S[2], Biller S[1], Fonseca C[3], Vaz F[4], Zentner L[2], Zanow F[5], Haueisen J[1]

[1]Institute of Biomedical Engineering and Informatics, Ilmenau University of Technology, Germany
[2]Department of Mechanism Technology, Ilmenau University of Technology, Germany
[3]Universidade do Porto, Faculdade de Engenharia, Rua Roberto Frias, 4200-465 Porto, Portugal
[4]Universidade do Minho, Centro de Física, Campus de Azurém, 4800 Guimarães, Portugal
[5]eemagine Medical Imaging Solutions GmbH, Berlin, Germany

patrique.fiedler@tu-ilmenau.de

Abstract: *New fields of application for electroencephalography (EEG) require robust measurement technologies for ubiquitous mobile monitoring. Fast, easy and failsafe application as well as stable signal quality are crucial requirements for the electrodes. The application of novel dry EEG electrodes requires direct, reliable contact with the human skin as well as stable electrochemical characteristics of the materials. We propose a novel biocompatible electrode based on Titanium Nitride (TiN) integrated into an adaptive cap system with active adduction mechanisms. We report electrode-skin impedance measurements to prove our cap system to provide reliable and stable electrode positioning and adduction.*

Keywords: *Electroencephalography, Dry electrodes, Biosignal acquisition, Adaptive cap system, Active adduction mechanisms*

Introduction

Silver/Silver-Chloride (Ag/AgCl) electrodes have been the gold standard in biosignal acquisition for several decades, but require extensive skin preparation and electrolyte gel application. Thus, they are inapplicable for upcoming new fields of application for electroencephalography (EEG) like Brain-Computer-Interfaces. Hence, dry electrode technologies have been developed for several years, eliminating the need for preparation and electrolyte gels or pastes [1]. Titanium-Nitride (TiN) based electrodes were shown to be mechanically and electrochemically stable in contact with human sweat [2]. EEG acquisition tests proved the signal quality of TiN electrodes to be comparable to conventional Ag/AgCl electrodes [3].

The function principle of dry electrodes requires reliable, reproducible and stable adduction. In this paper we describe a novel overall cap concept based on TiN electrodes integrated into active actuators, ensuring the necessary homogenous and reproducible electrode adduction. Based on electrode-skin impedance measurements, we prove the function and effect of our cap system in a study on volunteers.

Methods

We developed a novel pin-shaped electrode whose top diameter of only 1.5 mm allows for a rapid, reproducible interfusion of the hair layer and a stable contact to the scalp (see Fig. 1a).

The substrate of 99.96% pure titanium (GoodFellow Metals, London, UK) was turned into final shape using a CNC lathe (PD CNC AD 1515, Spinner Werkzeugmaschinenfabrik GmbH, Sauerlach, Germany). Subsequently a coating of a nano-sized layer of Titanium Nitride (TiN) was applied using a DC magnetron sputtering technique. Thus, the sensing element of the electrode exhibits excellent mechanical and electrochemical stability with good adhesion of the TiN coating [2]. The sensing element was connected to shielded coaxial cables using electrically conductive silver glue (Elecolit 325, Eurobond Adhesives Ltd, Sittingbourne, UK) and integrated into a silicone-based adduction actuator. The compliant actuator performs a translational movement if the internal pressure of the coherent, hollow structure is increased (see Fig. 1b). Hence, the adduction actuator allows for bypassing electrode-scalp distances of 2 to 8.5 mm.

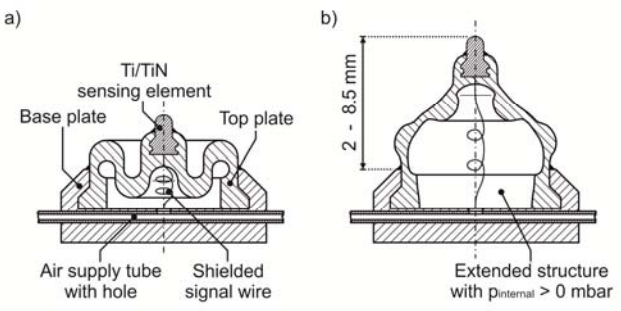

Figure 1: Novel pin-shaped TiN electrode integrated into an active adduction actuator: a) main components in initial position ($p_{internal}$ = 0 mbar, without counter-pressure), and b) translational adduction of the actuator ($p_{internal}$ > 0 mbar).

Up to 165 electrode elements can be arranged and interconnected to form a high-density dry EEG cap system. In the present study, a total of 32 elements were used and arranged according to the international 10–20 system for EEG acquisition. All actuators were connected to a central pressure supply.

In order to evaluate the performance and reproducibility of the actuators and the electrode adduction, we performed electrode-skin impedance measurements on three volunteers with normal hair length and density at room temperature and 40% air humidity. Therefore, a commercial impedance ana-

lyzer (4192A LF, Hewlett Packard, Palo Alto, USA) was used in combination with a custom-made security circuit. The impedance analyser is capable to measure impedances of $|Z| \leq 1.3$ MΩ. The security circuit immediately cuts the connection of volunteer and measurement system if the measurement current eventually exceeds 50 µA.

Two conventional Ag/AgCl electrodes were applied at AFz and Fz position on the head in combination with electrolyte gel (ECI Electro-Gel, Electro-Cap International Inc., Ohio, USA). The Ag/AgCl to Ag/AgCl impedance was always below 10 kΩ. We sequentially measured the impedances between all dry TiN electrodes and the Ag/AgCl electrode at AFz position. The measurement sequence was randomized in order to minimize the statistic influence of the time-to-measurement on the impedance results. We repeated the measurement with increasing internal pressure applied to the actuator structures. For each set of parameters (including subject, pressure, electrode position) 65 samples were recorded at a sampling frequency of 2 samples / second. The 65 samples were subsequently averaged.

Results

Figure 2 shows the influence of the internal pressure of the actuators on the electrode-skin impedance. The number of active channels, i.e. $|Z| \leq 1.3$ MΩ, continuously increases with increasing pressure. Due to the translational movement the sensing elements of the electrode better interfuse the hair layer. As the translation increases until electrode-skin contact is established, increasing pressure values allow for bridging of larger initial distances. As soon as the electrodes are in contact with the scalp, a further increase of the pressure causes decreasing impedance due to the electrode's tip causing an indentation in the scalp, thus leading to increased contact surface and better contact stability. The slightly increasing mean absolute impedance between 100 and 300 mbar is caused by the increased number of active channels rather than by increased per-electrode impedance.

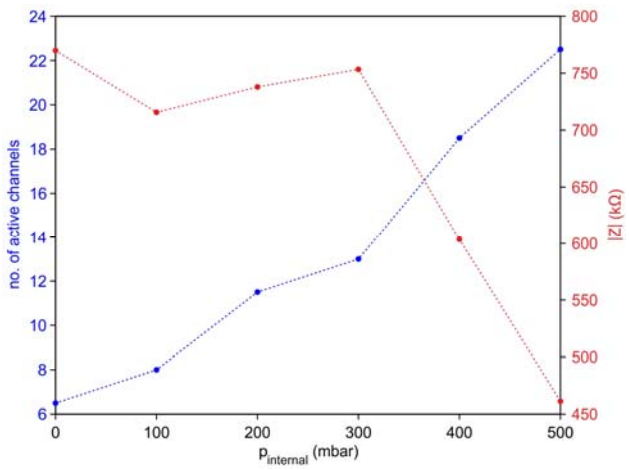

Figure 2: Influence of the applied internal pressure of the actuators on the electrode-skin impedance of three volunteers: number of active channels ($|Z| < 1300$ kΩ) shown in blue, and mean $|Z|$ over all active channels shown in red.

Figure 3 shows a mapping of the measured electrode-skin impedances at different electrode positions. While the frontal electrodes exhibit electrode-skin contact even without adduction, the adduction effects with increasing pressure are clearly visible. The remaining non-contact and high-impedance electrode positions are caused by technological limitations of the current cap system. The electrodes at F7 and the auricular positions require a tighter cap design. The O1 and P3 electrodes are affected by drag forces of the weight of the bundled electrode cables. Finally, the parietal electrodes on the right side of the head may suffer from decreasing internal pressure due to the current pressure distribution network design.

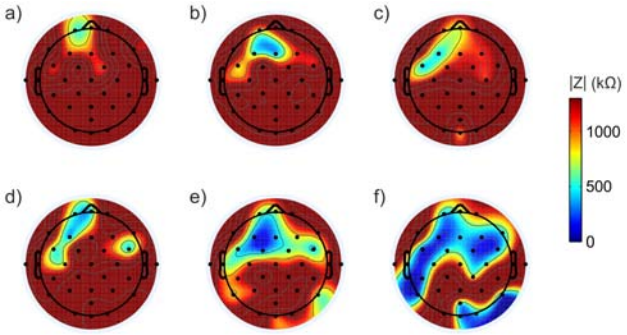

Figure 3: Mapping of the electrode-skin impedance (mean over all volunteers) for different internal pressure applied to the actuators: a) 0 mbar, b) 100 mbar, c) 200 mbar, d) 300 mbar, e) 400 mbar, and f) 500 mbar.

Discussion

We developed a novel cap system capable of enabling rapid dry EEG acquisition. Our experimental setup proved that the centrally controlled adduction actuators provide reproducible electrode-skin impedance. Furthermore, the translational movement and the applied contact pressure allow for increasing number of electrode-skin contacts and decreasing electrode-skin impedance. The biocompatible materials of the cap and the electrodes enable application in clinical routine as well as mobile and long-term measurements.

We will further improve the current cap design in order to eliminate current limitations like the lag of adduction at occipital and parietal electrode positions.

Bibliography

[1] Searle, A., and Kirkup, L.: A direct comparison of wet, dry and insulating bioelectric recording electrodes, *Physiol. Meas.*, vol. 21, pp. 271-283, 2000

[2] Cunha, L.T., Pedrosa, P. et. al.: The role of composition, morphology and crystalline structure in the electrochemical behaviour of TiNx thin films for dry electrode sensor materials, *Electrochim. Acta*, vol. 55, pp. 59-67, 2009

[3] Fiedler, P., Cunha, L.T. et. al.: Novel TiNx-based biosignal electrodes for electroencephalography, *Meas. Sci. Technol.*, vol. 22, article 025008, 2011

Biomed Tech 2013; 58 (Suppl. 1) © 2013 by Walter de Gruyter · Berlin · Boston. DOI 10.1515/bmt-2013-4430

PHYSIOLOGICAL NOISE REMOVAL FROM fNIRS SIGNALS

Bauernfeind G[1], Böck C[1], Wriessnegger SC[1] and Müller-Putz GR[1]

[1]Institute for Knowledge Discovery, Graz University of Technology, Austria

g.bauernfeind@tugraz.at

Abstract: *In the present study we report on the reduction of physiological rhythms in hemodynamic ((de)oxy-Hb) signals recorded with functional near-infrared spectroscopy (fNIRS). We investigated the use of three different signal processing approaches (spatial filtering, adaptive filtering and transfer function (TF) models) to reduce the influence of respiratory and blood pressure rhythms on the hemodynamic responses. The results show that all three methods are promising for reducing the influence from oxy-Hb signals, but only TF models fit for deoxy-Hb signals.*

Keywords: *Functional near infrared spectroscopy (fNIRS), physiological noise removal*

Introduction

In recent years multichannel fNIRS has been used to study hemodynamic responses (changes of oxygenated (oxy-Hb) and deoxygenated hemoglobin (deoxy-Hb)) of the cerebral cortex to cognitive, visual and motor tasks and was also proposed as a novel approach in the field of brain-computer interface (BCI) research [1]. A common challenge for using fNIRS is stable and reliable investigation and classification [1, 2], of spatio-temporal hemodynamic patterns. For this it is essential to reduce the influence of physiological noise. A spectral analysis of the optical signal reveals various quasi-periodic physiological rhythms, such as cardiovascular, vascular, respiratory and 3^{rd} order blood pressure (BP) rhythms, which may influence the recorded signals [1, 3] and superimpose the changes caused by cerebral activation. However, this fact is neglected by the majority of fNIRS studies. The sources of these influences are located in the tissue overlaying the brain as well as in the brain tissue itself. To decrement the influence of these global interfering signals, different methods are suitable.

The aim of this work is to compare three different approaches (spatial filters, adaptive filtering, and transfer function (TF) models) which reduce the systemic influences (respiration and BP waves) in the recorded fNIRS signals.

Methods

Data acquisition: The investigations were carried out on a group of five male subjects (aged 24.4 $\pm$ 3.1 years). The subjects performed 24 trials of cue-based mental arithmetic tasks (MA, serially subtract a one-digit number from a two-digit number for 12 s). For fNIRS recordings a multichannel continuous wave system (NIRScout1624, NIRx Medizintechnik, GmbH) was used. Additionally, the continuous BP signal (CNAP^{TM} Monitor 500, CNSystems Medizintechnik AG) and the respiration (resp) were recorded. From the BP signal the diastolic BP (BPdia) was extracted. These two signals (BPdia and resp) were band-pass filtered between 0.07-0.13 Hz and 0.2-0.4 Hz, respectively, and used in the TF approach to reduce the systemic influences in the recorded (de)oxy-Hb signals. In the following short descriptions of the used approaches are given:

Spatial filtering: Some methods to reduce the physiological noise evolve from approaches used in EEG analysis [2]. For example, spatial filters, like Laplacian derivation or common average reference (CAR), are used in the analysis of multichannel EEG signals. A new approach, for the first time implemented by our group in [4], is the application of CAR on fNIRS data. The idea behind this approach is the fact, that the global interfering signals influence all channels. For this purpose the mean of all channels is calculated and subtracted from each single channel and for every time point of the (de)oxy-Hb signals.

Transfer function (TF) models: A novel approach in the field of fNIRS, developed by our group and included in BioSig (http://biosig.sourceforge.net), is the use of TF models which were initially proposed by Florian et al. [5] to remove respiratory sinus arrhythmia in R–R interval series. In our approach, by using the BPdia and resp signals, TF models were applied to remove the related influences from the (de)oxy-Hb signals. These models are described by

$$\mathrm{X}[n] = \sum_{u=0}^{m} g_u \mathrm{Y}[n-u] + \mathrm{N}[n] \qquad (1)$$

where $\mathrm{X[n](n} = 1, 2, 3, \dots)$ denotes the time series of the recorded signal, $\mathrm{g_u(u} = 1, 2, .., \mathrm{m})$ the model parameters, Y the systemic influence and N the signal without the influence. For further details see [5].

Adaptive filtering (AF): This approach was introduced by Zhang et al. [6] and the idea behind the method is using hemodynamic signals recorded from additional detectors (Near-Detectors; see Fig. 1A) close to the sources to estimate changes in the overlaying tissue layers. These signals are further used by an adaptive filter (in the current study based on the Wiener-Hopf solution) to estimate global interference, which are then removed from the target signals [2].

Comparison: To compare all approaches the signal-to-noise ratio (SNR) improvements (averaged over all channels) of the (de)oxy-Hb signals were calculated. Therefore the ratios of the power in the non-influenced "signal" bands (P_{sig}; 0-0.07, 0.13-0.20 and 0.40-0.8 Hz) and "noise" bands (P_{noise}; 0.07-0.13 Hz, for BP influence, and 0.2-0.4 Hz, for respiration) were calculated before (SNR_{raw}) and after (SNR_{clean}) applying the different approaches. Finally the SNR improvement was calculated as the ratio of SNR_{clean} to SNR_{raw}.

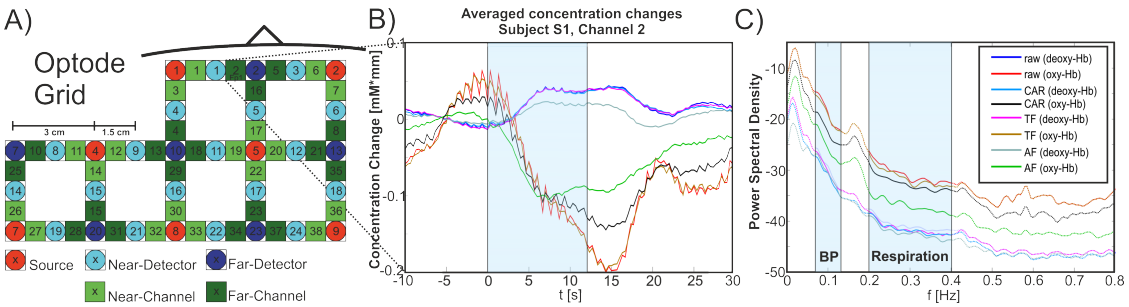

Figure 1: A) Schematic illustration of the multi-channel grid placed over the anterior prefrontal and left dorsolateral prefrontal cortex. B) Averaged task-related responses of oxy-Hb and deoxy-Hb (Subj. S1, Ch. 2). C) PSD (averaged over all channels) illustrating the SNR improvement for the same subject.

Table 1: SNR-improvement (%) for oxy-Hb and deoxy-Hb signals using common average reference (CAR), adaptive filtering (AF) and and transfer function (TF) models.

Subj.	**oxy-Hb**			**deoxy-Hb**		
	CAR	AF	TF	CAR	AF	TF
S1	31.2	23.4	12.1	8.4	-49.7	13.0
S2	16.5	52.6	40.3	-15.2	-26.9	20.2
S3	19.4	121.2	81.2	-12.8	-24.8	15.2
S4	-21.4	-28.7	24.3	-1.2	-6.8	3.4
S5	97.7	69.7	31.1	-11.1	-8.4	17.4
Mean	28.7	47.6	37.8	-6.4	-23.3	13.8
SD	43.3	55.5	26.4	9.8	17.4	6.4

Results

Table 1 summarizes the SNR-improvement (%) in oxy-Hb and deoxy-Hb using the three different approaches. For oxy-Hb a mean improvement of 28.7% over all subjects was possible using the CAR method. The TF approach caused an improvement of 37.8% and the highest improvement (47.6%) was reached by the AF method. For a better visualisation of the improvements, Fig. 1B displays the averaged responses of (de)oxy-Hb (representative subject S1, channel 2) during MA task performance, and Fig. 1C the power spectral density (PSD, averaged over all channel) before (raw) and after applying the CAR, AF and TF method. For deoxy-Hb only the TF approach caused an improvement ($13.8 \pm 6.4\%$). In contrast CAR and AF displayed a mean decrease of -6.4% and -23.3%, respectively.

Discussion

Summarizing all three approaches produce large reductions in BP and respiration influences on the oxy-Hb signals and therout improve the SNR. In contrast, for deoxy-Hb signals CAR and AF did not improve the SNR, moreover these methods degrade the SNR. However, these results are in line with the findings of Zhang et al. [2] and can be explained by the fact that the global interfering signals are primarily seen in oxy-Hb, and less prominent in the deoxy-Hb signals [3]. Furthermore, by applying CAR or AF not only the physiological noise will be reduced, also the "signal" bands will be influenced, causing a general amplitude reduction over the whole spectrum (see Fig. 1C) and thereout the SNR degrades. In contrast, for TF approach a small SNR-improvement in deoxy-Hb can be found, which can be explained by the fact that this approach only reduces the noise whereas the "signal" bands will not be influenced. Concluding, all three methods are promising for reducing the global influence from oxy-Hb signals, however CAR and AF should, in contrast to TF, be exclusively applied on oxy-Hb signals, not on deoxy-Hb.

Acknowledgement

This work was performed within the BioTechMed initiative.

Bibliography

[1] S. Coyle, T. Ward, and C. Markham, "Physiological noise in near-infrared spectroscopy: implications for optical brain computer interfacing," *Conf Proc IEEE Eng Med Biol Soc*, vol. 6, pp. 4540–4543, 2004.

[2] Q. Zhang, G. E. Strangman, and G. Ganis, "Adaptive filtering to reduce global interference in non-invasive NIRS measures of brain activation: how well and when does it work?," *Neuroimage*, vol. 45(3), pp. 788–794, 2009.

[3] C. E. Elwell, R. Springett, and E. Hillman, "Oscillations in cerebral haemodynamics - Implications for functional activation studies," *Adv Exp Med Biol*, vol. 471, pp. 57–65, 1999.

[4] G. Pfurtscheller, G. Bauernfeind, S. C. Wriessnegger, and C. Neuper, "Focal frontal (de)oxyhemoglobin responses during simple arithmetic," *Int J Psychophysiol*, vol. 76(3), pp. 186–192, 2010.

[5] G. Florian, A. Stancak, and G. Pfurtscheller, "Cardiac response induced by voluntary self-paced finger movement," *Int J Psychophysiol*, vol. 28(3), pp. 273–283, 1998.

[6] Q. Zhang, E. Brown, and G. Strangman, "Adaptive filtering for global interference cancellation and real time recovery of evoked brain activity: a monte carlo simulation study," *J. Biomed. Opt.*, vol. 12, p. 044014, 2007.

Biomed Tech 2013; 58 (Suppl. 1) © 2013 by Walter de Gruyter · Berlin · Boston. DOI 10.1515/bmt-2013-4431

ESTIMATING BRAIN CONNECTIVITY FROM SINGLE-TRIAL EEG RECORDINGS

Martin Billinger, Clemens Brunner, Reinhold Scherer and Gernot R. Müller-Putz

Institute for Knowledge Discovery, Graz University of Technology, Austria

martin.billinger@tugraz.at

Abstract: *Analysis of brain connectivity is an important tool in neuroscience. Connectivity estimates can be obtained from multi-channel electroencephalogram (EEG) recordings. This usually requires many repetitions (trials) of the condition under investigation. However, applications that rely on real-time signal analysis, such as brain-computer interfaces (BCIs), can only use single trials to estimate connectivity. We present a procedure for estimating single-trial connectivity from the EEG using vector autoregressive (VAR) models, and show for the first time that VAR based single-trial connectivity is possible and yields plausible results.*

Keywords: *brain connectivity, single trial estimation, electroencephalogram*

Introduction

Analysis of brain activity, for example in response to external stimuli, is well established in neuroscience. Brain activity can be observed in the electroencephalogram (EEG) as oscillations or changes in electrical potentials on the surface of the scalp. When e.g., the sensorimotor areas become active power in the mu band (8–12 Hz) decreases over that area [1]. Such processes are well understood and provide the basis for many neuroscientific paradigms [2].

Although the activity of brain areas provides information on the neural processes in the brain, additional knowledge can be gained from the interaction of brain areas, also known as connectivity [3]. Typically, connectivity is estimated from multivariate EEG time series. A common approach consists of fitting a vector autoregressive (VAR) model to multiple realizations (trials) of the time series, and subsequent extraction of various connectivity measures from the model [4]. This approach works well for offline analysis of pre-recorded data. However, to utilize connectivity in online applications such as brain-computer interfaces (BCIs), a method to obtain connectivity estimates from single trials is required. This is not a trivial task, because a large number of free parameters is estimated from a limited data set.

We present a procedure that, after initialization on pre-recorded data, estimates connectivity measures from individual time windows of multi-channel EEG. We pre-transform the data with Infomax independent component analysis (ICA), and estimate connectivity from the ICA sources. To reduce the amount of free parameters for VAR fitting, we select a subset of sources for further analysis. We focus on single-trial fitting of the VAR model. For details on how to extract connectivity measures see [4].

Methods

Initialization

The initialization step is applied to a set of pre-recorded data. First, we transform the raw EEG signals into source signals using the de-mixing matrix obtained from the Infomax ICA algorithm. Infomax has the property of minimizing the instantaneous statistical dependencies between signals, while time delayed dependencies are preserved (which can be modeled with a VAR model of order p).

The number of free parameters $\nu = M^2 p$ in a VAR model is proportional to the square of the number of signals M. The number of data points required to fit the model must be higher than ν. However, the number of available data points $\mu = MN$ is only linearly proportional to M and the estimation window length N. Thus, in order to model more signals, we need longer time windows to fit the VAR model. Likewise, we can reduce the required window length by selecting a subset of the signals.

We use all available signals and trials to obtain detailed connectivity estimates from long estimation windows. From these estimates, we select the most important sources to be used for single-trial estimation.

Single-Trial Estimation

The single-trial estimation step is applied to short windows of novel data. Using a sub-matrix of the de-mixing matrix obtained in the initialization step, we extract the selected source signals from the raw EEG. The lower number of signals in this step allows us to fit a VAR model to shorter time windows. Connectivity measures extracted from the VAR model fitted to short windows can be obtained at higher temporal resolution than signals estimated from long windows, but spatial resolution is lower due to the lower number of signals.

Evaluation on Real Data

We demonstrate our methods on motor imagery (MI) data recorded from one person. The data contains 90 trials of imagined right hand movement and 90 trials of imagined foot movement. 45 EEG channels were recorded, along with 3 electrooculogram (EOG) channels to reduce eye movement artifacts. We split the data into a training set containing 150 trials and a testing set containing 30 trials.

In the initialization step, we estimated the full frequency directed transfer function (ffDTF) [5] on the training set from

all 45 ICA sources with an estimation window length of 4.5 s. From these estimates, eight sources with the highest weighted degree were selected. The weighted degree of a source was calculated as the number of connections to and from the source, multiplied with the amount of correlation each connection contributes to discrimination of hand and foot MI. Subsequently, we performed single-trial estimation of the ffDTF between the selected sources on the testing set.

Results

For visualization purposes, we projected the ICA sources to their equivalent dipole locations. We averaged the ffDTF over the mu band (7–13 Hz), and indicated connectivities that exceed a threshold of ffDTF $>= 0.07$ with arrows between the dipoles. Fig. 1 shows the results for one of the trials.

When the subject was instructed to start MI ($t = 0\,\mathrm{s}$), no functional connectivity between the left and the right motor cortex can be observed. At $t = 2.7\,\mathrm{s}$, we can observe various causal influences from right to left motor cortex.

Although variance between trials is high, increased connectivity from right to left motor cortex can be observed for most of the trials in the testing set.

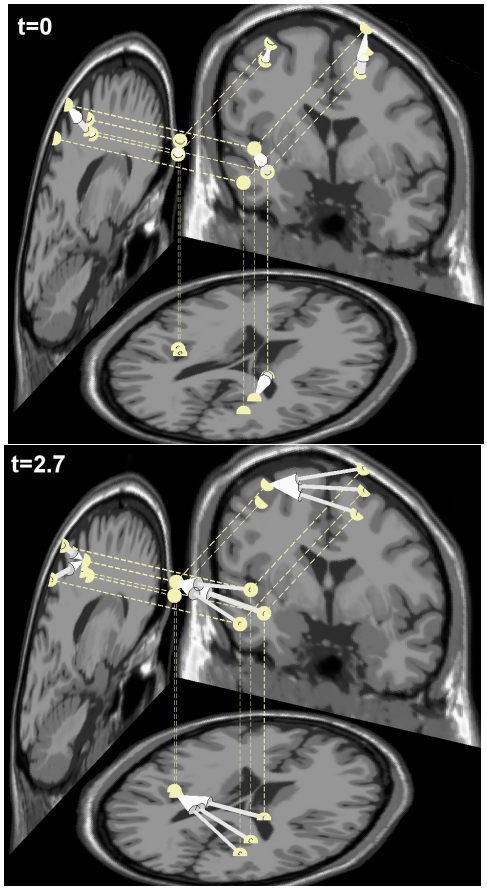

Figure 1: A single trial of ffDTF connectivity between dipole projections before and during imagined right hand movement in the mu band (7-13 Hz). Top: $t = 0\,\mathrm{s}$, Bottom: $t = 2.7\,\mathrm{s}$

Discussion

During hand movement imagination the brain area related to that hand is known to be active (mu power decrease), and the area related to the other hand shows an increase in mu power [1]. This indicates a functional connection between these areas. Thus, the increased connectivity we observed between left and right motor cortex during hand movement is plausible.

There is always a trade-off between temporal, spatial, and spectral resolution. While offline analysis can alleviate this trade-off by utilizing multiple trials, options for single-trial analysis are limited. By selecting a subset of source signals, we chose to reduce spatial resolution in order to obtain higher time resolution.

Connectivity varies between individual trials. This is not surprising, since the signals of interest are buried deeply in noise. Furthermore, there is no guarantee that the subject imagined the movement equally well in each trial. However, most of the trials have increased connectivity between left and right motor cortex. This indicates high robustness of our procedure, although this remains to be verified with detailed statistical analysis.

In summary, we could show for the first time that single-trial estimation of VAR based connectivity measures is possible and leads to plausible results.

Acknowledgement

This work was supported by the EU Project ABC (No. 287774) and the FWF Project (P20848-N15). This paper only reflects the authors' views and funding agencies are not liable for any use that may be made of the information contained herein.

Bibliography

[1] G. Pfurtscheller and F. H. Lopes da Silva, "Event-related EEG/MEG synchronization and desynchronization: basic principles," *Clinical Neurophysiology*, vol. 110, pp. 1842–1857, 1999.

[2] J. R. Wolpaw, N. Birbaumer, D. J. McFarland, G. Pfurtscheller, and T. M. Vaughan, "Brain-computer interfaces for communication and control," *Clinical Neurophysiology*, vol. 113, pp. 767–791, 2002.

[3] K. J. Friston, "Functional and effective connectivity: a review," *Brain Connectivity*, vol. 1, pp. 13–36, 2011.

[4] A. Schlögl and G. Supp, "Analyzing event-related EEG data with multivariate autoregressive parameters," in *Event-related dynamics of brain oscillations* (C. Neuper and W. Klimesch, eds.), pp. 135–147, Elsevier, 2006.

[5] A. Korzeniewska, M. Mańczak, M. Kamiński, K. J. Blinowska, and S. Kasicki, "Determination of information flow direction among brain structures by a modified directed transfer function (dDTF) method.," *J Neurosci Methods*, vol. 125, pp. 195–207, May 2003.

Biomed Tech 2013; 58 (Suppl. 1) © 2013 by Walter de Gruyter · Berlin · Boston. DOI 10.1515/bmt-2013-4432

TIME-DOMAIN CORRELATIONS OF IMAGINED ARM POSITIONS WITH BRAIN SOURCES

Ofner P[1] and Müller-Putz G R[1]

[1]Institute for Knowledge Discovery, Graz University of Technology, Austria

patrick.ofner@tugraz.at

Abstract: *We investigated how the assumed hand position of the right arm during movement imagination correlates with brain sources. Sources were calculated from the electroencephalogram (EEG) applying a brain imaging technique. We used frequencies below 1 Hz. In 4 out of 9 subjects, substantial correlations on the supplementary motor cortex were observed. This supports that decoding movement imaginations could be possible and it is neurophysiologically plausible.*

Keywords: *EEG, movement decoding, movement imagination*

Introduction

An important issue of tetraplegic persons is the restoration of the upper limb functionality. The nerves in the spinal cord are damaged and have to be bridged. For that purpose a functional electrical stimulation (FES) neuroprosthesis can be combined with a brain-computer interface (BCI) [1]. In general, a BCI measures brain signals and transforms them into control commands for devices. Here, the movement imagination (MI) is detected with a BCI and transformed into a real arm movement using the FES neuroprosthesis. Sensorimotor rhythms (SMR) based BCIs can detect power modulations in the mu-band accompanying MIs. However, SMR-based BCIs detect only the process of MI of a body part, but not the actual MI itself. As a consequence, different body parts usually have to be assigned to different neuroprosthesis movements. That means that e.g. a foot movement is assigned to an extension of the arm. A more natural control schema would be to decode the actual MI (e.g. the imagined position of the arm). Recent findings have shown that also low frequency time-domain signals (< 5 Hz) carry movement information when executing movements (e.g. [2]). In [3] low frequency electroencephalogram (EEG) components were used decode the velocity of executed arm movements. However, it is still an open question if this movement decoding can also be applied to imagined movements, and if so, which brain regions are involved. In this work we investigated if decoding of rhythmic movement imaginations is possible and which are the underlying brain regions.

Methods

Paradigm: We recruited 9 healthy right-handed subjects and measured the EEG during imagined arm movements. Subjects were seated comfortably in a chair, and in front of them was a computer screen displaying the cues. We asked subjects to imagine natural, round (not jaggy), repeated, rhythmic movements from left to right and back (transverse plane), and from bottom to top and back (sagittal plane). MIs were synchronised with a metronome with a frequency of 1 Hz. As a beat of the metronome corresponded to an endposition of the arm, the frequency of the imagined movements was 0.5 Hz. A trial started with a short beep tone together with a cue. The cue was either an arrow pointing right or up and was shown for 0.5 s. Subsequently, a cross was shown for the rest of the trial and subjects were asked to fixate their gaze on this cross to suppress eye movements. The metronome started beating 1.5–2.5 s after the trial start and stopped 20s later, this was also the end of the trial. We recorded 8 MI runs, each comprising 5 trials per movement plane. In this work we did not differentiate between the two different movement planes, leading to a combined set of 80 MI trials. To remove eye movements from the EEG with a linear regression method, we also recorded 2 runs with deliberate eye movements.

Recording: We recorded the EEG with 68 electrodes covering frontal, central and parietal areas. Reference was placed on the left ear, ground on the right ear. Furthermore, we recorded the electrooculogram (EOG) using 3 electrodes. Signals were acquired with g.USB amplifiers (g.tec, Graz, Austria) with a sampling frequency of 256 Hz and an 8th order Chebyshev bandpass filter with cut off frequencies at 0.01 Hz and 100 Hz and a notch filter at 50 Hz. The positions of the EEG electrodes were measured with a CMS 20EP system (Zebris Medical GmbH, Isny, Germany).

Preprocessing: To remove artefacts, we applied an independent component analysis and removed components suspected to be eye-, muscle- or technical artefacts. We also removed remaining influences of eye movements from the EEG with a linear regression method. For computational convenience, we applied an anti-aliasing filter and downsampled data to 16 Hz. Afterwards, we bandpass filtered the data with a zero-phase 4th order Butterworh filter with cut off frequencies at 0.3 Hz and 0.8 Hz, thus including the arm movement frequency of 0.5 Hz. To remove any remaining artefacts, we removed samples exceeding a threshold of 4.4 times the median absolute deviation. This corresponds approximately to 3 times the standard deviation when the data is normally distributed. We also removed samples 1 s before and after a detected artefact.

Analyis: We calculated the brain sources with the software Brainstorm. Here, we used the default anatomy data based on the Colin27 brain delivered with Brainstorm and cal-

Table 1: This table contains the maximum absolute canonical correlations over all brain sources for all subjects.

subject	s1	s2	s3	s4	s5	s6	s7	s8	s9
max abs corr	0.54	0.21	0.14	0.37	0.16	0.19	0.12	0.25	0.36

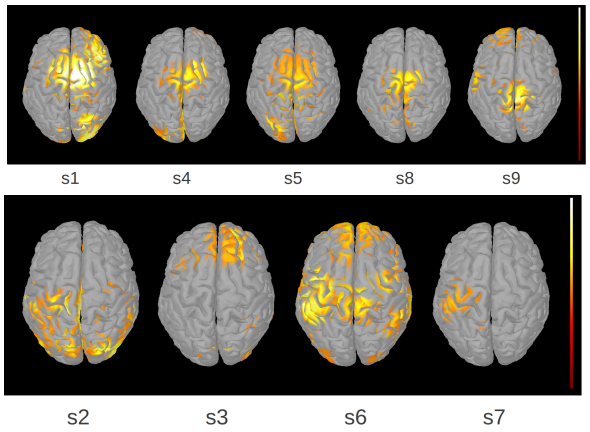

Figure 1: This figure shows the absolute canonical correlations for each subject. White (highest representable value) corresponds to a canonical correlation of 0.5 for s1, 0.4 for s4 and s9, 0.3 for s8 and 0.2 for all others. Canonical correlations below 50 % with respect to the highest representable value are not shown.

culated the boundary element head model. Subsequently, 15028 sources were calculated from the preprocessed EEG with the sLORETA method. The noise covariance matrix was set to the identity matrix. We build a feature vector for each source consisting of the current source value and 3 time delayed values with a time interval of 62.5 ms between them. Furthermore, we assumed that subjects imagined movement positions corresponding to a sine oscillation with a frequency of 0.5 Hz. Finally, we calculated for each source the canonical correlation between the feature vector and the sine oscillation. Here, to avoid any possible existing movement onset effects, we removed the first 2 s of MI data, leading to remaining 18 s of MI data per trial. As the canonical correlation builds a linear model of the independent variables (feature vector), the method described here is in fact the same as the position decoding described in [4].

Results

Tab. 1 shows the maximum absolute canonical correlations of all brain sources for each subject. Fig. 1 visualizes the absolute values of the canonical correlations of all brain sources. White corresponds to a canonical correlation of 0.5 for subject s1, 0.4 for s4 and s9, 0.3 for s8 and 0.2 for all others. Canonical correlations on the supplementary motor area (SMA) with the position of the rhythmic movement imagination are observable for subjects s1, s4, s5, s8. Subject s9 shows canonical correlations on the medial part of the motor cortex. Higher canonical correlations on the hand area of the primary motor cortex (M1) than on the SMA are observable for subjects s2, s6 and s7.

Discussion

We found correlations of brain sources with imagined rhythmic movements. Those correlations were observable on the SMA for 4 out of 9 subjects. However, we used a standard brain anatomy which can have caused inaccuracies and the central correlation pattern of s9 is similar to the ones of s1, s4, s5 and s8. Therefore, it is possible that this pattern has to be attributed to the SMA. The SMA is involved in motor control. Thus, these correlations are plausible from a neurophysiological point of view. Higher canonical correlations on the hand area of M1 than on the SMA were observed for 3 subjects only. Furthermore, they were always lower than 0.21. These findings suggest that in the *time-domain* primarily the SMA, and not M1, provides decodable information about rhythmic movement imaginations. Due to the lack of a control condition (metronome beat without MI), we do not know if these correlations exist also when just listening to a metronome. Indeed, [5] reports in an functional magnetic resonance imaging study an increased activity of the SMA during the perception of a beat. However, that is not conclusive for time-domain correlations. We have shown that rhythmic MI, synchronised to a beat, can be decoded from neurophysiological plausible brain sources. In the future, methods have to be improved to allow the decoding of non-rhythmic MI with sufficient accuracy to control neuroprotheses.

Bibliography

[1] G. R. Müller-Putz, R. Scherer, G. Pfurtscheller, and R. Rupp, "EEG-based neuroprosthesis control: a step towards clinical practice," *Neuroscience Letters*, vol. 382, pp. 169–174, 2005.

[2] S. Waldert, H. Preissl, E. Demandt, C. Braun, N. Birbaumer, A. Aertsen, and C. Mehring, "Hand movement direction decoded from meg and eeg," *The Journal of Neuroscience*, vol. 28, pp. 1000–1008, January 2008.

[3] T. J. Bradberry, R. J. Gentili, and J. L. Contreras-Vidal, "Reconstructing three-dimensional hand movements from noninvasive electroencephalographic signals," *Journal of Neuroscience*, vol. 30, pp. 3432–3437, 2010.

[4] P. Ofner and G. Müller-Putz, "Decoding of velocities and positions of 3d arm movement from eeg," in *Proceedings of the 34th Annual International Conference of the IEEE EMBS*, pp. 6406–6409, 2012.

[5] J. A. Grahn and M. Brett, "Rhythm and beat perception in motor areas of the brain," *Journal of Cognitive Neuroscience*, vol. 19, no. 5, pp. 893–906, 2007.

Biomed Tech 2013; 58 (Suppl. 1) © 2013 by Walter de Gruyter · Berlin · Boston. DOI 10.1515/bmt-2013-4433

SPATIAL-SPECTRAL IDENTIFICATION OF μ AND β EEG RHYTHM SOURCRS DURING ROBOT-ASSISTED WALKING

Seeber M[1], Scherer R[1], Wagner J[1], Solis-Escalante T[1], Müller-Putz G R[1]

[1]Institute for Knowledge Discovery, Graz University of Technology, Austria

gernot.mueller@tugraz.at

Abstract: *We are interested in studying cortical involvement during the gait to provide fundamental knowledge for stroke rehabilitation. In this work we analyze electroencephalographic (EEG) rhythms during a robot-assisted gait-training experiment from able-bodied participants. A computational 3D distributed source model based on individual anatomy was used to calculate EEG source maps. These functional brain topographies showed individual μ and β event-related desynchronization (ERD) activity in the sensorimotor area, where the β-ERD is located more focal and inter-subject consistent in the feet area than the μ-ERD. With this work we are providing a fully data-driven method capable to identify first, EEG rhythms for each subject individually without any spatial a priori region of interest and second, to localize these rhythmic changes on the cortical level.*

Keywords: *High-density EEG, inverse modelling, brain rhythms, gait analysis*

Introduction

Topographic analysis of high-density electroencephalography (EEG) is increasingly evolved to a capable brain imaging tool [1] due to progress in signal processing and the availability of computational power. In this work we apply EEG source imaging for individual subjects, since we are preparing methods for studying neuroplasticity during inpatient rehabilitation after stroke. From previous studies we have evidence that the spectral power of the EEG μ and β band decreases (ERD) [2] over sensorimotor foot areas [3] during isolated foot movements [4] [5] and walking [6], when compared to rest. Hence we aim to identify μ and β ERD activity for each individual subject by analyzing the EEG spectra and localize these changes in the EEG source topographies.

Methods

We recorded EEG from 120 electrodes placed according to the 5% 10-20 system from 8 able-bodied volunteers (26.3± 3.5 yr, 3 female) during 3 runs of upright standing (3 min each) and 4 runs of active walking (6 min each) in a robotic gait orthosis (Lokomat, Hocoma AG, Switzerland). EEG was sampled to 2.5 kHz, high pass filtered at 0.1 Hz and low pass filtered at 1 kHz, down-sampled to 250 Hz for further analysis and segmented into gait-cycles (time period between consecutive right heel contacts). Foot contact was measured with a mechanical foot switch placed over the calcaneus bone. Segments and channels with artifacts were excluded from further analysis (criteria based on statistical measures) and the remaining gait cycles were time warped. We used a 3D localizer (Zebris Elpos system, USA) to determine electrode positions and anatomical landmarks for each subject. Structural magnetic resonance imaging scans (Tim Trio, Siemens, Germany) were used to construct a four shell (layers: cortex, inner skull, outer skull and scalp surface) boundary element model (BEM) for each subject individually using Freesurfer [7] and OpenMEEG [8] toolbox. Electrode locations and the BEM were co-registered by anatomical landmarks (nasion, vertex left/right preauricular points). The bioelectric inverse problem was solved using a regularized minimum norm method [9] performed by the BrainStorm toolbox [10]. We computed z-score values of gait cycle segments versus standing condition segments (spilt into segments of gait cycle length). To identify the frequency component (individual 2 Hz bin from morlet wavelet time-frequency decomposition) that desynchronizes most for each subject individually, we calculated the mean of a population from 1% sources in the model that showed maximal ERD. Analyzing mean population activity considers the change of the amount and the strength of source activities for the different frequency bins. This approach does not necessarily imply focal activities that are organized in topographic clusters. Hence it is a global measure that is independent of any a priori spatial regions of interest.

Results

The spectra of cortical activity from the most desynchronizing sources showed individual spectral peak ERD slightly different, but consistent in the μ and β band (Fig.1, Table 1) in every subject. Brain topographies at these frequencies are illustrated in Fig.2 for the μ and in Fig.3 for the β rhythm.

Table 1: Peak ERD frequencies in the μ and β band of the individual subjects

Subject	μ-peak in Hz	β-peak in Hz
Subject A	12	26
Subject B	12	28
Subject C	10	28
Subject D	12	24
Subject E	12	22
Subject F	14	28
Subject G	12	30
Subject H	8	22
Average	11.5 ± 1.77	26 ± 3.02

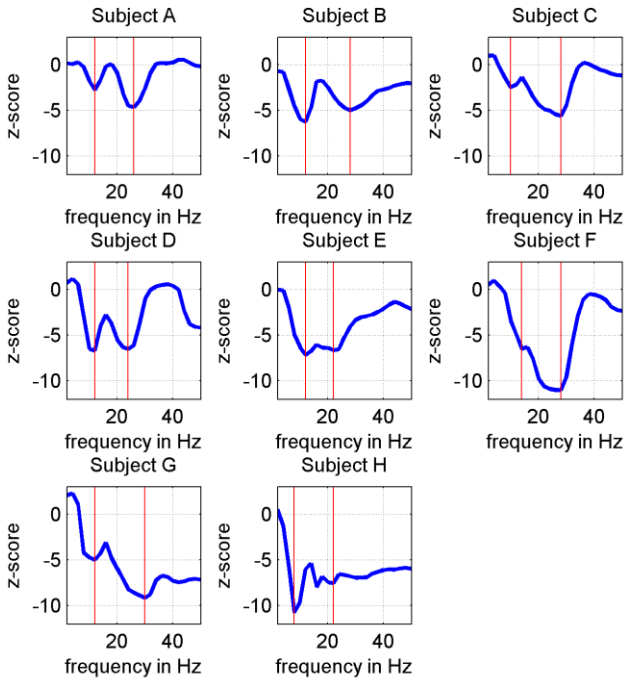

Figure 1: Mean spectral changes of the 1% EEG sources in the distributed source model that showed maximal ERD

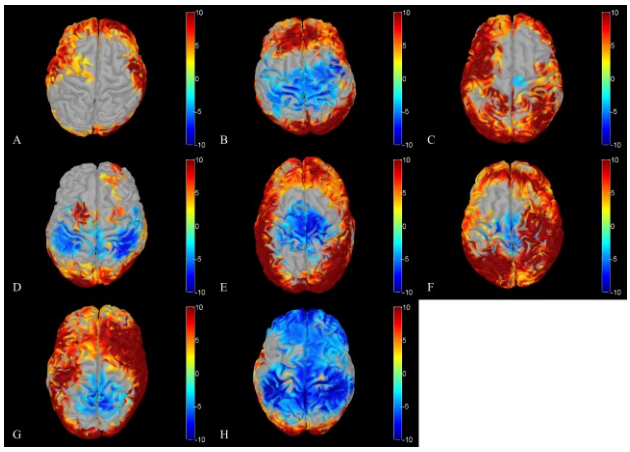

Figure 2: functional brain topographies of the μ ERD peak (ERD illustrated in blue) for all subjects, activity is in z-score values (>3, min. cluster size 10 vertices)

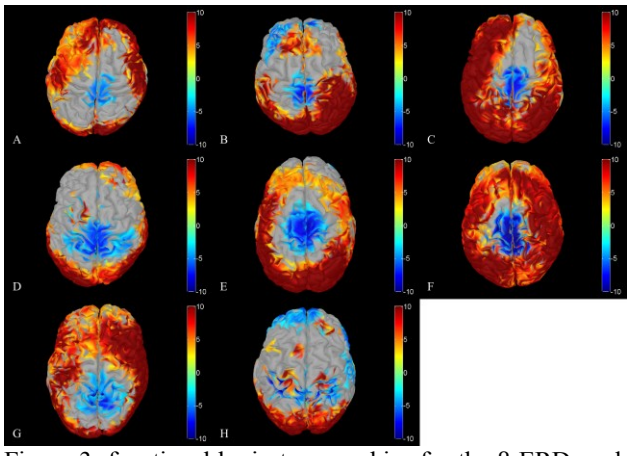

Figure 3: functional brain topographies for the β ERD peak for all subjects, figure settings as in Fig. 2

Discussion

Peak ERD frequencies were identified successfully for every subject in the μ and β band. The resulting spectral peaks lead to μ and β topographies for these frequencies. The β topographies showed inter-subject consistent focal ERD activity in the sensorimotor feet area reflecting the movement of lower limbs during walking. μ ERD is less inter-subject consistent and more widespread. These results are in line with previous studies showing brain activity during isolated foot movements [4] [5] and walking [6]. To our knowledge this is the first work showing distributed source model functional brain topographies of μ and β ERD based on individual anatomy during walking. Moreover, we showed a method that is capable to consider first, individual slight differences of the μ and β rhythms and second, to localize ERD activity of these rhythms on the cortical level.

Acknowledgement

This work was partly supported by the European Union research project BETTER and the Land Steiermark project BCI4REHAB. This paper only reflects the authors' views and funding agencies are not liable for any use that may be made of the information contained herein.

Bibliography

[1] Michel, C.M., Murray, M.: Towards the utilization of EEG as a brain imaging tool, *NeuroImage*, vol. 61, no. 2, pp. 371–385, 2012

[2] Pfurtscheller, G., Lopes da Silva, F.H.: Event-related EEG/MEG synchronization and desynchronization: basic principles. *Clin Neurophysiol*, vol. 110, pp. 1842–1857, 1999

[3] Jasper, H., Penfield, W.: Electrocorticograms in man: effect of voluntary movement upon the electrical activity of the precentral gyrus, *European Archives of Psychiatry and Clin. Neuology*, vol. 183, no. 1-2, pp. 163-174, 1949

[4] Hari, R., Salmelin, R.: Human cortical oscillations: a neuromagnetic view through the skull, *Trends in Neuroscience*, vol. 20, no. 1, pp. 44-49, 1997

[5] Pfurtscheller, G., Neuper, C. et. al: Foot and hand area mu rhythms, *International Journal of Psychophysiology*, vol. 26, pp. 121-135, 1997

[6] Wagner, J., Solis-Escalate, T. et. al: Level of participation in robotic-assisted treadmill walking modulates midline sensorimotor EEG rhythms in able-bodied subjects', *NeuroImage*, vol. 63, no. 3, pp. 1203–1211, 2012

[7] Dale, A., Fischl, B. et. Al: Cortical surface-based analysis. I. Segmentation and surface reconstruction, *NeuroImage*, vol. 9, no. 2, pp. 179-194, 1999

[8] Gramfort, A., Papadopoulo, T. et. al: OpenMEEG for M/EEG forward modeling: a comparison study, *Bio-Medical Engineering Online*, vol. 9/45, pp. 1-20, 2010

[9] Baillet, S., Moscher, J.C. et. al: Electromagnetic brain mapping, *IEEE Signal Processing Mag.*, pp. 14-30, 2001

[10] Tadel, F., Baillet, S. et. al: Brainstorm: A User-Friendly Application for MEG/EEG Analysis, Computational Intelligence and Neuroscience, 2011

Biomed Tech 2013; 58 (Suppl. 1) © 2013 by Walter de Gruyter · Berlin · Boston. DOI 10.1515/bmt-2013-4434

ROBOT ASSISTED WALKING AFFECTS THE SYNCHRONY BETWEEN PREMOTOR AND SOMATOSENSORY AREAS

J. Wagner[1], T. Solis-Escalante[1], C. Neuper[1,2], R. Scherer[1,3] and G. Müller-Putz[1]

[1]Institute of Knowledge Discovery, Graz University of Technology, Austria
[2]Department of Psychology, University of Graz, Austria
[3]Rehabilitation Clinic Judendorf-Strassengel, Austria

johanna.wagner@tugraz.at

Abstract: *We recorded the electroencephalogram (EEG) from 14 healthy volunteers during standing and active walking with a robotic gait orthosis. Infomax independent component analysis decomposed the EEG into independent components (ICs), representing brain, muscle and artifact sources. ICs were clustered across participants based on their anatomical position and spectral patterns. Coherence was computed between clusters. We show that walking compared to standing decreases α (8-12Hz) band coherence between sensorimotor areas. Additionally lower γ band (30-36Hz) coherence between the premotor cortex and the sensory cortex is enhanced. Our results suggest different functionalities at α and γ synchrony on sensorimotor processing during locomotion.*

Keywords: *EEG during walking, Coherence, brain oscillations, Neurorehabiltation, gait*

Introduction

In stroke patients, lesions can disrupt processing pathways between brain regions [1]. This can cause motor deficits not directly related to the function of the affected site. It is important to investigate which brain areas interact during the execution of a specific motor task to be able to target behavioral decifits during rehabilitation procedures. Little so far is known about the cortical processing pathways during locomotion. In this work we compared synchrony between cortical areas during standing and walking in a gait robot.

Methods

We recorded the electroencephalogram (EEG) from 120 sites from 14 healthy volunteers (24 ± 2 years, 8 male) during standing (3 runs of 3 min) and active walking (4 runs of 6 min) with a robotic gait orthosis (Lokomat, Hocoma). Fig. 1 summarizes the experiments.

EEG Analysis: Preprocessing included filtering from 1 to 200 Hz, resampling at 500 Hz and manual artifact rejection. Infomax independent component analysis [2] decomposed the EEG into independent components (ICs), representing brain, muscle and artifact sources. A single equivalent current dipole, was calculated for each IC. ICs were clustered across participants based on their anatomical position and spectral patterns [3]. The resulting clusters were checked for matching ICs from each subject (i.e. at least one IC per participant per cluster). Only cluster pairs that contained

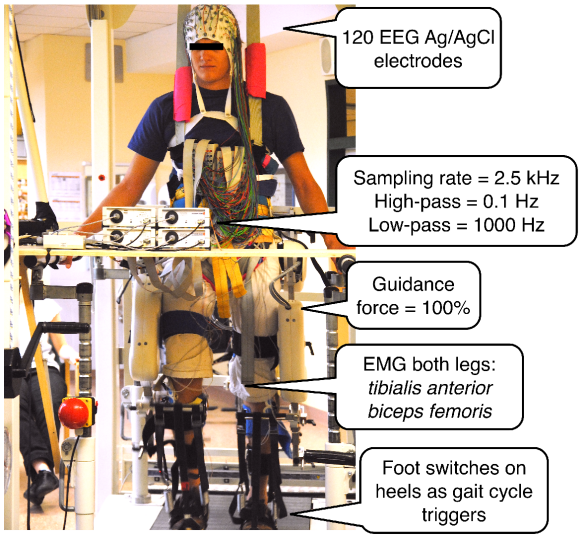

Figure 1: Experimental setup. Walking in the robotic gait orthosis. Speed ($\leq$ 2 km/h) and body weight support ($\sim$ 70 %) were adjusted for each participant

matching ICs from at least half of the participants were included in the following analysis. This procedure resulted in nine cluster pairs for comparison. Linear coherence was then computed between cluster pairs for matching ICs, from 1 to 46 Hz using two non overlapping time windows of 500 ms over 100 trials for each condition before and after the right heelstrike (time between controlateral steps 1 s). For standing, artificial epochs of 1 s were created. Coherence was computed according to Eq. 1

$$coh_{x,y}(f) = \frac{|S_{xy}(f)|^2}{S_{xx}(f)S_{yy}(f)} \quad (1)$$

where S_{xx} and S_{yy} are the autospectra of $IC1$ and $IC2$ for each condition and S_{xy} is the cross-spectra of the IC pair. Coherence was considered to be significant if it was greater than the 95% confidence limit CL [4]

$$CL = 1 - 0.05^{1/n-1} \quad (2)$$

where n is the number of trials used for spectral estimation. Coherence values between conditions were compared between pairs of clusters only for frequency ranges that showed significant coherence. Coherence between ICs was z-transformed and then averaged in the following bands:

θ (3-6Hz), α (8-12Hz), lower β (15-20Hz), upper β (22-30Hz) and lower γ (30-36Hz). Paired t-tests were computed with a bootstrap method and the significance level was Bonferroni corrected a priori at 0.05.

Results

Seven cluster pairs revealed significant coherence in at least one of the conditions. Three of these cluster pairs (see Fig. 2) showed significant differences between movement conditions (see Fig. 3). Tab. 1 shows single cluster properties. Coherence in the α band between BA6 (BA = Brodmann area) and BA5 is significantly suppressed during walking compared to standing while coherence in the lower γ band shows the opposite pattern (significant increase during walking vs. standing). Synchrony in the α band between BA6 and BA5 and between BA31 and BA6 is significantly increased during standing compared to the walking task.

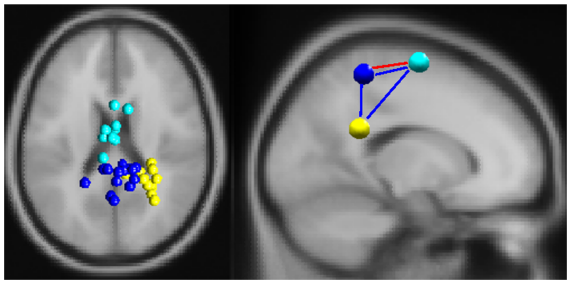

Figure 2: Spatial location of IC clusters (left: single dipoles, right: centroids) visualized in the MNI (Montreal Neurological Institute) brain volume: BA6 (turquois), BA5 (blue) and BA31 (yellow); Right: significant coherence between clusters is marke by a line (walking: red, standing:blue)

Table 1: Clusters of ICs showing significant differences in coherence between conditions

Cluster	Location of cluster centroid	Tailarach coordinates (x,y,z)	Subjects (S) & ICs
BA6	Premotor Area	1, -4, 63	9S 9ICs
BA5	Sensory Cortex	1, -38, 58	11S 14ICs
BA31	Cingulate Cortex	25, -43, 26	10S 12ICs

Note: cluster naming corresponds to Brodmann area.

Discussion

This is the first study showing that robot-assisted walking alters the coherence between brain areas.
Our analysis revealed that walking compared to standing decreases α band coherence between sensorimotor areas. Prior studies suggest that α band synchrony can be associated with the inactivation of cortical regions [5], thus we may consider that walking increases activation in sensorimotor areas. Interestingly, walking compared to standing increases lower γ band coherence between the premotor and the sensory cortex. In [6] the authors have shown that γ band synchrony (35-40Hz) is associated with a shortening of reaction times and could be related to preparatory top-down modulation of sensory processing. Thus during walking the premotor cortex might enhance preparatory activity in the sensory cortex via increased γ band synchrony. Our results support findings on different functionalities of α band (inhibitory) and γ band (excitatory) synchrony on motor processing and suggest that these effects are present during locomotion.

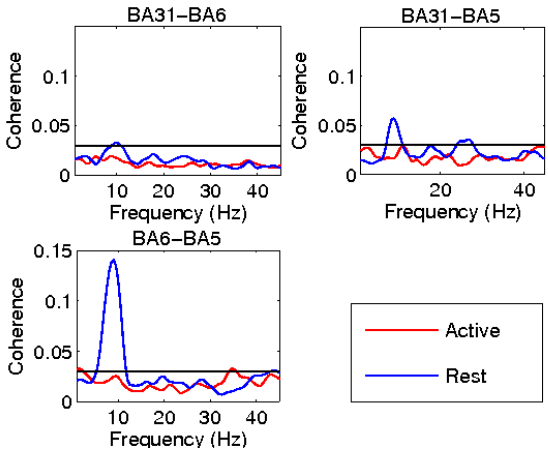

Figure 3: Coherence between clusters for different movement conditions. The significance level is marked by a black line.

Acknowledgement

This work was partly supported by the European Union research project BETTER (ICT-2009.7.2-247935) and the Land Steiermark project BCI4REHAB.

Bibliography

[1] C. Gerloff et al, "Multimodal imaging of brain reorganization in motor areas of the contralesional hemisphere of well recovered patients after capsular stroke.," *Brain*, vol. 129, pp. 791–808, 2006.

[2] S. Makeig et al, *Adv Neural Inf Process Syst*, ch. Independent Component Analysis of Electroencephalographic Data, pp. 145–151. MIT Press Cambridge, MA, 1996.

[3] J. Wagner et al, "Level of participation in robotic-assisted treadmill walking modulates midline sensorimotor eeg rhythms in able-bodied subjects," *NeuroImage*, 2012.

[4] J. R. Rosenberg et al, "The fourier approach to the identification of functional coupling between neuronal spike trains," *Prog Biophys. Mol. Biol.*, pp. 1–31, 1989.

[5] S. Palva and J. Palva, "New vistas for alpha-frequency band oscillations," *Trends in Neuroscience*, vol. 30, pp. 150–158, 2007.

[6] H. Jokeit et al, "Different event-related patterns of gamma-band power in brain waves of fast- and slow-reacting subjects.," *Proc. Natl Acad. Sci*, vol. 91, pp. 6339–6343, 1994.

Biomed Tech 2013; 58 (Suppl. 1) © 2013 by Walter de Gruyter · Berlin · Boston. DOI 10.1515/bmt-2013-4435

The hybrid Brain-Computer Interface: a bridge to assistive technology?

Müller-Putz G.R.[1], Schreuder M.[2], Tangermann M.[2], Leeb R.[3], Millán del R. J.[3]

[1] Institute for Knowledge Discovery, Graz University of Technology, Austria
[2] Machine Learning Lab, Technische Universität Berlin, Germany
[3] Chair in Non-Invasive Brain-Machine Interface, École Polytechnique Fédérale de Lausanne, Switzerland

gernot.mueller@tugraz.at

Abstract: *Brain-Computer Interfaces (BCIs) can be extended by other input signals to form a so-called hybrid BCI (hBCI). Such an hBCI allows the processing of several input signals with at least one brain signal for control purposes, i.e. communication and environmental control.*
This work shows the principle, technology and application of hBCIs and discusses future objectives.

Keywords: *hybrid BCI, electroencephalogram (EEG), assistive technology*

Introduction

Persons with movement disabilities can use a wide range of assistive devices (ADs). The set of ADs ranges from switches connected to a remote controller to complex sensors (e.g., mouth mouse, eye tracking systems) attached to a computer. All of these systems work very well after being adjusted individually for each person. However, there are still situations where the systems do not work properly, e.g., when residual muscles become fatigued or users have such severe disabilities that no movement is possible. In such situations, a Brain-Computer Interface (BCI) might be the only available option, since it uses mentally modulated brain signals (e.g., electroencephalogram, EEG) for control without requiring any movement.
BCIs are systems that establish a direct connection between the human brain and a computer, thus providing an additional means for communication. As noted, some people use a BCI because their disabilities make it impossible to use any interface which requires movements. BCIs can also be used to control neuroprostheses in patients suffering from a high spinal cord injury. After 20 years of research and development, Brain-Computer Interface technology is ready to leave the lab and to be used in practical applications in real world settings such as homes or hospitals.

A BCI could replace an existing AD. However, in some situations it would be even better to couple the BCI with the existing AD and develop a new system called a hybrid BCI (hBCI) [1,2,8]. Ideally, an hBCI should let the user extend the types of inputs available to an assistive technology, or choose not to use the BCI at all. The hBCI might decide which input channel(s) offer(s) the most reliable signal(s) and switch between input channels to improve information transfer rate and usability, or it could instead fuse various input channels to increase the SNR.

In the past as well as in the present, various studies about hBCIs have been conducted, but they always combined different brain signals or brain and other biosignals. A more general definition says that a hBCI does not depend on the BCI as an active input. Instead, it simply allows the BCI to function as an input channel when the BCI could increase the overall performance for that user. The hBCI can perform fusion to switch between multiple inputs, but (depending on the configuration) can also weight signals and combine/fuse them to achieve one control signal from a combination of multiple inputs.

Methods

The principle of an hBCI can be explained as following: in addition to the EEG-based BCI, there are other input and control signals possible [2]. These include other biosignals (e.g., electromyogram, [3]) as well as signals from manual controls such as from ADs (e.g., mouth mouse, push buttons, …[4,5]). A "fusion" collects all control signals and generates a new control signal out of all those inputs. Besides a quality check (e.g., artifact detection), those signals will be weighted and fused to a control signal, or the most reliable one will be chosen. Followed by the so-called "shared control", sensor signals from the application (neuroprosthesis [6], software [4], assistive robot [7]) will also be included and used to generate an accurate final control signal.

Results & Discussion

One major goal is to bring the BCI technology to a level where it can be used in an environment together with other assistive devices. To achieve this, however, the hBCI must be able to operate reliably for long periods. It has to recognize and adapt to changes since brain signals and patterns may change during a day. Reaching this goal requires that many different subsystems in the hBCI are able to work together. Examples include standard BCI processing, post processing (error potentials), mental state recognition (fatigue), artifact detection, adaptation of classifiers, and surveillance of signal quality (including EEG signals and those from additional input devices). Several of those modules are developed and tested successfully, however, the integration of all of them is still an open issue.

Acknowledgement

This work was supported by the EU FP7 projects TOBI (224631), and BackHome (288566) .

Bibliography

[1] Pfurtscheller, G.; Allison, B. Z.; Brunner, C.; Bauernfeind, G.; Solis Escalante, T.; Scherer, R.; Zander, T.; Müller-Putz, G.; Neuper, C.; Birbaumer, N.: The Hybrid BCI. - in: Frontiers in neuroprosthetics 4 (2010) , S. 1 - 11

[2] Müller-Putz, G.; Breitwieser, C.; Cincotti, F.; Leeb, R.; Schreuder, M.; Leotta, F.; Tavella, M.; Bianchi, L.; Kreilinger, A.; Ramsay, A.; Rohm, M.; Sagebaum, M.; Tonin, L.; Neuper, C.; del. R. Millán, J.: Tools for brain-computer interaction: a general concept for a hybrid BCI. - in: Frontiers in neuroinformatics 5 (2011) 30 , S. 1 - 10

[3] Leeb, R.; Sagha, H.; Chavarriaga, R. & d. R. Millán, J. A hybrid brain-computer interface based on the fusion of electroencephalographic and electromyographic activities. J Neural Eng, 2011, 8, 025011

[4] Clauzel, G.; Kaltner, B.; Breitwieser, C.; Müller-Putz, G.: Combining Hybrid BCI and signal quality monitoring to improve user experience. - in: 1st International DECODER Workshop. Boulogne-Billancourt, Frankreich am: 11.04.2012

[5] Kreilinger, A.; Kaiser, V.; Breitwieser, C.; Williamson, J.; Neuper, C.; Müller-Putz, G.: Switching between manual control and brain-computer interface using long term and short term quality measures. - in: Frontiers in neuroscience 5 (2012) 00147 , S. 1 - 11

[6] Rohm, M.; Schneiders, M.; Kreilinger, A.; Müller-Putz, G.; Rupp, R.: First evaluation results of a BCI-controlled hybrid neuroprosthesis for restoration of grasping in a high spinal cord injured individual. - in: Proceedings of TOBI Workshop lII. (2012), S. 8 - 9

[7] Tonin, L.; Carlson, T.; Leeb, R. & d. R. Millán, J. Brain-Controlled Telepresence Robot by Motor-Disabled People Proc. Annual International Conference of the IEEE Engineering in Medicine and Biology Society EMBC 2011, 2011, 4227-4230.

[8] Millán, J. d. R.; Rupp, R.; Müller-Putz, G.; Murray-Smith, R.; Giugliemma, C.; Tangermann, M.; Vidaurre, C.; Cincotti, F.; Kübler, A.; Leeb, R.; Neuper, C.; Müller, K. & Mattia, D. Combining Brain-Computer Interfaces and Assistive Technologies: State-of-the-Art and Challenges Frontiers in Neuroscience, 2010, 4, 161.

Biomed Tech 2013; 58 (Suppl. 1) © 2013 by Walter de Gruyter · Berlin · Boston. DOI 10.1515/bmt-2013-4436

ON THE USE OF NON-INVASIVE BRAIN-COMPUTER INTERFACE TECHNOLOGY IN NEUROREHABILITATION

Scherer R[1,2], Solis-Escalante T[1], Faller J[1], Wagner J[1], Seeber M[1] and Müller-Putz G[1]

[1]Institute for Knowledge Discovery, Graz University of Technology, Graz, Austria
[2]Clinic Judendorf-Strassengel, Judendorf-Strassengel, Austria

reinhold.scherer@tugraz.at

Abstract: *Brain-Computer Interfaces (BCIs) are devices that bypass the normal neuromuscular output pathways and translate a user's brain signal directly into action. Historically, BCIs were developed with the aim of restoring communication in completely paralyzed individuals and replacing lost motor function. In this work, we review recent developments towards the inclusion of BCI technology in the field of neurorehabilitation. Since years, our group at the Graz University of Technology, Austria, successfully researches and develops applications for non-invasive electroencephalogram-based (EEG) BCIs that are operated by modulation of sensorimotor rhythms. Our results demonstrate both the feasibility and possible utility of incorporating BCI technology into clinical practice.*

Keywords: *Brain-Computer Interfaces, Electroencephalogram, Neurological rehabilitation.*

Introduction

Brain tissue damage typically affects cognitive, emotional and physical aspects of human behavior. For recovering lost function, the nervous system has the capacity to reorganize neural pathways in response to environmental diversity. This ability of the central nervous system is known as neuroplasticity. Directed and early rehabilitation after brain injury aims at promoting neuroplasticity. Brain-Computer Interface (BCI) technologies allow monitoring and interpreting brain signals in real-time [1]. BCIs could thus be used to provide feedback on changes in brain activation that positively correlate with functional improvement before changes in behavior become evident.

Here, we review some recent work in the field of non-invasive electroencephalogram-based (EEG) BCI-assisted neurorehabilitation conducted at the Graz University of Technology. The review is divided into three parts. Firstly, we review our latest developments on EEG-based communication and control [2, 3]. Communication problems after brain injury are very common. Providing systems that enable basic communication in clinical settings can be very helpful. Secondly, using the example of gait rehabilitation, we outline how BCI technology can be helpful for assessing active participation of individuals during rehabilitation [4, 5]. Active participation is essential for successful rehabilitation. Thirdly, we present our first prototype of game-based functional motor mapping [6, 7]. Our aim is to develop systems that allow unobtrusively measuring motor and brain activity while individuals are engaged in computer games that require them to perform functionally meaningful tasks. Finally, we summarize the results of our work and provide an outlook on further development.

BCI technology in nerorehabilitation

Auto-calibration and self-optimizing BCIs

System calibration and user training is essential for operating BCIs that are controlled by modulation of the user's own brain rhythms [1]. Users have to learn to consistently generate EEG patterns that the machine can reliably detect. We recently introduced an adaptive BCI framework, which adapts its parameters in real-time to fit the users brain activity pattern [2]. Experiments in able-bodied individuals confirmed the validity of the proposed approach as ten (seven) out of twelve naive users achieved binary classification accuracies $\geq$70% (80%) within a 90 minutes time limit.

We are currently updating the parametrization to allow better characterization of EEG patterns in disabled individuals. Extensive offline simulations of real-time operation, using data previously recorded from five individuals with spinal cord injury (SCI) and four survivors of stroke, revealed performances $\geq$ 70% in seven out of the nine individuals after about 30 minutes of training [3]. Currently, real-time experiments are being performed in groups of individuals suffering from SCI and stroke. Experiments are still ongoing, however, first results suggest that achievable performances are comparable to those of able-bodied users.

Assessing participation during robot assisted walking

Active participation and contribution to motor rehabilitation is essential for encoding motor memory. Hence, the possibility to monitor an individual's level of participation would allow therapists to better design and tailor rehabilitation protocols to individual needs and capabilities.

With the aim of developing models that more accurately characterize the interplay between behavior (brain function) and brain structure, we started studying neural correlates of motor function [8] and the underlying mechanisms of motor control [4, 5, 9, 10]. Results of a basic study on active and passive walking with the robotic gait orthosis Lokomat (Hokoma, Switzerland) in able-bodied individuals revealed significant differences in cortical activation between active and passive movements [4].

Based on the above developed models and methods, we evaluated the feasibility to assess the level of participation

using EEG by classifying between active and passive movements during robotic assisted gait training in able-bodied individuals [5]. Off-line simulations revealed physiologically relevant patterns over central and parietal brain areas in five out of the six participants. Identified EEG patterns for active versus passive walking could be classified with an average accuracy of $68\% \pm 8\%$ by using a 10-times 10-fold cross validation statistic. These results suggest that classification of active and passive walking from the EEG is challenging but feasible.

Game-based functional brain mapping

One of our long-term goals is to study the effect of motor rehabilitation on neuroplasticity in individuals suffering from stroke and cerebral palsy. To achieve this goal, we need a practical data collection paradigm to be used during inpatient rehabilitation. Main features of the system include (i) the ability to track movements in an unobtrusive way and (ii) to allow users to perform functionally meaningful tasks in natural settings.

Recently, we proposed the use of the Kinect motion tracking sensor (Microsoft, Inc., Redmond, WA, USA) in a game-based paradigm for non-invasive EEG-based functional motor mapping [7, 6]. Results from an experimental study with able-bodied subjects playing a virtual ball-game suggest that the Kinect sensor is useful for isolating specific movements during the interaction with the game, and that the computed EEG patterns for hand and feet movements are in agreement with results described in the literature.

We are currently extending the game paradigm and (i) enhance the movement repertoire, (ii) add language based interaction with the game and (iii) add wireless EEG capabilities. This will allow users to perform behavioral tasks in a more natural setting and enable us to study brain activity and brain dynamics of functional behavior.

Summary and Discussion

This paper summarizes our efforts towards the adaptation of BCI technology for practical use in a clinical setting, and for its inclusion in neurorehabilitation. Special emphasis is put on the development of communication and monitoring applications that are easy to setup and use [2, 7], and hence are more likely to be accepted for clinical use. Additionally, we study mechanisms of motor control and EEG-correlates of motor function [8, 4, 5, 10, 9]. Gained knowledge will enable us to build better predictive models that more accurately characterize the interplay between brain activity, therapeutic intervention and functional outcome, and hence are more useful to monitor and document neuroplasticity. Future efforts will focus on the validation of developed methods in disabled individuals.

Acknowledgement

This work was partially supported by the FP7 EU Research projects ABC (287774), BRAINABLE (247447) and BETTER (247935), and the BCI4REHAB project funded by the Steiermärkische Landesregierung. This paper only reflects the authors' views and funding agencies are not liable for any use that may be made of the information contained herein.

Bibliography

[1] J. R. Wolpaw, N. Birbaumer, D. J. McFarland, G. Pfurtscheller, and T. M. Vaughan, "Brain-computer interfaces for communication and control," *Clin Neurophysiol*, vol. 113, pp. 767–791, 2002.

[2] J. Faller, C. Vidaurre, T. Solis-Escalante, C. Neuper, and R. Scherer, "Autocalibration and recurrent adaptation: Towards a plug and play online ERD-BCI," *IEEE Trans Neural Syst Rehabil Eng*, vol. 20, no. 3, pp. 313–319, 2012.

[3] J. Faller, C. Vidaurre, E. V. C. Friedrich, U. Costa, E. Opisso, J. Medina, C. Neuper, G. Müller-Putz, and R. Scherer, "Automatic adaptation to oscillatory EEG activity in spinal cord injury and stroke patients," in *Proc. of the 3rd TOBI Workshop*, pp. 12–13, 2012.

[4] J. Wagner, T. Solis-Escalante, P. Grieshofer, C. Neuper, G. Müller-Putz, and R. Scherer, "Level of participation in robotic-assisted treadmill walking modulates midline sensorimotor EEG rhythms in able-bodied subjects," *NeuroImage*, vol. 63, pp. 1203–1211, 2012.

[5] T. Solis-Escalante, J. Wagner, R. Scherer, P. Grieshofer, and G. Müller-Putz, "Assessing participation during robotic assisted gait training based on EEG: feasibility study," in *Proc. of the 3rd TOBI Workshop*, pp. 61–62, 2012.

[6] R. Scherer, J. Wagner, G. Moitzi, and G. Müller-Putz, "Kinect-based detection of self-paced hand movements: enhancing functional brain mapping paradigms," *Conf Proc IEEE Eng Med Biol Soc*, vol. 2012, pp. 4748–4751, 2012.

[7] R. Scherer, G. Moitzi, I. Daly, and G. Müller-Putz, "On the use of games for non-invasive EEG-based Functional Brain Mapping," *IEEE Trans Comput Intell AI in Games*, to be published.

[8] V. Kaiser, I. Daly, F. Pichiorri, D. Mattia, G. R. Müller-Putz, and C. Neuper, "Relationship between electrical brain responses to motor imagery and motor impairment in stroke," *Stroke*, 2012.

[9] M. Seeber, R. Scherer, J. Wagner, T. Solis-Escalante, and G. Müller-Putz, "EEG beta band sources modulated by gait cycle during robot-assisted walking," in *19th Annual Meeting of the Organization for Human Brain Mapping*, to be published.

[10] J. Wagner, T. Solis-Escalante, C. Neuper, R. Scherer, and G. Müller-Putz, "Interaction between parietal and premotor areas is disrupted during visually guided gait adaptation," in *19th Annual Meeting of the Organization for Human Brain Mapping*, to be published.

Biomed Tech 2013; 58 (Suppl. 1) © 2013 by Walter de Gruyter · Berlin · Boston. DOI 10.1515/bmt-2013-4437

BRAIN-ACTUATED ASSISTIVE MOBILITY FOR DISABLED END-USER

Leeb R, Carlson T, Tonin L and Millán JdR

Chair in Non-Invasive Brain-Machine Interface, École Polytechnique Fédérale de Lausanne, Switzerland

robert.leeb@epfl.ch

Abstract: *Brain-Computer Interfaces (BCIs) have been successfully used to control assistive mobility devices (like a telepresence robot or an electric wheelchair) using only motor imagery. Importantly, disabled end-users are able to achieve similar performances as healthy participants.*

Keywords: *Brain-Computer Interfaces, electroencephalogram, motor imagery, shared control, robot, wheelchair*

Introduction

Brain-Computer Interface (BCI) technology enables people to control machines not by manual operation, but by mere "thinking". Thereby, the electrical activity from the brain (the electroencephalogram, EEG) is analyzed in real-time and control parameters are extracted. BCIs are no longer only used by healthy subjects under standardized laboratory conditions, but are also introduced to end-users controlling applications in their homes [1]. Applications range from simple control of computers, by reestablishing communication via writing programs, to motor substitution and games. For people with motor disabilities, regaining mobility is a big issue. In this work, we want to present our latest results from two assistive mobility devices (a telepresence robot and an electric wheelchair) controlled by disabled end-users directly from a rehabilitation center.

Methods

Brain-Computer Interface and signal processing: All participants used motor imagery (e.g. of the left hand, right hand, feet) to control the BCI. Therefore, the brain activity was acquired via 16 EEG channels over the motor cortex. From the Laplacian filtered EEG, the power spectral density was calculated and classified with a Gaussian classifier (more details see [2]). The output of the BCI is visualized on a screen and used to control the application.

Application prototypes: In case of the telepresence application, the subject remotely controlled the robot, steering it to the left or to the right within an office environment [3]. If no commands were delivered, the default behavior of the robot was activated, which consisted of moving forward and avoiding obstacles with the help of a shared control system using its on-board sensors.

The second application was a powered wheelchair equipped with sonars and webcams, whose movements can be controlled similarly to the telepresence robot, except that the subject was co-located with it [4]. The subject had to drive the wheelchair to reach several targets.

Both applications were quite demanding for the subjects, since besides the increased workload and the split attention [2], a certain temporal precision was required.

Results and Discussion

Up to now, 9 end-users (aged 37.7±12.2 year) tested the telepresence application. They achieved a ratio between the time needed to reach the targets with manual control vs. BCI control of 0.87 ± 0.09 (whereby 1 would correspond to perfect and 0 to no control). These performances are similar to healthy participants [3]. In case of the wheelchair only one person tested it and achieved an amazing 0.97.

Most importantly we could demonstrate that all end-users who achieved good BCI performance could also control the applications successfully with the help of the shared control system. This is very important, because having a good BCI control does not guarantee good control over the application, due to the necessary split attention between the application and the BCI, and the temporal constraints [2].

In the future we have to add a start/stop or a pausing functionality for the movement of the robotic device. In the framework of a hybrid BCI, such commands could also be delivered through other channels such as residual muscular activity, which can be controlled reliably—but not very often, because of the quick fatigue.

Acknowledgement

This work was supported by the European ICT Programme Project TOBI FP7-224631.

Bibliography

[1] J. d. R. Millán, R. Rupp, et. al., "Combining brain-computer interfaces and assistive technologies: State-of-the-art and challenges," *Front Neurosci*, vol. 4, p. 161, 2010.

[2] R. Leeb, S. Perdikis, et. al., "Transferring brain-computer interface skills: from simple bci training to successful application control," *Artif Intell Med*, 2013, in revision.

[3] L. Tonin, T. Carlson, et. al., "Brain-controlled telepresence robot by motor-disabled people," in *Conf Proc IEEE Eng Med Biol Soc*, pp. 4227–4230, 2011.

[4] T. Carlson and J. d. R. Millán, "Brain–controlled wheelchairs: A robotic architecture," *IEEE Robot Autom Mag*, vol. 20, no. 1, pp. 65–73, 2013.

Biomed Tech 2013; 58 (Suppl. 1) © 2013 by Walter de Gruyter · Berlin · Boston. DOI 10.1515/bmt-2013-4438

Applying the user-centred design to evaluation of Brain-Computer Interface controlled applications

Kübler A[1], Zickler C[2], Holz E[1], Kaufmann T[1], Riccio A[3], Mattia D[3]

[1]Institute of Psychology, University of Würzburg, Würzburg, Germany
[2]Institute of Medical Psychology and Behavioural Neurobiology, University of Tübingen, Tübingen, Germany
[3] Neuroelectrical Imaging and BCI Lab, Fondazione Santa Lucia IRCCS, Rome, Italy

andrea.kuebler@uni-wuerzburg.de

Abstract: *In recent years different applications have been linked to BCI control and tested by severely motor impaired users in the field. An effort has been made to apply objective and standardised evaluation metrics to foster a user-centred design process in the development of BCI controlled applications. The user-centred design appears appropriate to bridge the reliability and translational gap faced by BCI research that aims at providing people in need with an optimally adapted assistive BCI driven technology.*

Keywords: *BCI, end-user, reliability, user-centred design, evaluation, workload, satisfaction, efficiency, effectiveness*

Introduction

Studies with BCI controlled applications have become numerous, yet those with targeted end-users, i.e. is patients with severe motor impairment (locked-in) are still sparse. Thus, BCI research is facing a translational gap as profound knowledge about how to transfer BCI technology from the laboratory to the field does not exist. There is also a reliability gap such that the pre-requisites for long-term stability of the brain signal of interest are sparse. To bridge these gaps, the user-centred design has been adapted and applied to evaluate BCI-controlled applications with end-users in the field [1].
The user-centered design was standardized in the ISO 9241-210 and adopts the concept of usability which is the "extent to which a … product … can be used by specified users to achieve specified goals with effectiveness, efficiency and satisfaction in a specified context of use [2].
Its principles and steps of the developmental process are listed in Table 1.

For evaluating BCI-controlled applications according to these principles, metrics were defined and applied to BCI-controlled applications tested by end-users.

Methods

Operalisation of usability in the BCI context:

- **Effectiveness**
  - Accuracy (correct selections of total selections)[1]
- **Efficiency**
  - ITR (information transfer rate) [1]
  - Workload (NASA questionnaire) [2]
- **Satisfaction**
  - Extended QUEST (adapted for BCI) [2]
  - VAS satisfaction, joy, frustration (visual analogue scale, quick assessment) [1]
  - ATD PA (Assistive Technology Device Predisposition Assessment) – expected technology benefit[2]
  - Open interview[2]

[1]Metrics assessed in each session
[2]Metrics assessed at the end of the evaluation period

Table 1: Principles of the user-centred design and iterative steps needed for implementation

The Principles
➢ understand the user, the task and environmental requirements
➢ encourage early and active involvement of users
➢ be driven and refined by user-centered evaluation
➢ include iteration of design solutions
➢ address the whole user experience
➢ encourage multi-disciplinary design
The Steps
➢ understand and specify the context of use; 2, specify the user requirements
➢ specify the user requirements
➢ produce design solutions to meet user requirements; and
➢ evaluate the designs against requirements

Four applications were brought to end-users (N=17) diagnosed with diseases affecting the motor system including locked-in patients. Table 2 summarizes the applications.

Table 2: Summary of applications

Application	**Input signal for BCI**	**Domain**	**Number of patients involved**
Spelling with commercial AT software (Qualilife) [1]	P300	communication	4
Brain Painting [3,4]	P300	entertainment	5
Spelling with AT software – hybrid [5]	P300 + EMG[3]	communication	4
Connect 4 [6]	SMR[4]	entertainment	4

[3]electromyogram; [4] sensorimotor rhythms

End-users were involved in 4 to 8 sessions in their home environment. In the Brain Painting applied independently at home 140 sessions were conducted [4].

Results

Table 3 summarizes the results for effectiveness, efficiency, and satisfaction for the three prototypes.

Table 3: Summary of evaluation results.

Application	Effectiveness	Efficiency ITR	Efficiency NASA	Satisfaction VAS	Satisfaction QUEST	Satisfaction ATD PA	Use in daily life
Spelling	70-100%	4.0-8.6	9-49	4.2-9.0	2.8-4.8	-	☹
Brain Painting	80-100%	4.0-6.7	5-49	5.0-7.9	3.3-4.9	3.4-4.3	😐
Spelling hybrid	68-100%	Mean 3.9	-	-	-	-	☹
Connect 4	40-80%	0.05-1.44	17-72	6.0-10.0	2.8-4.4	2.3-4.3	☺
Brain Painting at home	-	-	-	0-10	-	5	☺

NASA scale is 0-100; QUEST scale is 1-5; VAS is from 0-10; ATD PA scale 1-5 with 4-5 meaning good match, 3-3.9 need for improvement, < 3 risk of non-use.

In the open interview the users stated several caveats of the BCI that prevent independent home use. These were (1) time consuming set-up of hardware and software, (2) need for washing hair after use due to gel for electrode cap, (3) uncomfortable cap, (4) restricted mobility when using the BCI, (5) eye-catching look of the cap, and (6) low speed. In contrast, reliability and learnability of the BCI was rated high.

Discussion

Effectiveness was high for P300 and low for SMR controlled applicatons. Efficiency as measured with ITR and the NASA was moderate. Satisfaction was overall moderate but high for independent home use. Use in daily life seems possible even with moderate effectiveness. It is important to note that satisfaction can be high even when performance is moderate provided that the BCI application is not aiming at basic needs for interaction, i.e. communication.

To conclude, the user-centred approach has been successfully implemented in evaluation of BCI-controlled application. It can be used in an iterative manner to provide information about steps that need to be taken to bring BCIs to end-users home and enable independent home use, i.e. to bridge the translational gap. To bridge the reliability gap long-term studies need to be conducted with end-user in their home environment.

Acknowledgement

This work is supported by the European ICT Program Project FP7-224631 (TOBI) and FP7- 288566 (Backhome). This manuscript only reflects the authors' views and funding agencies are not liable for any use that may be made of the information contained herein.

Bibliography

[1] Zickler C, Riccio A, et al.: A brain-computer interface as input channel for a standard assistive technology software, *Clin EEG Neurosci*. 42(4):236-44, Oct 2011.

[2] ISO 9241-210: Ergonomics of human-system interaction - Part 210: Human-centred design for interactive systems (ISO, Genf, 2010).

[3] Zickler C, Halder S, et al.: Brain Painting: usability testing according to the user-centered design in end users with severe motor paralysis, *Artific Intell Med*, in revision.

[4] Holz EM, Botrel L, & A. Kübler: Bridging Gaps: Long-term independent BCI home-use by a locked-in end-user, Proc TOBI Workshop IV (Sion, Switzerland, 2013).

[5] Holz EM, Riccio A, et al.: Hybrid-P300 BCI: Usability testing by severely motor-restricted end-users, Proc TOBI Workshop IV (Sion, Switzerland, 2013).

[6] Holz EM, Höhne J, et al.: BCI-Controlled Gaming: Evaluation of Usability by Severely Motor Restricted End-Users, *Artific Intell Med*, in revision.

Biomed Tech 2013; 58 (Suppl. 1) © 2013 by Walter de Gruyter · Berlin · Boston. DOI 10.1515/bmt-2013-4439

ZERO TRAINING FOR BCI – REALITY FOR BCI SYSTEMS BASED ON EVENT-RELATED POTENTIALS

Michael Tangermann[1], Pieter-Jan Kindermans[3], Martijn Schreuder[2], Benjamin Schrauwen[3], Klaus-Robert Müller[2]

[1]Excellence Cluster BrainLinks-BrainTools, University of Freiburg, Germany
[2]Dept. Machine Learning, BBCI Group, Technical University Berlin, Germany
[3]Electronics and Information Systems Department, Ghent University, Belgium

mt@we-are.de

Abstract: *This contribution reviews how usability in Brain-Computer Interfaces (BCI) can be enhanced. As an example, an unsupervised signal processing approach is presented, which tackles usability by an algorithmic improvement from the field of machine learning. The approach completely omits the necessity of a calibration recording for BCIs based on event-related potential (ERP) paradigms. The positive effect is twofold - first, the experimental time is shortened and the productive online use of the BCI system starts as early as possible. Second, the unsupervised session avoids the usual paradigmatic break between calibration phase and online phase, which is known to introduce data-analytic problems related to non-stationarity.*

Keywords: *Brain-Computer Interface, Machine Learning, Unsupervised Classification, Event-Related Potentials, Spatial Auditory Attention, Usability*

Introduction

Usability challenges in Brain-Computer Interfaces so far have impeded their application in every-day scenarios. Recently, this problem has been recognized and addressed by a number of research projects, which have taken the field closer to a true usability for patients. Among them hybrid BCI paradigms [1, 2], simplified user interfaces [3], dry electrode systems [4, 5], reduced electrode sets [6, 7], transfer learning approaches [8, 9], shared control principles [10], improvements in BCI paradigms [11, 12] and stimulus modalities [13, 14, 15] need to be recognized.

Methods

Now, another brick has been placed to form this important fundament - a completely unsupervised signal processing approach [16]. Discarding calibration recordings completely – even for novel subjects – this method allows for a kick-start usage of BCI systems, which are based on event-related potentials (ERP) like the P300.

Making use of an established six-class auditory spelling paradigm [12], examples of the online experience with this Bayesian unsupervised approach are presented, and a comparison to the traditional approach involving supervised LDA classification and explicit calibration recordings is made.

Results

The positive effect of the unsupervised classification approach for ERPs is twofold. First, the overall experimental time is shortened by the unsupervised approach, as the productive online use of the BCI system starts as early, as enough evidence has been collected from the data. Second, the unsupervised session is monolithic in the sense, that it does not undergo any paradigmatic change and the feedback mode remains the same throughout the session. This strategy avoids the usual paradigmatic break between calibration phase and online phase, which is known to introduce data-analytic problems related to the increasing non-stationarity of the data.

Acknowledgement

The authors are thankfor for funding by the BOF-GOA Project Home-MATE (Ghent University Special Research Fund), by the Bernstein Focus Neurotechnology (01GQ0850) and by the DFG (MU987/14-1).

Bibliography

[1] J. d. R. Millán, R. Rupp, G. Müller-Putz, R. Murray-Smith, C. Giugliemma, M. Tangermann, C. Vidaurre, F. Cincotti, A. Kübler, R. Leeb, *et al.*, "Combining brain–computer interfaces and assistive technologies: state-of-the-art and challenges," *Frontiers in neuroscience*, vol. 4, 2010.

[2] G. R. Müller-Putz, C. Breitwieser, F. Cincotti, R. Leeb, M. Schreuder, F. Leotta, M. Tavella, L. Bianchi, A. Kreilinger, A. Ramsay, *et al.*, "Tools for brain-computer interaction: a general concept for a hybrid BCI," *Frontiers in neuroinformatics*, vol. 5, 2011.

[3] T. Kaufmann, S. Völker, L. Gunesch, and A. Kübler, "Spelling is just a click away–a user-centered brain–computer interface including auto-calibration and predictive text entry," *Frontiers in Neuroscience*, vol. 6, 2012.

[4] F. Popescu, S. Fazli, Y. Badower, B. Blankertz, and K.-R. Müller, "Single trial classification of motor

imagination using 6 dry EEG electrodes," *PloS one*, vol. 2, no. 7, p. e637, 2007.

[5] T. O. Zander, M. Lehne, K. Ihme, S. Jatzev, J. Correia, C. Kothe, B. Picht, and F. Nijboer, "A dry EEG-system for scientific research and brain–computer interfaces," *Frontiers in neuroscience*, vol. 5, 2011.

[6] C. Sannelli, C. Vidaurre, K.-R. Müller, and B. Blankertz, "CSP patches: an ensemble of optimized spatial filters. an evaluation study," *Journal of Neural Engineering*, vol. 8, no. 2, p. 025012, 2011.

[7] T. N. Lal, M. Schröder, T. Hinterberger, J. Weston, M. Bogdan, N. Birbaumer, and B. Schölkopf, "Support vector channel selection in BCI," *Biomedical Engineering, IEEE Transactions on*, vol. 51, no. 6, pp. 1003–1010, 2004.

[8] M. Krauledat, M. Tangermann, B. Blankertz, and K.-R. Müller, "Towards zero training for brain-computer interfacing," *PLoS One*, vol. 3, no. 8, p. e2967, 2008.

[9] S. Fazli, C. Grozea, M. Danoczy, B. Blankertz, F. Popescu, and K.-R. Müller, "Subject independent EEG-based BCI decoding," *Advances in Neural Information Processing Systems*, vol. 22, pp. 513–521, 2009.

[10] F. Galán, M. Nuttin, E. Lew, P. W. Ferrez, G. Vanacker, J. Philips, and J. d. R. Millán, "A brain-actuated wheelchair: asynchronous and non-invasive brain–computer interfaces for continuous control of robots," *Clinical Neurophysiology*, vol. 119, no. 9, pp. 2159–2169, 2008.

[11] V. V. Nikulin, F. U. Hohlefeld, A. M. Jacobs, and G. Curio, "Quasi-movements: A novel motor–cognitive phenomenon," *Neuropsychologia*, vol. 46, no. 2, pp. 727–742, 2008.

[12] M. Schreuder, T. Rost, and M. Tangermann, "Listen, you are writing! speeding up online spelling with a dynamic auditory BCI," *Frontiers in Neuroscience*, vol. 5, 2011.

[13] S. Schaeff, M. S. Treder, B. Venthur, and B. Blankertz, "Exploring motion VEPs for gaze-independent communication," *Journal of Neural Engineering*, vol. 9, no. 4, p. 045006, 2012.

[14] M. Tangermann, M. Schreuder, S. Dähne, J. Höhne, S. Regler, A. Ramsay, M. Quek, J. Williamson, and R. Murray-Smith, "Optimized stimulation events for a visual ERP BCI," *Int J Bioelectromagnetism Volume*, vol. 13, no. 3, pp. 119–120, 2011.

[15] J. Höhne, K. Krenzlin, S. Dähne, and M. Tangermann, "Natural stimuli improve auditory BCIs with respect to ergonomics and performance," *Journal of Neural Engineering*, vol. 9, no. 4, p. 045003, 2012.

[16] P.-J. Kindermans, D. Verstraeten, and B. Schrauwen, "A bayesian model for exploiting application constraints to enable unsupervised training of a P300-based BCI," *PloS one*, vol. 7, no. 4, p. e33758, 2012.

Biomed Tech 2013; 58 (Suppl. 1) © 2013 by Walter de Gruyter · Berlin · Boston. DOI 10.1515/bmt-2013-4440

THINK2GRASP - BCI-CONTROLLED NEUROPROSTHESIS FOR THE UPPER EXTREMITY

Rupp R[1], Rohm M[1], Schneiders M[1], Weidner N[1], Kaiser V[2], Kreilinger A[2], Müller-Putz GR[2]
[1] Heidelberg University Hospital, Spinal Cord Injury Center, Heidelberg, Germany
[2] Institute for Knowledge Discovery, Graz University of Technology, Graz, Austria
Ruediger.Rupp@med.uni-heidelberg.de

Abstract: *By application of grasp neuroprostheses a restricted hand function can be successfully improved. The introduction of hybrid neuroprostheses based on Functional Electrical Stimulation (FES) and orthosis holds promise to compensate for a substantial loss of upper extremity function in individuals with high spinal cord injury (SCI). Novel user interfaces are necessary to make use of their additional degrees of freedom. In the European Project TOBI (Tools for Brain-Computer Interfaces) a motor imagery (MI) based, hybrid BCI (hBCI) for control of an upper extremity hybrid neuroprosthesis was evaluated following a user-centered design. This technology allowed several end users with SCI to successfully perform activities of daily living and may therefore serve as a valuable assistive device for functional rehabilitation of severely motor impaired individuals.*
Keywords: *Electroencephalogram (EEG), spinal cord injury, Brain-Computer Interface (BCI), upper extremity neuroprosthesis, evaluation, assistive technology*

Introduction

A spinal cord injury (SCI) leads to different degrees of impairment depending on the segmental level of lesion. The main needs of highly paralyzed individuals with restricted upper extremity function are manipulation and communication [1]. However, in this patient group only a few residual motor functions are preserved that can be used for control of assistive devices. For this purpose non invasive Brain-Computer Interfaces (BCI) exploiting the subject's electroencephalogram (EEG) are currently introduced outside lab conditions to offer an additional channel for control. One work package of the European Integrated Project TOBI (Tools for Brain-Computer Interaction) aims at the restoration of a weak or missing elbow and hand function in individuals with high spinal cord injury by means of a motor imagery (MI) Brain-Computer Interface (BCI) controlled upper extremity neuroprosthesis. This manuscript is intended to give an overview of one of the end user studies conducted in the framework of TOBI, which specific goal is to evaluate the efficiency, effectiveness of and satisfaction with a MI-BCI-controlled upper extremity hybrid neuroprosthesis.

Methods

For this purpose a neuroprosthesis based on a combination of non invasive Functional Electrical Stimulation (FES) of innervated upper arm and forearm muscles and orthotic components mainly consisting of an electrically de-/lockable elbow joint has been developed [2]. Several submodules for individualization including an electrode fixation sleeve, a wrist orthosis for elbow-coupled ulnar deviation or rotation, a weight support system for the elbow and even a small electrical drive that flexes the elbow of the end user's arm reliably were provided (Fig. 1). The latter is intended to be used in end users, in whom the M. biceps/triceps do not generate enough force with the use of FES.

Figure 1: End user of the modular upper extremity neuroprosthesis during a BCI classifier setup session

The brain-controlled neuroprosthesis was evaluated in four end users with SCI who gave informed consent for study participation. The end user satisfaction was assessed by the TUEBS, which is a questionnaire developed on the basis of the QUEST 2.0 [3] and aims at assessing the satisfaction with the special features of BCI applications. Participants are asked to rate their satisfaction on a 5-point Likert scale and to indicate the reasons for their satisfaction or dissatisfaction. Furthermore, the ATD-PA [4] and a Visual Analog Scale (VAS) were used to assess the user satisfaction and the NASA-TLX [5] to measure the subjective workload.

Results

In a first step a subcomponent of the BCI-controlled neuroprosthesis, namely the hybrid-FES orthosis, was evaluated. The results obtained from one individual with SCI show that the non-invasively generated grasp patterns are comparable to those of the most sophisticated grasp neuroprosthesis - the implanted Freehand system - in terms of functionality and strength [6]. By introduction of the electrode fixation forearm sleeve a reproducible generation of the grasp patterns was achieved. Two of the participating end-users with missing elbow and hand func-

tion used the MI-BCI to switch the analog signal of a shoulder position sensor to either the control the FES of the elbow or the hand. Two SCI end users with preserved elbow flexion used shoulder movements for control of an FES generated opening/closing the hand and the MI-BCI for switching between a lateral and palmar grasp pattern. All four end users successfully performed activities of daily living with the neuroprosthesis, which they could not do without it. All four end users were quite satisfied with the device (TUEBS mean score 3.75/5). The most important properties were "dimensions", "effectiveness" and "reliability". After the testing sessions the overall satisfaction of all end users assessed by a Visual Analogue Scale was quite high (mean 6.8/10). Furthermore, the overall mean workload in all end users measured by the NASA-TLX was only moderate (mean of 46/100). "Mental demand", "physical demand" and "effort" contributed most to workload. The usability rating measured by the ATD-PA is remarkably lower (2.8/5). Nevertheless, users stated that they could imagine integrating it in their daily life.

During the recruitment phase ˜50% of the screened patients were not eligible for study inclusion. The main reasons for this were joint contractures in the finger and hand, a high degree of severely denervated muscles not accessible to FES.

Discussion

Initially, end users with very high SCI were in the project's focus, in whom not many residual functions for setup of a neuroprosthesis' user interface are available. Throughout the evaluation sessions of the first prototypes, in which a user centered design approach was consequently applied, we realized that not the end user has to fit to the technology we are able to offer, but that our technology has to be adapted to the capabilities, needs and priorities of each individual end user. Consequently the neuroprosthesis was redesigned in a highly modular manner and its functionality has been extended to allow for inclusion of a larger population of end user.

Based on the high number of screening failures we estimate that only 10-15% of the total tetraplegic SCI end users may be able to use and profit from an upper extremity neuroprosthesis. But even those end users that basically fulfilled all inclusion criteria were not all (dropout rate 25%) successful in finishing the evaluation study, because not all managed to regularly perform the FES training in their home environment or at their nursing home. More important, about 30% of the potential end users did not have an initial level of BCI performance sufficient for a reliable control of the neuroprosthesis. Additionally, in some of the end users no improvement of the performance occurred even after a long period of training. Based on the screening results it may be concluded that the BCI performance of high spinal cord injured end users is lower compared to non motor impaired subjects. Of course, this preliminary result needs to be confirmed in studies involving more end users. In any case a better understanding of the lesion induced changes on event related de-/synchronization (ERD/ERS) of brain waves by MI is necessary.

With the extensive implementation of intelligent shared control mechanisms uncertainties and non-stationarities, which are inherent to non-invasive MI-BCIs, may be partly tackled. Nevertheless, we would not consider a MI-BCI as an add-on to established control interfaces, if the initial BCI performance is below 70% and not stable over sessions.

In general, the setup and handling of current BCI systems is relatively complicated and needs the (tele-)presence of technical experts. Thus, BCIs have to be improved to a stage, in which end users together with their care givers are able to apply the systems independently at home. First steps into this direction have been undertaken in the European TOBI project (www.tobi-project.org), however there is still room for improvement.

When talking of a MI-BCI, one has to be aware that at the current stage of technology this is far away from any intuitive control, because the imageries of movements are used that cause the highest ERD/ERS effects. This might even be feet movements, which is then used for control of an upper extremity neuroprosthesis. Hence, a real breakthrough in neuroprosthesis control would be the decoding of body movements from EEG. First attempts into this direction have been started recently, which might pave the way for non-invasive BCI systems with a more natural control scheme [7]. For this a deeper understanding of the underlying brain physiology has to be attained.

Acknowledgement

This research is supported by the European Project "Tools for Brain-Computer Interaction – TOBI" (FP7-224631).

Bibliography

[1] Zickler, C., Riccio, A. et al.: A brain-computer interface as input channel for a standard assistive technology software. *Clin EEG Neurosci.*, vol. 42(4), pp. 236-244, 2011

[2] Rohm, M., Müller-Putz. GR. et al.: Modular FES-hybrid orthosis for individualized setup of BCI controlled motor substitution and recovery, *Int J Bioelectromagnetism*, vol. 13, pp. 127-128, 2011

[3] Demers, L., Monette, M. et al.: Reliability, validity, and applicability of the Quebec User Evaluation of Satisfaction with assistive Technology (QUEST 2.0) for adults with multiple sclerosis, *Disabil Rehabil*, vol. 24, pp. 21-30, 2002

[4] Scherer, MJ., Cushman, LA.: Determining the content for an interactive training programme and interpretive guidelines for the Assistive Technology Device Predisposition Assessment, *Disabil Rehabil*, vol. 24, pp. 126-130, 2002

[5] S. Hart and L. Staveland. "Development of NASA-TLX (Task Load Index): Results of empirical and theoretical research" in *Human Mental Workload*, (P.A. Hancock and N. Meshkati, eds.) pp. 139–183. Amsterdam: North Holland Press, 1988

[6] Rupp, R., Kreilinger A. et al.: Development of a non-invasive, multifunctional grasp neuroprosthesis and its evaluation in an individual with a high spinal cord injury, *Conf Proc IEEE Eng Med Biol Soc*, pp. 1835–38, 2012

[7] Ofner, P., Müller-Putz, G.R.: Decoding of velocities and positions of 3D arm movement from EEG, *Conf Proc IEEE Eng Med Biol Soc*, pp. 6406-6409, 2012

Biomed Tech 2013; 58 (Suppl. 1) © 2013 by Walter de Gruyter · Berlin · Boston. DOI 10.1515/bmt-2013-4441

A tactile P300-based BCI for communication and detection of awareness

Ortner R.[1], Prückl R.[1], Guger C[1]

[1]g.tec Guger Technologies OG, Graz, Austria
ortner@gtec.at

Abstract: *In this publication a tactile P300-based Brain-Computer Interface (BCI) is presented. It can be used for communication, but is also aimed for testing the consciousness in nonresponsive patients. Three different settings were evaluated: two stimulators for testing if a P300 could be detected; three stimulators that could be used for simple communication, and a setup with eight stimulators that provides more classes and is hence suitable for advanced communication. The BCI was evaluated on 12 healthy users showing a mean accuracy of 100% for classification in the two stimulator approach, 80% in the three stimulator approach and 69.4% in the eight stimulator approach.*

Keywords: *EEG, P300, vibrotactile stimulation, minimal conscious state, persistent vegetative state.*

Introduction

Brain-Computer Interfaces (BCIs) for communication are usually controlled via a P300 paradigm. During the last 25 years, several P300 spellers based on visual stimulation have been developed. But for users suffering visual impairments or even in a minimally conscious state, visual stimulation cannot be used any more. For these groups of users, a tactile stimulation can be used to elicit the event related potential (ERP). Hence, one can use this way of stimulation for communication and also for assessment of the level of consciousness in patients classified as non-responsive. Kotchoubey et al. tested ERPs to stimuli of different complexity levels in patients with persistent vegetative state (PVS) and minimal conscious state [1]. They found a P300 also in PVS patients although it was associated more frequent to patients with lower level of disability.

Therefore, testing only for the existence of a P300 response is not sufficient to decide about the consciousness of the patient, but it is the first step that could lead to further tests with the proposed BCI.

Next, one should present certain commands to the patient, like selecting a specific sequence of symbols. If the user is able to follow the sequence, the patient could be classified as responsive.

For a visual P300 speller, it was shown that healthy users reach an average control accuracy of 91% [2] and a group of fifteen people suffering motor impairments reached 70.1% [3]. In this paper, we evaluate the control accuracy of a tactile P300 speller on twelve healthy users.

Methods

Three different scenarios were tested. In the first paradigm, two vibrotactile stimulators (g.VIBROstim, g.tec medical engineering, Austria, see Fig. 1) were placed on the user's wrists. One stimulator delivered a train of standard stimuli (one stimulus was a short vibration of the stimulator). The stimulator on the other wrist produced the deviant stimulus with a probability of 12.5%. If the user was asked to concentrate on the deviant stimulus, one could evaluate if this person has a P300 response. The second paradigm used three stimulators. Again, one of the stimulators (placed on the user's back) delivered a train of standard stimuli. The deviant stimuli were now delivered on the left and right wrist, one of which conveyed "yes" the other of which conveyed "no". The user had to concentrate on the stimuli given on one of the two wrists to select the answer. This setup could be used for communication if only a simple yes/no response is desired. In the third paradigm, eight stimulators were used instead of three. They were placed on the fingers (little finger, ring finger, middle finger, index finger) of the left and right hand. Each stimulator flashed with the same probability (12.5%). During one run, the user had to concentrate on each finger in a random order, the commands on which stimulator the user should concentrate actually were give via voice.

In each session of the three paradigms, two runs were performed: one to set up a classifier and a second run to test the classifier. Each run of the two-stimulator and three-stimulator paradigm consisted of 5 sequences, with 15 target events per sequence. The runs of the eight stimulator experiment consisted of eight sequences, again with 15 target events per sequence. For each session the accuracy was calculated.

Figure 1: Eight g.VIBROstim stimulators plugged into the g.STIMbox that drives them

Table 1: Accuracy (%) of the single users.

User	*two-stimulators*	*three-stimulators*	*eight-stimulators*
1	100	100	50
2	100	100	-
3	100	100	100
4	100	60	-
5	100	40	100
6	100	60	75
7	100	100	62.5
8	100	60	25
9	100	80	100
10	100	100	-
11	-	-	100
12	-	-	12.5
mean	100	80.0	69.4
STD	0	23.1	34.3

Results

Table 1 summarizes the results of the twelve persons. The mean accuracy was at 100% for the two stimulators, 80% in the three stimulator approach and 69.4% in the eight stimulator experiment. Not all persons had enough time to process all of the three approaches, hence some field in the table are empty. When looking at the mean accuracy of the people participating to all three approaches (S1, S3, S5, S6, S7, S8, S9) the mean accuracy was: 100%, 77.1% and 73.2%.

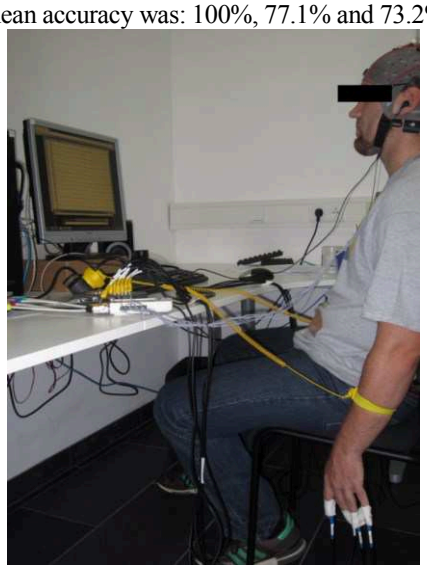

Figure 2: One user during the eight stimulator experiment

Discussion

Patients with visual impairments or unknown levels of consciousness need new ways to present the stimuli that will elicit the P300 response, since visual P300 BCIs are not practical for such users. The presented tool could be used for both: for communication and for detection of consciousness in nonresponsive persons. The accuracy in the three stimulator experiment was higher than in the eight stimulator experiment, but with the higher number of classes the information transfer rate would be higher in the eight stimulator experiment.

Details such as the exact duration of the stimuli or the best location of the stimulator are points for further investigation. Also, the methods used in this study, and the potential applications and users, will be expanded. Promising tests on people suffering Locked in Syndrome were already performed and are planned to be published soon [4].

Acknowledgement

This work was funded by the EC projects Decoder and Brainable.

Bibliography

[1] Kotchoubey, B., Lang, S. et al.: Information processing in severe disorders of consciousness: Vegetative state and minimally conscious state, *Clin. Neurophysiol*, vol. 116(10), pp. 2441-2453 2005.

[2] Guger, C., Daban, S. et al.: How many people are able to control a P300-based brain-computer interface (BCI)?, *Neurosci. Lett.*, vol. 462, pp. 94-98, 2009.

[3] Ortner, R., Aloise, F., et al.: Accuracy of a P300 Speller for People with Motor Impairments: a Comparison, *Clin. EEG Neurosci.*, , vol. 42(4), pp. 214-218, 2011

[4] Lugo Z. Rodriguez, J., et al.: A vibrotactile P300-based BCI for consciousness detection and communication, *Clin. EEG and Neuroscience*, submitted.

Biomed Tech 2013; 58 (Suppl. 1) © 2013 by Walter de Gruyter · Berlin · Boston. DOI 10.1515/bmt-2013-4442

Auditorily elicited neural oscillations associated with motor execution, motor imagery and non-motor mental tasks

Horki P[1], Klobassa DS[1], Pokorny C[1], and Müller-Putz GR[1]

[1]Institute for Knowledge Discovery, Graz University of Technology, Graz, Austria
petar.horki@tugraz.at

Abstract: In this work we investigated whether brisk feet dorsiflexion execution/imagery and a cognitive task related to working memory and perception of human voice elicited statistically significant event-related desynchronization/synchronization (ERDS) patterns in an auditory scanning paradigm. Following the auditory presentation of the target letter, seven out of ten participants displayed a central beta re-bound after brisk feet motor execution, whereas five out of ten participants also displayed similar, albeit weaker, ERDS patterns after imagination of the same movement. Six out of ten participants displayed frontal theta ERS in the non-motor cognitive task.
Keywords: EEG, brain-computer interface (BCI), motor execution, motor imagery, working memory, auditory scanning.

Introduction

Auditory electroencephalogram (EEG)-based brain-computer interfaces (BCI) for spelling applications have mainly been pursued by means of event-related potentials [1, 2]. However, spelling has also been successfully demonstrated by means of an event-related desynchronization/synchronization (ERDS) based BCI in the visual modality [3]. Furthermore, it was shown that ERDS can be used for communication both in visual [4] and binary choice auditory scanning mode [5]. Surprisingly, no attempts have been made towards ERDS based BCI spelling in auditory modality.

As a first step towards ERDS based BCI spelling in auditory modality, we investigated whether motor execution/imagery or a non-motor cognitive task could be detected in a multi-choice auditory scanning paradigm. To that end, we evaluated whether execution/imagery of brisk feet dorsiflexion [6, 7] and a cognitive task related to working memory [8, 9], and perception of human voice [10] elicited statistically significant ERDS patterns.

Our aim was to evaluate, if a multi-choice auditory scanning paradigm will lead to similar findings as previously described visually cued paradigms – i.e. if motor execution (ME) and motor imagery (MI) will lead to central ERS in the beta band (15-40 Hz), and that the cognitive task will lead to frontal ERS in the gamma band (4-7 Hz).

Methods

Ten healthy people (5 male, 5 female, college aged) participated in this experiment. Participants gave informed consent prior to the beginning of the experiments and received monetary compensation afterwards.

The EEG was recorded with 29 active electrodes overlying the frontal, central, and parietal scalp areas. The electrooculogram (EOG) was recorded with three active electrodes, and the electromyogram (EMG) with four electrodes from both legs. The EEG amplifiers were set up with a bandpass filter between 0.5 and 100 Hz, and a notch filter at 50 Hz. The EEG and EOG were sampled at 512 Hz, the EMG at 2000 Hz.

Spoken letters of the English alphabet, generated by a text-to-speech program, were presented sequentially (stimulus onset asynchrony 550 ms including 50 ms pause; 14.3 s for the whole alphabet) through a right headphone for one of several predefined words: “brain”, ”power”, “husky” and “magic”. Presenting acoustic cues through one ear only, keeps the other ear free for incoming communication from surroundings. For each target letter, the alphabet was presented two to four times.

The participants performed one of the following three tasks in the copy spelling mode: (1) brisk feet motor execution/imagery triggered by the target letter (ME/MI); (2) discrimination of the target voice’s gender and comparison to the following repetition (i.e. whether the target voice’s gender has changed or it remained the same, reporting through single/double button press) as a cognitive task (COG); and (3) mental repetition of the target letter as a control condition.

We balanced the order of motor and cognitive tasks, and voice of presentation. We randomized the order of words, and pseudorandomized the cognitive task and the control condition. Participants received no feedback.

Data analysis: We analyzed the central beta rebound in the ME/MI task and frontal theta band oscillations in the cognitive task.

To analyze the percentage of power decrease (ERD) or power increase (ERS) relative to a reference interval (0.5 s preceding the stimulus onset), a time-frequency map for frequency bands between 4 and 40 Hz (35 overlapping bands using a band width of 2 Hz) was calculated. Logarithmic band power features, calculated by band-pass filtering, squaring and subsequently averaging over the trials, were used to assess changes in the frequency domain. To determine the statistical significance of the ERD/ERS values a t-percentile bootstrap algorithm with a significance level of α=0.01 was applied.

Table 1: Results of ERDS analysis for all participants. The ERDS analysis for ME and MI task was conducted on a single orthogonal Laplacian derivation centered at Cz electrode position, whereas analysis for COG task was conducted on a single bipolar derivation AFz-Fz. Shown here are only significant(p=0.01) results.

Subj	S1	S2	S3	S4	S5	S6	S7	S8	S9	S10
***central β* ERS$_{ME}$**	-	+	+	-	+	+	-	+	+	+
***central β*-ERS$_{MI}$**	-	+	+	-	+	+	-	-	-	+
***frontal ϑ*-ERS$_{COG}$**	+	-	+	-	+	+	+	-	-	+

Results

Seven out of ten participants displayed central beta rebound following brisk feet motor execution, whereas five out of ten participants also displayed similar, albeit weaker, ERDS patterns following imagination of the same movement (see Table 1). Six out of ten participants displayed frontal theta ERS in the cognitive task. Fig. 2 and Fig. 3 show examples of central beta ERS following brisk feet motor execution and of frontal theta ERS following the non-motor cognitive task, in one participant.

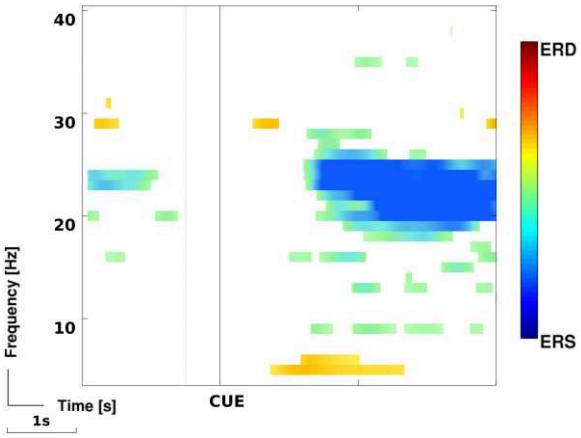

Figure 2: Central beta ERS following brisk feet motor execution in one participant.

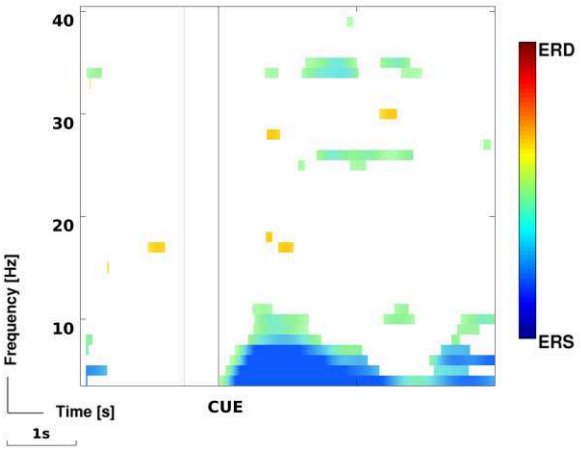

Figure 3: Frontal theta ERS following the COG task in one participant.

Discussion

The initial results indicate that task related ERDS changes in EEG could be exploited for auditory spelling. In future work we will investigate whether both ERDS and event-related potentials as combination can be used to determine which letter the participant was focusing on.

Acknowledgement

This research was supported by the European ICT Programme Project FP7-247919 (DECODER). This paper only reflects the authors' views and funding agencies are not liable. The authors would like to thank C. Breitwieser and M. Billinger for advice and assistance in the development of aspects of the BCI systems used in this work.

Bibliography

[1] Schreuder, M., Rost, T. et. al. Listen, You are Writing! Speeding up Online Spelling with a Dynamic Auditory BCI. Front. Neurosci., vol. 5, 2011

[2] Höhne, J., Schreuder, M. et. al. A novel 9-class auditory ERP paradigm driving a predictive text entry system. Front. Neurosci., vol. 5, 2011

[3] Scherer, R., Müller, G.R. et. al.: An asynchronously controlled EEG-based virtual keyboard: improvement of the spelling rate, IEEE Trans. Biomed. Eng., vol. 51, pp. 979-984, 2003

[4] Friedrich, E.V., McFarland, D.J. et. al. A scanning protocol for a sensorimotor rhythm-based brain-computer interface Biol. Psychol. vol.80, pp. 169-175, 2009.

[5] Müller-Putz, G.R., Pokorny, C. et. al. A single-switch BCI based on passive and imagined movements: towards restoring communication in minimally conscious patients Int. J. Neural Syst., vol. 23, 2013

[6] Pfurtscheller, G., Solis-Escalante, T.: Could the beta rebound in the EEG be suitable to realize a "brain switch"? Clin. Neurophysiol., vol. 120, pp. 24-29, 2009

[7] Müller-Putz, G.R., Kaiser, V. et. al.: Fast set-up asynchronous brain-switch based on detection of foot motor imagery in 1-channel EEG Med. Biol Eng. Comp., vol. 48, pp. 229-233, 2010

[8] Ruchkin, D.S., Johnson, R.et. al. Distinctions and similarities among working memory processes: an ERP study Cog. Brain Res., vol. 1, pp. 53-66, 1992.

[9] Klimesch, W., Doppelmayr, M. et. al. Theta synchronization during episodic retrieval: neural correlates of conscious awareness Cog. Brain Res., vol. 12, 2001

[10] Xu, H., Zhang, D. et al. Employing an active mental task to enhance the performance of auditory attention-based brain-computer interfaces Clin. Neurophysiol., vol. 124, pp. 83-90, 2013

Biomed Tech 2013; 58 (Suppl. 1) © 2013 by Walter de Gruyter · Berlin · Boston. DOI 10.1515/bmt-2013-4443

BCI AND FES TRAINING OF A SPINAL CORD INJURED END-USER TO CONTROL A NEUROPROSTHESIS

Kreilinger A [1], Kaiser V [1], Rohm M [2], Rupp R [2] and Müller-Putz GR[1]

[1]Institute for Knowledge Discovery, Graz University of Technology, Austria
[2]University Hospital, Spinal Cord Injury Center, Heidelberg, Germany

alex.kreilinger@tugraz.at

Abstract: *This article exemplarily summarizes the steps necessary for application of a brain controlled neuroprosthesis in one spinal cord injured end-user. After screening an extensive training has to be performed until the final use of a neuroprosthesis based on functional electrical stimulation (FES) and controlled by a motor imagery (MI) brain-computer interface (BCI) is possible. The end-user maintained a very high BCI performance over a period of more than one year and successfully managed to control synchronous and asynchronous BCI applications.*

Keywords: *EEG, BCI, FES, neuroprosthesis*

Introduction

A spinal cord injury (SCI) above the neurological level of C5 leads to a loss of motor and sensory functions in the lower and upper extremities. Tetraplegic patients are normally wheelchair bound and no longer able to perform grasping or even elbow or shoulder movements. To compensate this motor impairment, end-users can be provided with neuroprostheses based on functional electrical stimulation (FES). These neuroprostheses induce contractions of innervated muscles by applying short current pulses via surface electrodes placed near dedicated motor points. The FES-generated movement patterns can be modulated by any kind of control signal originating from unaffected parts of the body. This signal can be obtained e.g. from a shoulder position sensor but also from a brain-computer interface (BCI) which translates thoughts—e.g., motor imagery (MI)—into commands by evaluating brain activity directly at its origin [1]. Control signals from different sources can be merged in a hybrid BCI [2]. Here, we introduce two control techniques tested in one end-user with SCI. First, a combination of a shoulder position sensor for analog control of the grasp and a BCI for switching between grasp patterns. Second, a neuroprosthesis for restoration of hand and elbow movements with BCI as the sole control signal.
The aim of this article is to present the steps from the first screening until the final successful control of BCI applications together with evaluation results.

Methods

End-user: the 31 years old male end-user is diagnosed with a motor and sensory complete lesion (ASIA Impairment Scale A) at the level of C5 caused by an accident in 2010. He is not able to move his hand/fingers but has residual muscle control of his shoulder and partly the elbow. His range of motion of hand and finger joint is not restricted. All hand and finger muscles are paralyzed but innervated.
Data recording and processing: initially, in June 2011, EEG was recorded with 15 electrodes placed on the head to have Laplacian and/or bipolar derivations around the motor cortex. Signals were acquired with a g.USBamp (Guger Technologies, Austria) with a sample rate of 512 Hz and filtered between 0.5 and 100 Hz with a notch filter at 50 Hz. Later, different electrode layouts were used as well, mostly consisting of nine electrodes at positions C3, Cz, and C4 and anterior and posterior.
Data were analyzed for significant changes in band power in certain frequency bands, depending on the type of mental strategy. This was realized by plotting event-related desynchronisation/synchronisation (ERD/ERS) maps [3] between 5–40 Hz which show relative changes in band power in different frequency bands during MI for the three relevant channels C3, Cz, and C4. The most promising frequency bands of the best channels for the mental tasks with the best distinguishable patterns were selected manually as features to generate LDA (linear discriminant analysis) classifiers for later online use. In a 10×10 cross-validation process the best point in time for classification was found and used to set up the final classifier.
Data of online sessions were also analyzed with ERD/ERS maps. Additionally, performance was evaluated via classification accuracy, speed, or number of false positives/min.
Training: the end-user started training with a BCI based on motor imagery (MI), i.e., the imagination of movements of hands or feet. Thereby generated brain patterns, in this case ERD, were intended to be found in a first screening session performed with the standard Graz-BCI paradigm [1]. The goal was to find limbs for which imagination of movements produced distinct patterns and then to proceed online with this mental strategy. In addition to BCI training, we also started with FES-assisted muscle training to achieve a fatigue resistance in both arms sufficient to control a grasp neuroprosthesis.
Online BCI sessions: training was continued by applying the LDA classifier online to control a liquid-cursor feedback to reach cue-paced tasks in a two-class BCI. In fact, the end-user performed offline training only once at the beginning and once after one year after the start of training. Online training was performed in eight sessions, classifying left hand versus feet MI. After offline and online

training, two neuroprosthesis applications were controlled by the end-user. In the first one he could choose between a lateral grasp or a palmar grasp pattern with a BCI and open/close his hand continuously with a shoulder position sensor. Individual stimulation profiles and electrode positions were used to realize both grasp patterns [4]. In this experiment he was asked to move objects with the dedicated grasp type in a limited time period and switch between the grasps when necessary.
In the second BCI application he controlled a neuroprosthesis for hand and elbow functions solely with BCI [5]. In both applications he used time-coded MI, the best active class (feet MI) versus a rest condition. Depending on the length of the performed imagination, either different switches were triggered, or commands were executed as long as the command was active. He had to perform ten predefined sequences, consisting of short commands to open/close the hand and long commands to move the arm upwards or downwards continuously.

Results

Fig. 1 shows ERD/ERS maps after the first screening (S1) and after the second offline training session (S2) one year later. The pattern on Cz in the beta frequency range did not change and was used constantly in all online sessions, including the two BCI-driven neuroprosthesis applications.

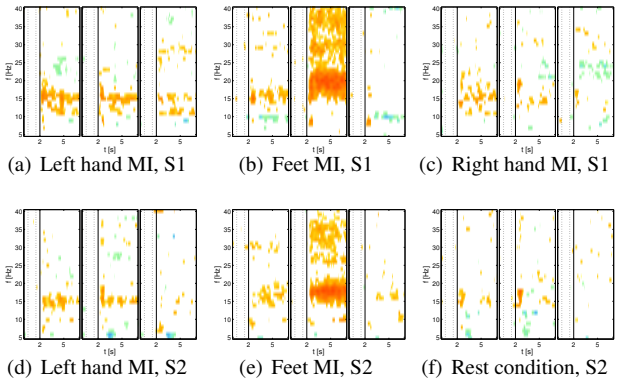

(a) Left hand MI, S1 (b) Feet MI, S1 (c) Right hand MI, S1

(d) Left hand MI, S2 (e) Feet MI, S2 (f) Rest condition, S2

Figure 1: ERD/ERS maps from the first screening session and an offline training session one year later. For each session three images show relative changes in band power for different frequency bands on the three channels C3, Cz, C4 (from left to right). In S2 Right hand MI was replaced by a Rest condition to set up a classifier for discriminating an active versus a rest class.

On average he achieved 82.7±7.9 % classification accuracy for the eight online BCI training sessions. He could control the first BCI application and moved 215 objects within 24 min and switched between grasp types in 16.9±12.2 s.
In the hand/elbow neuroprosthesis he performed second best among nine healthy subjects [5]: the true positive rate (correct use of short or long commands) was 73.7 % and he could successfully perform 8 out of 10 sequences. During active control he managed to trigger 6.9 commands/min, as opposed to only 2 commands/min during resting periods.

Discussion

This work shows that several prerequisites must be fulfilled for a successful use of non-invasive BCI-controlled neuroprostheses. The end-user needs to be compliant to FES training, has to be able to generate distinct ERD patterns and has to be able to voluntarily activate these patterns in an MI-BCI. Our end-user fulfilled all of them which seems not always to be the case [6]. He was able to control the grasp neuroprosthesis for functional tasks and in everyday life settings. He is not in need of an elbow neuroprosthesis but he successfully showed that such a form of control, solely based on BCI, is feasible in end-users with impaired elbow and shoulder functions. Therefore, controlling a neuroprosthesis with BCI based on MI seems to be a promising way for restoration of the upper extremity function in selected end-users.

Acknowledgement

This work is supported by the European ICT Programme Project FP7-224631 and BioTechMed Graz.

Bibliography

[1] G. Pfurtscheller and C. Neuper, "Motor imagery and direct brain-computer communication," *Proceedings of the IEEE*, vol. 89, pp. 1123–1134, 2001.

[2] G. R. Müller-Putz, C. Breitwieser, F. Cincotti, R. Leeb, M. Schreuder, F. Leotta, M. Tavella, L. Bianchi, A. Kreilinger, A. Ramsay, M. Rohm, M. Sagebaum, L. Tonin, C. Neuper, and J. del R. Millán, "Tools for Brain-Computer Interaction: a general concept for a hybrid BCI (hBCI)," *Frontiers in Neuroinformatics*, 2011.

[3] B. Graimann, J. E. Huggins, S. P. Levine, and G. Pfurtscheller, "Visualization of significant ERD/ERS patterns in multichannel EEG and ECoG data," *Clinical Neurophysiology*, vol. 113, pp. 43–47, 2002.

[4] R. Rupp, A. Kreilinger, M. Rohm, V. Kaiser, and G. Müller-Putz, "Development of a non-invasive, multifunctional grasp neuroprosthesis and its evaluation in an individual with a high spinal cord injury," in *4th Annual International Conference of the IEEE EMBS*, 2012.

[5] A. Kreilinger, M. Rohm, V. Kaiser, R. Leeb, R. Rupp, and G. R. Müller-Putz, "Continuous and discrete control of a hybrid neuroprosthesis via time-coded motor imagery BCI," in *Proceedings of TOBI Workshop lV*, 2013.

[6] V. Kaiser, A. Kreilinger, G. Müller-Putz, and C. Neuper, "Long-term BCI training for grasp restoration in a patient diagnosed with cervical spinal cord injury," in *5th International BCI Conference 2011*, 2011.

Biomed Tech 2013; 58 (Suppl. 1) © 2013 by Walter de Gruyter · Berlin · Boston. DOI 10.1515/bmt-2013-4444

AUTOMATIC ADAPTATION TO POST-MOVEMENT EVENT-RELATED SYNCHRONIZATION IN A BRAIN-COMPUTER INTERFACE

Faller J[1*], Solis-Escalante T[1*], Scherer R[1] and Müller-Putz G R[1]

[1]Institute for Knowledge Discovery, Graz University of Technology, Austria

gernot.mueller@tugraz.at

*These authors contributed equally.

Abstract: *We simulate how an adaptive, two-class brain-computer interface system based on only one Laplace derivation at Cz automatically calibrates and adapts to post-movement event-related synchronization (ERS) data from 20 healthy volunteers. This is an important intermediate step towards adapting to post-movement imagery (MI) ERS signals in an online BCI. Our system performs rigorous outlier rejection, initially calibrates after only five trials per class, and re-calibrates at every five trials per class. In our analysis, the newest classifier was always applied to the ensuing trials. The results showed a high average peak accuracy over all participants of* $81.0 \pm 9.1\,\%$*. The high efficacy of this system on post-movement ERS data encourages us to test our system with post-MI data with the final aim to implement an online BCI system.*

Keywords: *Electroencephalogram, Adaptive Brain-Computer Interface, Event-Related Synchronization*

Introduction

Electroencephalogram (EEG) based brain-computer interfaces (BCI) can establish a non-muscular channel of communication for severely disabled individuals [1]. To achieve this, BCIs rely on the fact that humans can voluntarily modulate the amplitude of sensorimotor rhythms in the perirolandic EEG by performing motor tasks, such as movement execution (ME) or movement imagery (MI) of the feet. Using machine learning techniques, BCI systems translate patterns of these amplitude changes into control signals that can drive spelling systems, wheelchairs or other assistive technology.

Producing these oscillatory responses is a skill-full action, which requires training of varying extent [2]. For this training process, co-adaptive BCI paradigms have proven very intuitive and effective [3, 4]. The purpose of a BCI training paradigm is to allow for fast auto-calibration and effective online training that leads to satisfactory online control in a short time for most users.

Analogous to [4], our simulation initially calibrates based on only five trials per class (TPC) and re-calibrates whenever five new TPC are available. The novel aspect here is that our system operates on post-movement beta event-related synchronization (ERS, [5]) data. This phenomenon, also called the beta rebound is a very distinctive and robust phenomenon in the EEG [6, 5] and appears at the offset of both ME and MI. Previous work successfully set up BCI systems based on this phenomenon [7, 8]. Our aim is to evaluate the efficacy of the adaptive BCI concept on ME data, to finally create an online BCI setup based on MI.

Methods

For our adaptive BCI simulation we used previously recorded EEG data from 20 healthy volunteers [9]. The data was sampled at 250 Hz and filtered between 0.5 and 100 Hz. There was a notch filter at 50 Hz. Specifically, we recorded EEG from 3 Laplace derivations at C3, Cz and C4. We only used Cz for this analysis.

Seated in a comfortable arm chair, the participants performed a Go/NoGo task (see Figure 1) where they visually fixated a green cross on a computer monitor. The system displayed a filled, green circle instead of the cross to indicate the Go condition, where the participants executed one single, brisk (≈ 1.6 s, [9]) dorsiflexion of both feet. The NoGo condition was indicated analogously by a filled, red circle. For this condition, participants were instructed to withhold any motor response and to relax. The sequence in which cues for either condition occurred was random with each condition being equally probable.

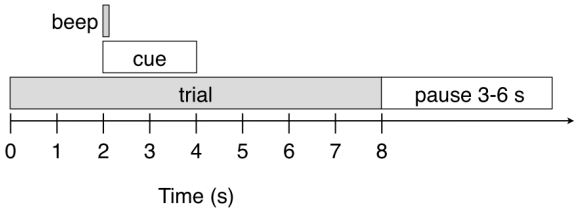

Figure 1: Scheme of the trial structure in the Go/NoGo paradigm.

Based on [4] and [10], our simulation ran through the data trial by trial, performing rigorous outlier rejection based on different methods [10] including time domain signal thresholding, kurtosis, and probability. As soon as five artifact free TPC were available, the system auto-calibrated the first time. To simulate online performance, we always applied the newest classifier to every new trial. Whenever five new artifact free trials were available the system recalibrated. In every calibration step the BCI trained a linear discriminant analysis (LDA) classifier. We always used the one of four logarithmic bandpower features ($\beta_{low} = 13\ to\ 23\,Hz$, $\beta_{mid} = 16\ to\ 26\,Hz$, $\beta_{high} = 20\ to\ 30\,Hz$ and $\beta_{full} = 13\ to\ 30\,Hz$; cf. [6]) from the Laplace derivation at Cz that yielded the highest separability according to Fisher score.

To evaluate the performance of our BCI system, we calculated the classification accuracy for every sample point in all test trials. Averaging across all test trials gave us a trial time series that showed how accurate our system was in classifying the users brain activity in every sample point. We report the peak accuracy in the window of 3 to 7 s. Noteworthy, the level of significantly (p = 0.01) better than chance binary classification accuracy with 31 TPC is 66.1 % [11].

Results

From 20 participants, 19 achieved significantly better than chance peak accuracies at an overall average of $81.0 \pm 9.1\,\%$. The feature β_{low} was dominant for most participants (40 %), followed by β_{high} (30 %), β_{full} (25 %) and β_{mid} (5 %). See Figure 2 for details on the accuracies.

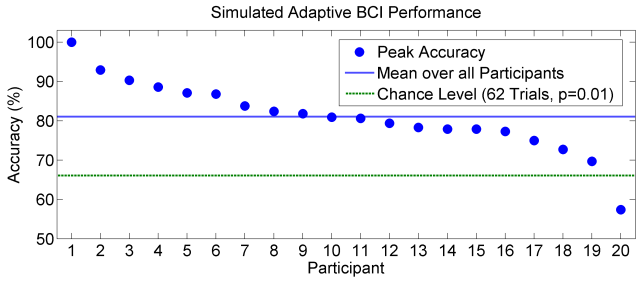

Figure 2: Accuracy for all 20 participants.

Discussion

The successful auto-calibration and adaptation of our system in this simulation led to significantly better than chance accuracy for 95 % of the novice users. 90 % of the participants performed above a commonly assumed threshold level of 70 % accuracy, required to effectively operate a spelling program [12]. Even more interesting: Participants either performed a very brisk motor task or did nothing (i.e. withheld movement); in a previous online study [4] participants had to perform distinct motor tasks for two conditions for over five seconds. In comparison with [4], the required user effort in the present system is much lower, while the resulting accuracy in excess of the chance level is not significantly different (p = 0.65; two-tailed, independent samples t-test). These promising results with executed movement encourage us to investigate the efficacy of adaptive BCI systems on data from post-movement imagery ERS data with the final aim to create an online system based on brisk imagined movement.

Acknowledgement

Supported by the EU research projects Better (No. 247935) and Backhome (No. 288566). This paper only reflects the author's views and funding agencies are not liable for any use that may be made of the information contained herein.

Bibliography

[1] J. R. Wolpaw, N. Birbaumer, D. J. McFarland, G. Pfurtscheller, and T. M. Vaughan, "Brain-computer interfaces for communication and control," *Clinical Neurophysiology*, vol. 113, pp. 767–791, 2002.

[2] A. Kübler, F. Nijboer, J. Mellinger, T. M. Vaughan, H. Pawelzik, G. Schalk, D. J. McFarland, N. Birbaumer, and J. R. Wolpaw, "Patients with ALS can use sensorimotor rhythms to operate a braincomputer interface," *Neurology*, vol. 64, pp. 1775–1777, 2005.

[3] C. Vidaurre, C. Sannelli, K.-R. Müller, and B. Blankertz, "Co-adaptive calibration to improve BCI efficiency," *J Neural Eng*, vol. 8, p. 025009, 2011.

[4] J. Faller, C. Vidaurre, T. Solis-Escalante, C. Neuper, and R. Scherer, "Autocalibration and recurrent adaptation: Towards a plug and play online ERD-BCI," *IEEE T Neur Sys Reh*, vol. 20, pp. 313–319, May 2012.

[5] G. Pfurtscheller and F. H. Lopes da Silva, "Event-related EEG/MEG synchronization and desynchronization: basic principles," *Clinical Neurophysiology*, vol. 110, pp. 1842–1857, 1999.

[6] C. Neuper and G. Pfurtscheller, "Post movement synchronization of beta rhythms in the EEG over the cortical foot area in man," *Neuroscience Letters*, vol. 216, pp. 17–20, 1996.

[7] T. Solis-Escalante, G. R. Müller-Putz, C. Brunner, V. Kaiser, and G. Pfurtscheller, "Analysis of sensorimotor rhythms for the implementation of a brain switch for healthy subjects," *Biomedical Signal Processing and Control*, vol. 5, pp. 15–20, 2010.

[8] G. R. Müller-Putz, V. Kaiser, T. Solis-Escalante, and G. Pfurtscheller, "Fast set-up asynchronous brain-switch based on detection of foot motor imagery in 1-channel EEG," *Medical and Biological Engineering and Computing*, vol. 48, pp. 229–233, 2010.

[9] T. Solis-Escalante, G. R. Müller-Putz, G. Pfurtscheller, and C. Neuper, "Cue-induced beta rebound during withholding of overt and covert foot movement," *Clinical Neurophysiology*, vol. 123, pp. 1182–1190, 2012.

[10] J. Faller, C. Vidaurre, E. V. C. Friedrich, U. Costa, E. Opisso, J. Medina, C. Neuper, G. Müller-Putz, and R. Scherer, "Automatic adaptation to oscillatory EEG activity in spinal cord injury and stroke patients," in *TOBI Workshop 2012*, 2012.

[11] G. R. Müller-Putz, R. Scherer, C. Brunner, R. Leeb, and G. Pfurtscheller, "Better than random? A closer look on BCI results," *Int J Bioelectromag*, vol. 10, pp. 52–55, 2008.

[12] J. Perelmouter and N. Birbaumer, "A binary spelling interface with random errors," *IEEE T Rehabil Eng*, vol. 8, pp. 227–232, 2000.

Biomed Tech 2013; 58 (Suppl. 1) © 2013 by Walter de Gruyter · Berlin · Boston. DOI 10.1515/bmt-2013-4445

INTRODUCTION OF A UNIVERSAL P300 BRAIN-COMPUTER INTERFACE COMMUNICATION SYSTEM

Andreas Pinegger[1], Selina Wriessnegger[1], Gernot Müller-Putz[1]

[1]Institute for Knowledge Discovery, Graz University of Technology , Austria

a.pinegger@tugraz.at

Abstract: *We developed a new P300-based BCI communication system. The design is tripartite: One part operates as a universal data acquisition unit, which allows to easily use different data acquisition devices. The second part is a rapid prototyping platform based on Matlab/Simulink ® for data processing, which can be modified in an easy way. The last part is a graphical user interface, which also acts as main controller. Every single part is state-of-the-art designed and implemented. Connected together they are a very powerful tool not only for scientists and research issues, but also for non-expert users.*

Keywords: *P300, BCI, user-centered-design, famous faces*

Introduction

A brain-computer interface (BCI) is an interface that connects a human brain directly with a computer. It recognizes mentally induced changes of brain signals, in our case the electroencephalogram (EEG) and forms a control signal.
There are different kinds of brain activity patterns which can be used for a BCI. One of them, the P300 phenomenon, is an event-related potential (ERP), triggered by unexpected, rare, or particularly informative stimuli. It is described as a positive peak visible in the EEG approximately 300 ms after the stimuli.
Donchin and colleagues presented in [1] the first P300-based BCI, also called P300 speller, which permits to spell words. A 6×6 matrix filled with letters and symbols is presented to the user, and entire columns or rows are flashed one after the other in random order. When the column/row containing the desired letter is flashed, a P300 is elicited.
If the stimulus is more complex than just a flash, other ERPs are generated too. Kaufmann and colleges showed in [2] that the use of famous face images as stimuli cause two further negative deflections, the N170 and N400f, and that these can be additionally used for classification. This modification improves the classification rates significantly.

In this work we present our newly developed universal P300-famous faces speller, see Fig.1, based on the ideas of Donchin and Kaufmann. With this BCI the user is able to spell, to control a multimedia player, or to browse the Internet.

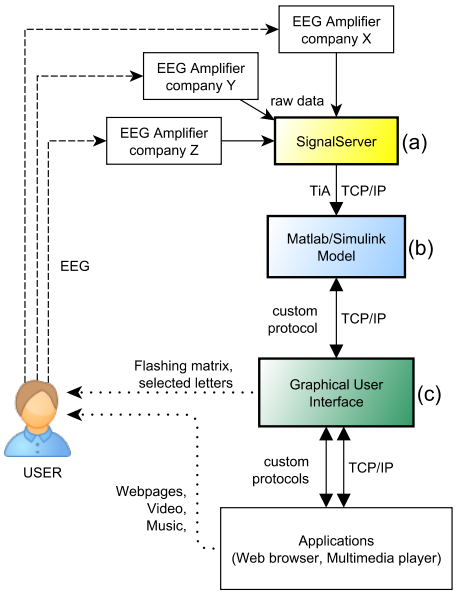

Figure 1: Design sketch of the universal P300 BCI communication system.

Methods

Data acquisition:
For data acquisition the TOBI SignalServer software [3] is used, see Fig. 1a). The big advantage of this software is that it can handle many different data acquisition devices [4].
Paradigm:
The paradigm is inspired by the work of Donchin [1] which has been described before. The only differences are (i) the matrix has a fixed size of 6×6 just during the calibration and can have an $n \times 6$ $(with\ n = 6...14)$ size afterwards, and (ii) the intensification of the rows /columns is done with famous faces instead of flashing them.
Data processing:
Matlab/Simulink ® (*The MathWorks, USA*) is used for data processing, see Fig. 1b). The processing itself is mainly based on results found in [5] with some deviations.
For each channel, 800 ms segments of data following each intensification are extracted. Afterwards a baseline correction with 200 ms pre-stimulus data is performed. The segments are then moving average filtered and decimated by equivalent values. The resulting data segments are concatenated by channel for each intensification (highlighting

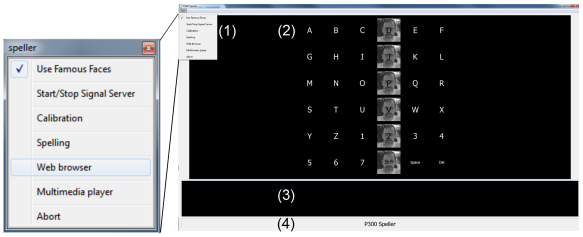

Figure 2: Screen-shot of a) the user menu and b) the P300 user interface. The different areas are (1) the menu, (2) the P300 matrix, (3) the text field, and (4) the status bar. Normally famous faces are used which are not shown in this figure due to print license.

of a row or column), creating a single feature vector. For each stimulus one feature vector per sequence (all rows and columns highlighted once) is generated and averaged over all sequences (maximum 15 per selection).
In training mode this is done for ten letters and afterwards a classifier is trained using stepwise linear discriminant analysis (SWLDA) [6]. To get the best trade-off between speed and accuracy the lowest number of sequences is calculated with a leave-one-out cross-validation (LOOCV) and successive adding of sequences to the test set. However, the practically best number of sequences is determined afterwards as described in [7].
In spelling mode the calculated classifier and the determined best number of sequences will automatically be used.

Results

We developed a P300 BCI system which is based on three main components: The TOBI SignalServer for data acquisition and distribution, a Matlab/Simulink ® model for data processing and an in C++ implemented graphical user interface and paradigm control, see Fig. 2. Within the application it is possible to start and stop the data acquisition software (SignalServer). Once the Matlab/Simulink ® model is running in the background the training or spelling session can be started just by one click. Also the image (preferred famous face) for highlighting can be selected freely just by three mouse clicks.
The communication with Matlab/Simulink ® is done via a network (TCP/IP) connection. Two further TCP/IP connections to control other applications are already implemented: One to control a web browser and one to control a multimedia player. To fulfill the needs of these two applications the size of the matrix adapts automatically, as described before.

Discussion

This work introduces a state-of-the-art P300 BCI system based on famous faces. It was designed and developed for the EC founded project BackHome (www.backhome-fp7.eu). It should be easy and intuitive in use with simultaneous consideration of the latest research results. To achieve this, it combines the universal data acquisition interface idea from [4] with the improvements of Kaufmann and colleges [2] and [7] showing letters highlight as famous faces and a user-centered, easy-to-use graphical user interface design. Regarding the data processing part the design is focused on best on-line performance as it is described in [5] and [7].
From a scientific perspective the use of Matlab/Simulink ® as data processing and partly control software allows scientific users to easily implement and test new algorithms or paradigm control structures to address research questions.
The two implemented interfaces to external applications (multimedia player and web browser),which are still under development, round off the universal applicability of this system.

Acknowledgement

Supported by the FP7 research project BackHome (No. 288566). This paper only reflects the author's views and funding agencies are not liable for any use that may be made of the information contained herein.

Bibliography

[1] E. Donchin, K. Spencer, and R. Wijesinghe, "The mental prosthesis: Assessing the speed of a p300-based brain- computer interface," *IEEE Transactions on Rehabilitation Engineering*, vol. 8, no. 2, pp. 174–179, 2000.

[2] T. Kaufmann *et al.*, "Flashing characters with famous faces improves erp-based brain-computer interface performance," *Journal of Neural Engineering*, vol. 8, no. 5, 2011.

[3] C. Breitwieser *et al.*, "Proposing a standardized protocol for raw biosignal transmission," *IEEE Transactions on Biomedical Engineering*, vol. 59, no. 3, pp. 852–859, 2012.

[4] G. R. Müller-Putz *et al.*, "Tools for brain-computer interaction: a general concept for a hybrid bci (hbci)," *Frontiers in Neuroinformatics*, vol. 5, no. 30, 2011.

[5] D. Krusienski *et al.*, "Toward enhanced p300 speller performance," *Journal of Neuroscience Methods*, vol. 167, no. 1, pp. 15 – 21, 2008.

[6] D. J. Krusienski *et al.*, "A comparison of classification techniques for the p300 speller," *Journal of Neural Engineering*, vol. 3, no. 4, p. 299, 2006.

[7] T. Kaufmann *et al.*, "Spelling is just a click away – a user-centered brain-computer interface including auto-calibration and predictive text entry," *Frontiers in Neuroscience*, vol. 6, no. 72, 2012.

Biomed Tech 2013; 58 (Suppl. 1) © 2013 by Walter de Gruyter · Berlin · Boston. DOI 10.1515/bmt-2013-4446

CORTICAL ACTIVATION PATTERNS OF CUE-PACED FOOT MOVEMENT IN SUBACUTE STROKE PATIENTS

T. Solis-Escalante[1], J. M. Belda-Lois[2], and G. R. Müller-Putz[1]

[1]Institute for Knowledge Discovery, Graz University of Technology, Austria

[2]Instuto de Biomecánica de Valencia, Universitat Politécnica de Valencia, Spain

teodoro.solisescalante@tugraz.at

Abstract: *Limb movement is associated with well defined cortical activation patterns. Structural and functional changes in the brain affect the characteristics of these patterns (strength and topography). Novel strategies for post-stroke motor rehabilitation could monitor cortical activity as an additional index of engagement and/or recovery. In this work we analyze differences in cortical activation related to movements of the affected vs. unaffected foot (dorsiflexion). Our results show stronger cortical activation during movements of the affected foot, and stronger responses at the vertex. Online assessment of cortical activation and the experiment described in this work could be added to traditional motor rehabilitation.*

Keywords: *Event-related (de)synchronization, Post-movement beta rebound, Subacute stroke, EEG*

Introduction

Novel strategies for improving post-stroke motor rehabilitation may monitor cortical activation during therapy [1, 2]. Cortical activation patterns related to limb movement are visible in the EEG as changes in the amplitude of sensorimotor rhythms. These changes are described as event-related desyncrhonization (ERD) and event-related synchronization (ERS) [3]. In general, ERD can be interpreted as a correlate of an active cortical area, while ERS can be associated with a deactivated or inhibited state of large neuronal networks. After a stroke, structural and functional changes in the brain affect the characteristics of ERD and ERS patterns, i.e., strength and topography [4, 5, 6]. In this work, we investigate the cortical activation patterns of subacute stroke patients during foot movements of the affected and unaffected side of their body.

Methods

Experimental paradigm and data acquisition: Eleven subacute stroke patients (ischemic stroke, time after lesion 8±2 months, age 63±14 yr., right handed, 5 female, 8 with left hemiparesis) were recruited by the Instituto de Biomecánica de Valencia, Spain. The participants' task was to perform left or right foot dorsiflexions following cues shown on a computer screen (8 runs with 10 movements per leg). Movement side (left and right) and duration (3 to 4 s) were randomized. Online feedback, representing muscle activity, was presented to assist patients with the execution of the foot movements. The experiment

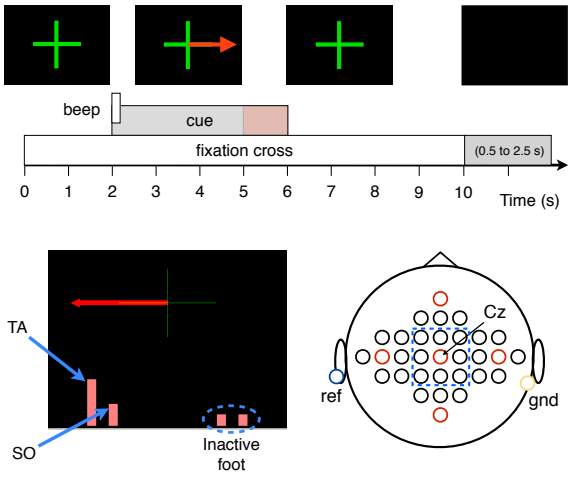

Figure 1: Experimental paradigm, online feedback, and electrode montage. Top: Schematic of the paradigm timing. Bottom left: Online feedback shows the muscle activity of both legs. Bottom right: Thirty-one electrodes around the vertex (electrode position Cz) used to record EEG. Electrode positions in red are Fz, C3, Cz, C4, and Pz.

was approved by the local ethics committee and all participants gave written informed consent. EEG was recorded from 31 sites using a custom cap (Easycap, Herrsching, Germany) and active electrodes (g.tec, Schiedelberg, Austria). The reference electrode was on the left earlobe and the ground electrode was on the right mastoid. EMG was recorded from each leg: extensor hallucis longus (HL), tibialis anterior (TA), soleus (SO), and gastrocnemius (GA). Two monopolar channels were recorded from each muscle using adhesive Ag/AgCl electrodes (reference on the right hip). Signals were acquired at 1.2 kHz using biosignal amplifiers (g.USBamp) with filters between 0.1 and 100 Hz for EEG, 0.1 and 500 Hz for EMG, and a notch filter (50 Hz). Fig. 1 illustrates the paradigm timing, the cues on screen, the online feedback, and the EEG montage.

Cortical activation: Laplacian filters were applied to the EEG data to improve the SNR [7]. Afterwards, the EEG was filtered between 6 and 40 Hz and downsampled to 600 Hz. Incorrectly performed trials (wrong leg movement, left/right co-contraction, late reaction time) and trials with artifacts (EEG>25μV) were rejected. Only nine derivations close to electrode position Cz were considered (see Fig. 1), because ERD and ERS related to foot movements are prominent at the vertex [8, 9]. Onset and offset of in-

dividual movements were identified from the TA signals and used as triggers. The analysis focused on the peri-movement ERD and the post-movement ERS. Frequency bands showing the strongest ERD or ERS (average from 500 ms to 1.5 s relative to movement onset/offset) were selected for further analysis. ERD and ERS waveforms were computed for each patient using a participant-specific frequency band. To summarize cortical activation, ERD was integrated in a 2.5 s window following movement onset, whereas ERS was integrated between 500 ms and 1.5 s, relative to movement offset.

Statistical analysis: Statistical significance was evaluated for the ERD and ERS independently, with two-way ANOVAs with factors SIDE $\times$ ELECTRODE. The factor SIDE had two levels: affected vs. unaffected side of the body, whereas the factor ELECTRODE had nine levels: anterior-ipsilateral, anterior-central, anterior-contralateral, central-ipsilateral, vertex, central-contralateral, posterior-ipsilateral, posterior-central, and posterior-contralateral; relative to the affected side of the body. Significance values were corrected (Greenhouse-Geiser) if sphericity violations occurred.

Results

Peri-movement ERD: The average frequency band for ERD was 10.7 ± 5.2 and 22.4 ± 7.5 Hz. Significant differences were found for the main factor SIDE ($F(1,10) = 8.21$, $p<0.05$), indicating that the ERD was stronger during movements of the affected foot (-381 ± 293) than during movements of the unaffected foot (-275 ± 226).

Post-movement ERS: The average frequency band for ERS was 17.1 ± 5.1 and 24.1 ± 6.1 Hz. Significant differences were found for the main factor ELECTRODE ($F(8,80)=4.11$, $p<0.05$, Greenhouse-Geiser corrected) and for the interaction SIDE $\times$ ELECTRODE ($F(8,80)=2.34$, $p<0.05$). Multiple comparisons between electrode positions revealed significant differences ($p<0.05$, Bonferroni corrected) between the vertex and the electrode positions anterior ipsilateral, anterior contralateral, and central contralateral, i.e., the ERS at the vertex is stronger (147 ± 171) than the anterior locations (ipsilateral: 9 ± 66, contralateral: 45 ± 90) and the central contralateral to the affected foot (affected hemisphere: 10 ± 75). The multiple comparisons did not show significant differences for the interaction SIDE $\times$ ELECTRODE.

Discussion

The aim of our work was to investigate the cortical activation patterns of foot movements in subacute stroke patients. We found higher levels of cortical activity (ERD) for movements of the affected foot than during movements of the unaffected foot. Also, the post-movement response (ERS) at the vertex was stronger than pre-central positions and the central-contralateral to the affected foot (i.e., affected hemisphere). Experimental sessions of cue-paced active foot movement (with feedback) could be used as a novel strategy for motor rehabilitation. Online monitoring of cortical activation and comparisons between movements of both feet, could be useful to assess motor recovery (i.e., changes in cortical activation) [4, 5, 6]. Further work will focus on the post-movement ERS and possible differences between subacute stroke patients and healthy persons.

Acknowledgement

This work was supported by the FP7 EU Research Project BETTER (247935). The authors are thankful to Silvia Mena del Horno and Javier Bonilla for assistance during the experiments.

Bibliography

[1] J. J. Daly and J. R. Wolpaw, "Brain-computer interfaces in neurological rehabilitation," *The Lancet Neurology*, vol. 7, pp. 1032–1043, 2008. Review of BCIs in neurological rehabilitation.

[2] M. A. Dimyan and L. G. Cohen, "Neuroplasticity in the context of motor rehabilitation after stroke.," *Nature Reviews Neurology*, vol. 7, pp. 76–85, 2011.

[3] G. Pfurtscheller and F. H. Lopes da Silva, "Event-related EEG/MEG synchronization and desynchronization: basic principles," *Clinical Neurophysiology*, vol. 110, pp. 1842–1857, 1999.

[4] M. Stępień, J. Conradi, G. Waterstraat, F. U. Hohlefeld, G. Curio, and V. V. Nikulin, "Event-related desynchronization of sensorimotor EEG rhythms in hemiparetic patients with acute stroke.," *Neuroscience Letters*, vol. 488, pp. 17–21, Jan 2011.

[5] V. Kaiser, I. Daly, F. Pichiorri, D. Mattia, G. R. Müller-Putz, and C. Neuper, "Relationship between electrical brain responses to motor imagery and motor impairment in stroke," *Stroke*, 2012.

[6] K. Laaksonen, E. Kirveskari, J. P. Mäkelä, M. Kaste, S. Mustanoja, L. Nummenmaa, T. Tatlisumak, and N. Forss, "Effect of afferent input on motor cortex excitability during stroke recovery.," *Clinical Neurophysiology*, vol. 123, pp. 2429–2436, Dec 2012.

[7] B. Hjorth, "An on-line transformation of EEG scalp potentials into orthogonal source derivations," *Electroencephalography and Clinical Neurophysiology*, vol. 39, pp. 526–530, 1975.

[8] C. Neuper and G. Pfurtscheller, "Post movement synchronization of beta rhythms in the EEG over the cortical foot area in man," *Neuroscience Letters*, vol. 216, pp. 17–20, 1996.

[9] G. R. Müller-Putz, D. Zimmermann, B. Graimann, K. Nestinger, G. Korisek, and G. Pfurtscheller, "Event-related beta EEG-changes during passive and attempted foot movements in paraplegic patients," *Brain Research*, vol. 1137, pp. 84–91, 2007.

Biomed Tech 2013; 58 (Suppl. 1) © 2013 by Walter de Gruyter · Berlin · Boston. DOI 10.1515/bmt-2013-4447

DARK ADDAPTED PUPILLARY LIGHT REFLEX DUE TO SHORT TIME LASER BEAM EXPOSURE

Beckmann D, Reidenbach HD, Dollinger K and Al Ghouz I

Research Laboratory of Medical Tedchnology and Non-Ionizing Radiation,
Cologne University of Applied Sciences, Germany

Dirk.Beckmann@FH-Koeln.de

Abstract: *The Pupillary Light Reflex (PLR) controls the amount of light entering the eye. This might protect the retina when exposed to laser radiation. Higher radiation power causes the pupil to close more and more rapidly. Using a 532 nm laser beam with radiation power between 100 pW and 100 μW causes the pupil diameter to decrease between 15.4 % to 42.4 %. The decrease starts after a latency period ranging from 160 ms to 300 ms. Contraction takes additional 360 ms to 1100 ms and is increasing with power. A duration of more than 600 ms passes before the pupil size reaches the minimum. The response varies with wavelength and it is shown, that the Spectral Luminous Efficiency Function can not be used to describe dependency.*

Keywords: *Pupillary light reflex, wavelength, radiation power, laser pointer, short exposure*

Introduction

Handheld laser pointer with different wavelengthes and increasing power became available in the last years. These pointers can cause temporary blinding, dazzle or glare, even over huge distances. The PLR is a response which controls the amount of light entering the eye and therefore might protect the eye from laser beam exposure. In [1] the author stated that the PLR might be suitable. Preliminary investigations showed that the accuracy of handheld laser pointer is low and no test person was able to hit a target for more than 200 ms. However even small exposure duration and low radiation power can cause a temporary loss of sight. Various studies explored the PLR for diagnostic purpose [2], but investigations with short time laser exposure are rare.

Methods

The PLR was measured with infrared pupillography. This technique, where an array of infrared diodes is used to illuminate the pupil, is well known and had often been used to measure the pupil size and PLR. A camera (The Imaging Source - DMK 22AUC03) with a frame rate of 120 frames per second and resolution of 320 x 240 was used. Leading to a time resolution of about 8.3 ms and pupil size resolution of about 81 μm.
Laser modules with 405 nm, 445 nm, 532 nm, 635 nm and 670 nm wavelength had been used. The laser beam was focused on a distant point and therefore entered the eye with a small divergence. With the aid of variable neutral density filters (Thorlabs NDC-50C-4M) the light power entering the eye was controlled. Seven power settings, 100 pW, 1 nW, 10 nW, 100 nW 1 μW, 10 μW, and 100 μW, had been applied for each wavelength.
6 subjects (4 male, 2 female) in the age from 26 to 70 (41 $\pm$ 18 years) participated in this investigation. Due to the small number of subjects, attributes like gender, age or eye color could not be considered. The effect, that pupil size is decreasing with age, was reduced by using the relative amplitude rather than the absolute value.
A ten minute dark adaptation and readaptation was done before each test. In total each subject participated in 35 tests, except from 1subject missing the 445 nm laser. One subject showed blink reflexes for values higher than about 1 μW and this videos had been excluded.
In order to compute the latency a threshold is often used. In order to determine a more precise value additionally a window of 100 ms was used and shifted until the signal was not monotonous decreasing. The contraction time is defined as time between the first change in pupil size until the minimum was detected. The amplitude is defined as the pupil size in the moment when the laser was switched on and the minimal pupil size.
Often logarithmic functions had been used to describe the changes of these attributes. Least square fitting of equation (1) was done to describe the mean value of the above described attributes.

$$y = a \cdot log_{10}(P) + b \tag{1}$$

An curve fitting example using the relative amplitude versus Power in W after exposure to a 635 nm laser as a function of power P is shown in Figure 1. Additionally the fit through maximal and minimal response is displaedy.

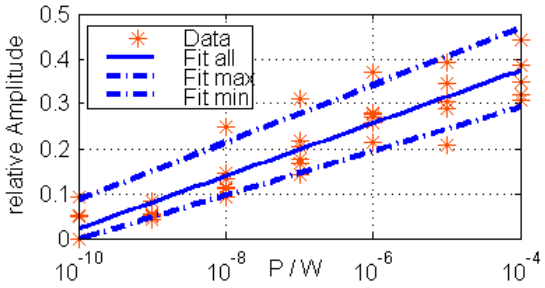

Figure 1: Measured relative amplitude and fitting through the data points. Data was collected by using a 635 nm laser

Table 1: Coefficients and statistics of fittings

Wave-length	a_{amp}	b_{amp}	$rmse$ amp	r^2_{amp}	a_{lat}	b_{lat}	$rmse$ lat	r^2_{lat}	a_{cont}	b_{cont}	$rmse$ $cont$	r^2_{cont}
405 nm	0.058	0.642	0.050	0.847	-0.035	0.045	0.089	0.491	0.056	1.281	0.114	0.699
445 nm	0.050	0.569	0.068	0.650	-0.034	0.042	0.070	0.419	0.049	1.220	0.068	0.844
532 nm	0.045	0.604	0.066	0.660	-0.025	0.062	0.041	0.595	0.098	1.651	0.160	0.705
635 nm	0.059	0.608	0.049	0.859	-0.045	-.021	0.051	0.738	0.027	1.000	0.077	0.761
670 nm	0.054	0.544	0.048	0.839	-0.043	0.022	0.048	0.727	-.008	0.773	0.166	0.128

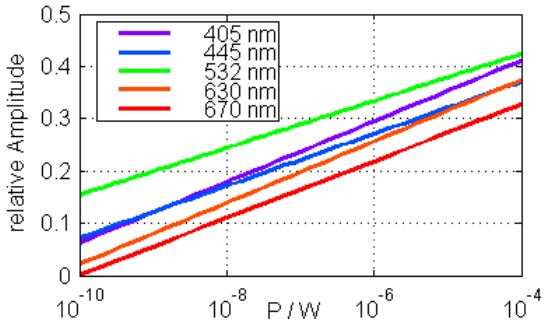

Figure 2: Radiation power versus relative amplitude

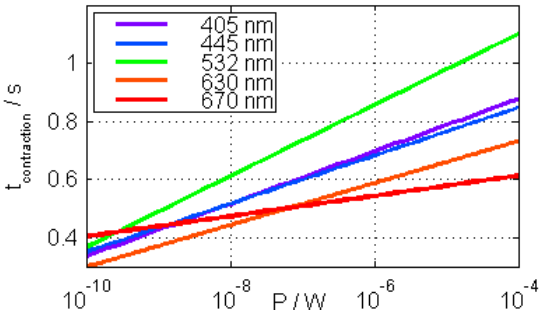

Figure 4: Radiation Power versus contraction time

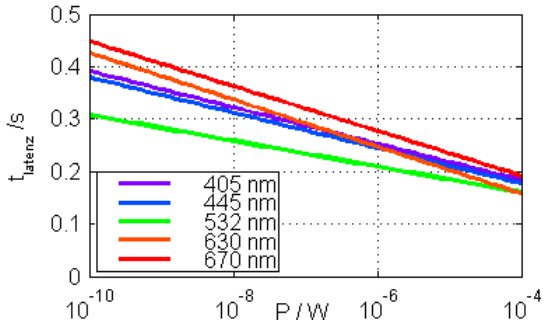

Figure 3: Radiation power versus latency period

Results

As shown in figure 1 the response varies strongly around the fitted curve. Different age, gender, subject condition and other parameter influence the measurment. This leads to a low r-squared value. Table 1 lists next to the coefficients of the curve the r-squared and root mean square error.

The amplitude of the pupil response increases with power (Figure 2). The green 532 nm laser is causing the highest response and the radius decreases in average 15.4 %, even when radiation power is only 0.1 nW. Using a power 100 μW reduces the diameter 42.4 %. In order to cause a 20 % reduced diameter with a green laser about 1nW is necessary. Same effect is caused by 405 nm and 24 nW, 445 nm and 39 nW, 630 nm and 113 nW and 670 nm and 475 nW. The lower response to wavelength of 630 nm and 670 nm than 405 nm and 445 nm shows that spectral luminous efficiency function of the CIE is not suitable to describe the wavelength dependency. Park et. al. stated that the response is caused not only by the rods and cones, also retinal ganglion cells containing the photopigment melanopsin contribute to the PLR [3].

When considering the latency it becomes visible that the time until the pupil size starts changing is decreasing with increasing power. With a response time of in average 159 ms and a deviation of 47 ms the 532 nm laser causes the fastest response when a power of 100 μW is used. After contraction started the closure of the eye took up to 1.1 s before it reaches the minimum. The contraction time is increasing with power. Even for small changes in the pupil size more than 300 ms are needed (figure 3).

Discussion

The sum of latency period and contraction time is longer than half a second. This is not suitable to protect the eye from laser radiation, which might cause damage or hazardous glare. Most exposures due to laser pointer are expected to be shorter than 100 ms.

Bibliography

[1] D. A. Stamper, D. J. Lund, J. W. Molchany, and B. E. Stuck, "Human pupil and eyelid response to intense laser light: implications for protection," *Perceptual and motor skills*, vol. 95, no. 3, pp. 775–782, 2002.

[2] C. Ellis, "The pupillary light reflex in normal subjects.," *British Journal of Ophthalmology*, vol. 65, no. 11, pp. 754–759, 1981.

[3] J. C. Park, A. L. Moura, A. S. Raza, D. W. Rhee, R. H. Kardon, and D. C. Hood, "Toward a clinical protocol for assessing rod, cone, and melanopsin contributions to the human pupil response," *Investigative ophthalmology & visual science*, vol. 52, no. 9, pp. 6624–6635, 2011.

Biomed Tech 2013; 58 (Suppl. 1) © 2013 by Walter de Gruyter · Berlin · Boston. DOI 10.1515/bmt-2013-4448

Investigation of noise levels in intensive care units

Kletzenbauer G[1], Fruhwald S[2], Schröttner J[1]

[1]Institute of Health Care Engineering, University of Technology Graz, Austria

[2]Department of Anesthesiology and Intensive Care Medicine, Medical University of Graz, Austria

gerald.kletzenbauer@student.tugraz.at

Abstract: *To investigate noise levels in intensive care units sound level measurements were carried out for several weeks both in patient's areas as well as in staff working and monitoring areas. The time course of the sound pressure level was investigated and the characteristics in terms of minimum, maximum and rating levels were determined and assessed. Preliminary results show that the noise level is very high for patients at any given time. Furthermore, the legal noise limit for intellectual activities (50dB) at the workplace was exceeded at all times, although the limit for simple office work (70dB) was not exceeded. Solutions should be developed to minimize the noise disturbance to staff and patients.*

Keywords: *Noise, ICU, hospital, decibel (dB), patients*

Introduction

In recent years, due to an increase in patient numbers and the available treatment options, the noise levels in intensive care units (ICU) have increased significantly. In addition to the main influence noise factors (personnel, visits, preparations for patient care) the device-specific noise is becoming increasingly dominant in existing noise-related problems. Sound measurement is the first step to evaluate the current noise situation thoroughly. In a next step, after evaluating the results, appropriate arrangements will be suggested to improve the overall situation. [1]

Methods

The comparison of the noise situation in a special surgery ICU with given limits (Regulation for noise and vibration), requires the determination of the rating level $L_{A,r}$ (see eq 2) in accordance with ÖNORM S 5004:2008 and EN ISO 9612:2009. This allows us to assess the noise exposure of the employees. The patient's situation can only be compared with international guidelines which are relevant to the energy-equivalent permanent sound level (see eq 1). [1, 2, 3]

$$L_{A,eq} = 10 \lg \frac{1}{T} \int_{t1}^{t2} \frac{p_A(t)^2}{p_0^2} dt \qquad (1)$$

With:
- $p_A(t)$ sound pressure
- p_0 reference sound pressure
- T testing time
- $L_{A,eq}$ energy-equivalent permanent sound level

$$L_{A,r} = L_{A,eq,8h} + K \qquad (2)$$

With:
- $L_{A,eq,8h}$ energy-equivalent permanent sound level with a reference period of 8 hours
- K additional added pulse or tone level

The noise level was captured with an NL-32 sound level meter (see Fig. 1). The instrument was set to record one measurement per second. The instrument was mounted at a height between 1.1m and 1.5m. The measurement strategy was based on stationary, multi-full-day measurements.

The measurements were carried out at representative locations, which were selected by an on-site inspection. Overall, six different sites were chosen. Three Measurements were carried out to record the noise impact on the staff (three positions at monitoring and working areas). On the other hand additional positions were chosen to monitor the noise exposure of patients. In these cases the sound level meter was placed near the patients head of occupied beds (see Fig. 1) - whenever possible. Again three measurement locations were chosen: a 1-bed ICU room, a 3-bed ICU room and a 4-bed ICU room.

In addition to the noise level the background level was recorded in order to identify and evaluate atypical influences [2]. For privacy reasons, the audio signal was distorted (adjustment of the pitch), resulting in unintelligible conversations where people could no longer be identified, but other types of noise were assignable.

To accustom staff and patients to the measurement situation, we measured at each point for several days [2] (six days for the workplace measurements and four days for patient-sites). Any first day of the noise-level tests was used to get an overview and also check the measurement to impulsiveness. Then a 5 - respectively 3 - days measurement with the following parameters followed: frequency rating "A" and time rating "fast". [3]

The measured data - more than 2 million data points - were analysed and processed (trend analysis, peak detection, artefact control and plausibility control) with the help of Matlab (The MathWorks, Inc.).

Figure 1: Sound level meter in the 4-bed patient room

Results

The overall results of the six measurement locations are shown in Figure 2 and 3. Figure 2 shows the results of the workplace measurements as a rating level and Figure 3 shows the results of the patient-site measurements as an energy-equivalent permanent sound level. Each day was hereby divided into three sections: a morning section from 6am until 2pm, an afternoon section from 2pm to 10pm and a night section from 10pm to 6am. The results show the average values of the last 72 hours per measurement location [2].

According to [4] the comparison of the measurements results of the workplaces and the patient-sites requires the impulsiveness to be added to latter, which is 6dB in our case.

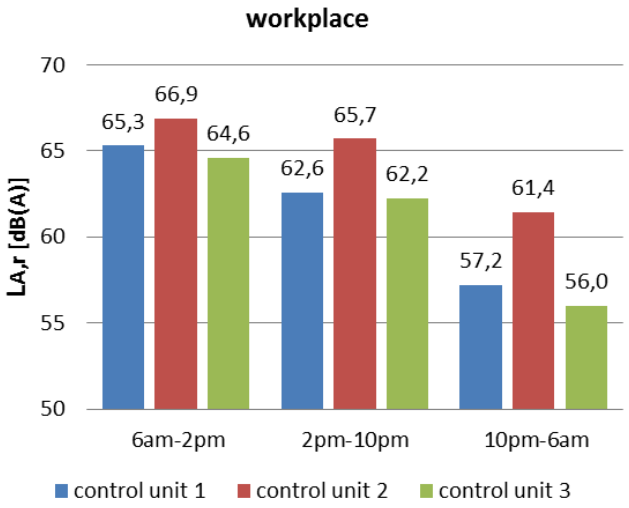

Figure 2: Results of the three workplace measurements

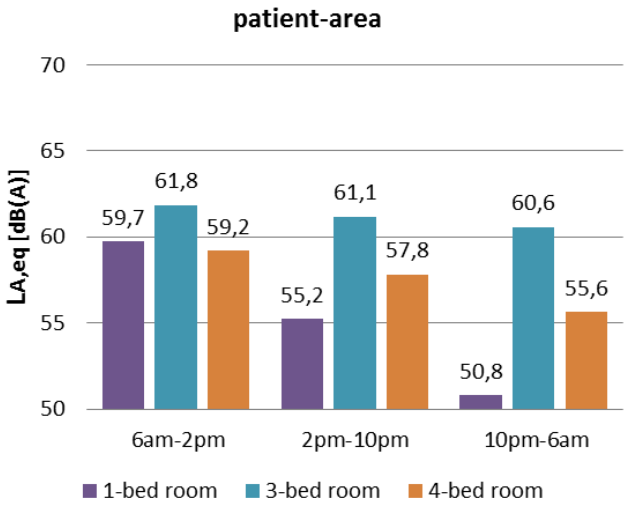

Figure 3: Results of the three patient area measurements

Discussion

The Environmental Protection Agency (EPA) has established guidelines recommending noise levels not to exceed 45dB during the day and 35dB at night in hospital patient rooms [6]. The World Health Organization (WHO) recommends a limit of the energy-equivalent permanent sound level of 35dB [5].

As the results show, not even one measurement was close to these recommendations. This recommended noise level was exceeded by more than 25dB in the 3-bed intensive care room at night. Even in the most quiet room, the 1-bed ICU room, this level was exceeded by 15dB.

The main reasons for the high sound level in the 3-bed ICU room can be explained as follows: First, the room is very close to the control-unit 2 and the main entrance of the intensive care unit. And second, special beds are used for the sickest patients, which produce a very high noise level.

The regulation of noise and vibration defines two limits for certain areas in the workplace. First, a rating level of 50 dB in rooms where mostly intellectual activities are performed and second, a rating level of 70 dB in rooms where simple office work or similar activities are performed [4]. The noise limit for intellectual activities was exceeded at all times whereas the noise limit for simple office work was still in legal boundaries. However, the latter only marginally comply.

Results acquired by secondary literature [1 ,7] are similar, but the results presented in this paper indicate an upward trend.

In a next step, solutions will be developed to minimize the noise disturbance for staff and patients.

Bibliography

[1] Arnold, J., Kornadt, O. et. al.: Lärm auf Intensivstationen in Krankenhäusern, *Bauphysik-Kalender 2009*, pp. 657-679, 2009.

[2] ÖNORM EN ISO 9612:2009, Bestimmung der Lärmexposition am Arbeitsplatz – Verfahren der Genauigkeitsklasse 2 (Ingenieurverfahren), 2009-09-01.

[3] ÖNORM S 5004:2008, Messung von Schallimmissionen, 2008-12-01.

[4] VOLV, Rechtsvorschrift für Verordnung Lärm und Vibrationen, 2012-10-01.

[5] Berglund, B.; Lindvall, T.; Schwela, D. H.: Guidelines for community noise, Genua: OMS (World Health Organization), 1999.

[6] U.S. Environmental Protection Agency, Office of Noise Abatement and Control. 1974. Information on levels of environmental noise requisite to protect public health and welfare with an adequate margin of safety (550/9-74-004). Retrieved March 6, 2013, from: http://www.nonoise.org/library/levels74/levels74.htm

[7] Jar-Yuan, P., A Study in Hospital Noise - A Case From Taiwan, *International Journal of Occupational Safety and Ergonomics (JOSE)*, Vol. 13, No. 1, pp. 83–90, 2007

Biomed Tech 2013; 58 (Suppl. 1) © 2013 by Walter de Gruyter · Berlin · Boston. DOI 10.1515/bmt-2013-4449

Breath analysis using Ion Mobility Spectrometry (IMS) as diagnostic tool in equine reproduction medicine

Klein CC[1], Wietstock S[2], Hoffmann M[2]

[1]Equine Clinic, fzmb GmbH, Bad Langensalza, Germany
[2]Instrument Development Unit, fzmb GmbH, Bad Langensalza, Germany

cklein@fzmb.de

Abstract: *Diagnosing reproduction processes is a main activity of veterinarians concerning farm animals. So it would be eligible to replace this physically demanding work by other procedures. Aim of the presented study was to investigate, whether results of breath analysis are related to sexual hormone levels in equine females. Breath samples of 25 mares as well as regularly taken samples of ambient air were analysed using Ion Mobility Spectrometry (IMS). Peak heights of three clusters were found to correlate moderately strong to blood serum levels of equine chorionic gonadotropine (eCG) and / or progesterone (P) as well.*

Keywords: *Ion mobility spectrometry, IMS, breath analysis, sexual hormone level, horse*

Introduction

Rectal examination of females is usually done for detection of pregnancy or estimation of best moment for mating in bovine and equine species. This procedure provides an immediate diagnosis, but is a physically demanding labour for the veterinarian in large animal practice. Analysis of different sexual hormones in blood serum samples is a precise, but unfortunately a time consuming and expensive method.
First results in human studies revealed, that exhaled volatile organic compounds (VOC) could be detected by means of spectrometric techniques and are suitable for specification of several diseases, medication and gravidity testing [1, 2, 3]. These encouraging results were inspiration to use breath samples for the detection of pregnancy in horses, which was successfully done two years ago [4]. Since the formerly utilised technical system is not available commercially any longer, a new device basing on Ion Mobility Spectrometry (IMS) was used to test versus analysis of blood serum levels of these sexual hormones: equine chorionic gonadotropine (eCG), progesterone (P) and estrone sulphate (ES).

Methods

The animal study was approved by the department of animal protection of provincial government of Thuringia (Registration number 14-102/12). An IMS (STEP GmbH, Pockau, Germany), coupled to a gas chromatography column, was adapted to the animals via face mask and completed by various other components (valves and tubes) (Fig. 1). Clusters of peaks representing the same volatile organic compound were analysed using special statistical algorithm.
Breath and blood serum samples of 25 mares (14 pregnant and 11 non pregnant) of a stud farm were taken in alternating order. After each animal sampling, measurements of ambient air were performed. Because of the quantity of measurements, investigations were done on two consecutive days.
Clusters only associated to ambient air on the two sampling days were excluded from further evaluation. Peak heights of remaining clusters were related to serum hormone levels of eCG, P and ES by Spearman rank correlation analysis at first. Only pairs of variables with significant correlations were used in the following simple regression analysis.

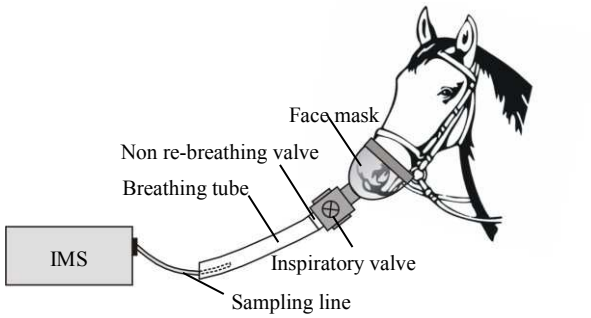

Fig. 1: Principle of adaption of IMS to equine species

Results

Analysis of breath samples provided 113 clusters with peaks in at least one group (ambient air, animals). Peak heights of 18 clusters were significantly correlated to the levels of at least one of the sexual hormones (Spearman rank correlation, $p \leq 0.05$). Regression analysis resulted in 13 clusters with significant correlation of peak heights to the blood serum levels of one or two hormones and a correlation coefficient of more than 0.5. A critical check of the data pool was performed once more and all clusters influenced by the sampling day were removed.
Regression equations and statistical data of the four remaining peak height and hormone level pairs are given in Tab. 1. Results for each pair of variables are shown as plots of the best fitted model (Figures 2 to 5). The equation of the fitted model is shown as a blue line. The plot includes both confidence limits for the means (the middle red lines) and the prediction limits (the outer pink lines).

Table 1: Peak heights in selected clusters versus blood serum hormone levels in 25 mares; simple regression analysis, equations of best fitted models, p-values, correlation coefficients and coefficients of determination (r^2)

Pair of variables	Equation of best fitted model p-value; correlation coefficient; r^2-value
c3 vs. eCG	c3 = 0.0017 + 0.00003 * eCG p = 0.0064; r = 0.5301; r^2 = 28.1065 %
c8 vs. eCG	c8 = 0.0011 + 0.00007 * eCG p = 0.0001; r = 0.7076; r^2 = 50.0730 %
c8 vs. P	c8 = (0.0267 + 0.00071 * P)^2 p = 0.0024; r = 0.5795; r^2 = 33.5935 %
c12 vs. eCG	c12 = (0.03229 – 0.00025 * eCG)^2 p = 0.0001; r = 0.7125; r^2 = 50.7653 %

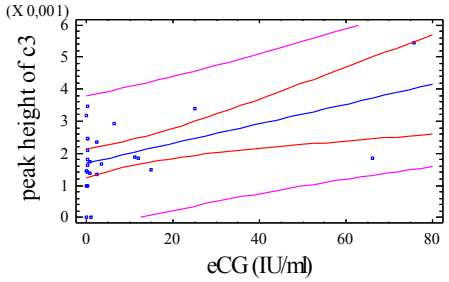

Fig. **2**: Peak heights of cluster c3 versus blood serum eCG levels in 25 mares, results of fitting a linear model (simple regression analysis)

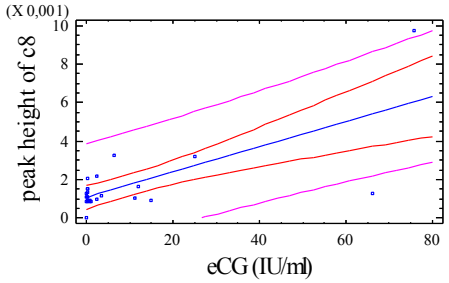

Fig. **3**: Peak heights of cluster c8 versus blood serum eCG-levels in 25 mares, results of fitting a linear model (simple regression analysis)

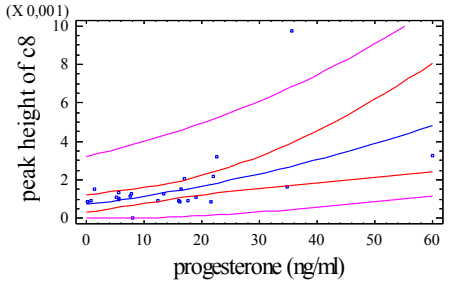

Fig. **4**: Peak heights of cluster c8 versus blood serum progesterone levels in 25 mares, results of fitting a square root-Y model (simple regression analysis)

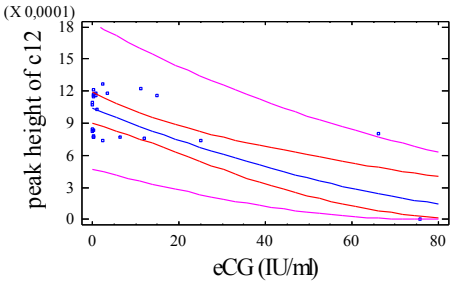

Fig. 5: Peak heights of cluster c12 versus blood serum eCG levels in 25 mares, results of fitting a square root-Y model (simple regression analysis)

Discussion

Functioning of estrus cycle and gravidity in females are determined by fine tuned regulation of sexual hormones like gonadotropins and the steroids ES and P. In addition to these, a specific gonadotropin (i.e. eCG) is found only in equine species between the 50th and 100th day of gestation [5]. The detected four pairs of variables indicate a moderately strong relationship between the peak heights of selected clusters and the blood serum levels of sexual hormones. Certainly, the hormones are not detected directly by IMS, but volatile compounds produced by the metabolism in hormonally regulated processes [3]. Breath analysis for diagnosis in veterinary reproduction medicine is a promising tool. However, to tap the full potential of this method optimisation and standardisation of sampling and analysing procedures is necessary.

Acknowledgement

This study was granted by the German Federal Ministry of Economics via the Euronorm GmbH (Registration number VF090056). The authors appreciate the kind support of Katrin Frankenfeld for eCG analysis and of Petra Prokop for proof-reading the manuscript.

Bibliography

[1] Phillips, M., Cataneo, R.N., et al.: Volatile markers of breast cancer in the breath, *Breast J.*, Vol. 9, pp. 184–191, 2003

[2] Perl, T., E. Carstens, et al.: Detemination of propofol concentrations by breath analysis using ion mobility spectrometry, *Br. J. Anaest.* Vol. 103, pp. 822 – 827, 2009

[3] Moretti, M., Phillips, M., et al.: Increased breath markers of oxidative stress in normal pregnancy and in preeclampsia, *Am. J. Obstet. Gynecol.,* Vol. 190, pp. 1184-1190, 2004

[4] Klein, C.C., Becher, G., et al.: Detection of pregnancy in horses by breath analysis using differential ion mobility spectrometry (DMS), *Eur. Resp. J.*, Suppl., Vol. 55, p. 219s, 2011

[5] Allen, W.R.: Fetomaternal interactions and influences during equine pregnancy, *Reproduction,* Vol. 121, pp. 513-527, 2001

Biomed Tech 2013; 58 (Suppl. 1) © 2013 by Walter de Gruyter · Berlin · Boston. DOI 10.1515/bmt-2013-4450

SINGLE TRIAL MOTOR IMAGERY CLASSIFICATION IN EEG MEASURED DURING FMRI IMAGE ACQUISITION - A FIRST GLANCE

Steyrl D[1], Wriessnegger S C[1], Müller-Putz G R[1],

[1]Institute for Knowledge Discovery, BCI Lab, Graz University of Technology, Austria

david.steyrl@tugraz.at

Abstract: *Non-invasive electroencephalogram (EEG) based Brain-Computer Interfaces (BCIs), which rely on event related desynchronization (ERD), are often affected by large fluctuations of their accuracy. We want to overcome this drawback by using simultaneous EEG and functional magnetic imaging (fMRI). The question we are addressing in this work is if ERD is still classifiable in EEG on a single trial basis after the removement of fMRI related artefacts. In a first single participant recording we found the classical ERD distribution and were able to compute a leave-one-out-cross-validation (LOOCV) accuracy of 78%, which is significantly higher than chance level.*

Keywords: *Brain-Computer Interface (BCI), EEG, fMRI, Motor Imagery (MI), classification*

Introduction

The simultaneous measure of the electroencephalogram (EEG) and functional magnetic resonance imaging (fMRI), is on the edge to make the breakthrough and to become a broader used neuroscience tool. EEG-fMRI offers the unique opportunity to measure two different brain activity related signals simultaneously. First, the electrical activity and second, the oxygen consumption of the brain. Although the relationship between these two brain signals is not clear yet, the bimodal view allows new insights into the brain functionality [1].

Brain-Computer Interfaces (BCIs) are devices which provide control signals out of brain activity signals. One common brain signal used for EEG based non-invase BCIs, is the event related desynchonization (ERD) of sensory motor rhythms (SMR). This desynchronization can be induced by the imagery of limb movements, called motor imagery (MI) [2]. Unfortunately this kind of BCIs are often unreliable. Reasons for that can be found in the data; noise and outliers, high dimensionality, time information, non-stationarity, poor signal-to-noise ratio (SNR) and small training-sets for the machine learning algorithms.

We want to study the processes of MI by measuring EEG and fMRI simultaneously for future improvements of existing BCI systems. This work addresses the question if MI induced ERD is classifiable on a single trial basis in EEG measured with fMRI simultaneously.

Methods

Participant: The participant (male, 23 years old), a known good MI performer, was lying in the fMRI scanner and was looking at a screen via a mirror. He got instruction for MI by a paradigm similar to the classical Graz-BCI [3].

Exp. paradigm: At the start of each trial a white cross appeared. At second 3, a white arrow was added, indicating the kind of MI and removed after 1.25 s. Right hand and feet MIs were used in a randomized order. In this work we reported only the right hand imagery data. The participant was asked to perform sustained MI until the white cross disappeared (at second 10). Following there was a break (black screen) with a random length between 6 s and 8 s. We measured 5 runs with 10 right hand MI trials each, but we had to reject the last 2 runs due to movement artefacts. Finally, we got 30 trials of right hand MI for further analysis.

Data acquisition: We used a "BrainCap-MR" electrode system by EasyCap (EASYCAP GmbH, Herrsching, Germany), which consists of 66 MRI compatible Ag/AgCl pin electrodes with safety resistors. One ground, one reference, one electrocardiogram (ECG) and 63 EEG electrodes. The EEG electrodes were rectangularly arranged with distances of 2.5 cm. The rectangular grid was centred on the 10-20 system positions C3, Cz and C4. The electrodes and the cables were fixed on the cap to prevent looping, which would be a safety risk because of eddy currents and therefore, heating. We recorded the EEG with a "BrainAmp MR" amplifier system, an fMRI compatible shielded EEG amplifier by BrainProducts (Brain Products GmbH, Gilching, Munich, Germany). The amplifiers and the batteries were positioned directly in the MRI scanner, in the near of the subject's head. Recording settings: Low pass filter at 1000 Hz, high pass filter at 0.1 Hz, sampling rate 5 kHz. The EEG recording was performed in a Siemens Skyra 3T (Siemens AG, Munich, Germany), during a fMRI echo planar imaging (EPI) sequence with a TR of 3000 ms. We used a head coil for sending and receiving. For this work we did not report the fMRI data.

Data analysis: The simultaneous EEG-fMRI measurement is highly contaminated by two types of fMRI related artefacts. First, the gradient artefact due to gradient switching during the image acquisition and second, the cardiac related artefact, due to micro movements and blood speed changes in the high static magnetic field during a cardiac cycle [1]. For both artefact types, we used the template subtraction approach invented by Allen et al. [4] [5] and as implemented in the BrainVision Analyzer2 (Brain Products GmbH, Gilching, Munich, Germany) software.

The event related desynchronization/synchronization (ERDS) time-frequency maps were computed according to [6].

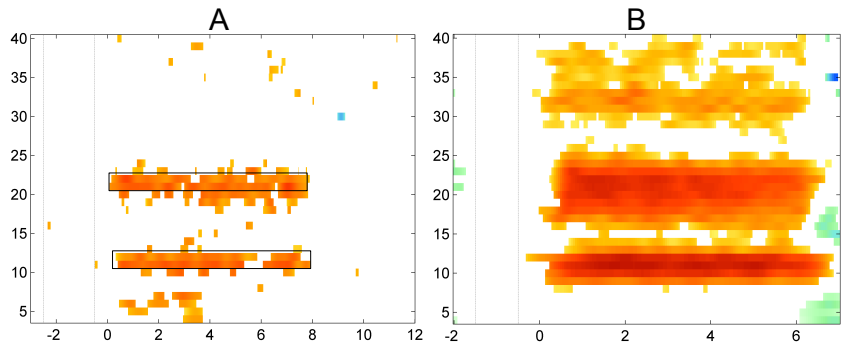

Figure 1: ERDS maps (BP). A/B: Lap C3, Trials: 30/90, classes: 1, fs: 250/512 Hz, time: [-3, 0, 12]/[-2, 0.05, 7] s, ref: [-2.5, -0.5]/[-1.5, -0.5] s, f borders: [4, 40] Hz, f bandwidths: 2 Hz, f steps: 1 Hz, Bootstrap significance test ($\alpha = 0.01$)

We used two time segments of each trial's laplacian derivation at C3 for classification. One time segment (start t = 1 s, length 1 s) was during reference period and is called the rest condition. The other segment (start t = 4.5 s, length 1 s) was during the MI period and is called the MI condition. We calculated the absolute values of the segment's Fourier transformations and used two bands of the values as features for a linear discriminant analysis (LDA). First band (11-12 Hz) was in the mu band and second band (21-22 Hz) was in the beta band. To estimate a single trial classification accuracy, we used a leave-one-out-cross-validation (LOOCV).

Results

Fig. 1 shows significant ERDS maps of the same participant with frequency bands from 4-40 Hz for position C3. Fig. 1 A was calculated with the data recorded simultaneously with fMRI (30 trials). The resulting signal patterns are highlighted. Fig. 1 B was calculated using data measured outside the scanner (90 trials).

The results of the single trial classification showed that 78,33% of the samples were correctly classified in the LOOCV. Two rest condition samples and 11 MI condition samples were wrong classified. The chance level was 64,54% according to [7].

Discussion

The observed ERD patterns (Fig. 1 A), one in the mu band (11-12 Hz) and one in the beta band (21-22 Hz), are similar to the patterns found in the measurement outside the fMRI scanner (Fig. 1 B) and are in line with other work [8]. Due to more trials the bands are more pronounced in Fig. 1 B. Our findings suggest, that the fMRI artefact correction algorithms can restore the underlying EEG and preserves the ERD phenomena, which is a requirement for a successful single trial MI classification. With these two pattern as features for an LDA, we computed an LOOCV accuracy of 78% which is significantly better than chance level (65%).

In summary, ERD phenomena can be classified on single trial basis although when the raw EEG is contaminated with fMRI related artefacts.

Acknowledgement

This work was performed within the BioTechMed initiative.

Bibliography

[1] C. Mulert and L. Lemieux, *EEG-fMRI Physiological Basis, Technique, and Applications*. Springer, Berlin, 2010.

[2] G. Pfurtscheller and C. Neuper, "Motor imagery and direct brain-computer communication," *Proceeding IEEE*, vol. 89 no. 5, p. 1123–1134, 2001.

[3] G. Pfurtscheller, G. R. Müller-Putz, A. Schlögl, B. Graimann, R. Scherer, R. Leeb, C. Brunner, C. Keinrath, F. Lee, G. Townsend, C. Vidaurre, and C. Neuper, "15 years of bci research at graz university of technology: current projects," *IEEE Transactions on Neural Systems and Rehabilitation Engineering*, vol. 14, pp. 205–210, 2006.

[4] P. J. Allen, G. Polizzi, K. Krakow, D. R. Fish, and L. Lemieux, "Identification of eeg events in the mr scanner: The problem of pulse artifact and a method for its subtraction," *NeuroImage*, vol. 8, p. 229–239, 1998.

[5] P. J. Allen, O. Josephs, and R. Turner, "A method for removing imaging artifact from continuous eeg recorded during functional mri," *NeuroImage*, vol. 12, p. 230–239, 2000.

[6] B. Graimann, J. Huggins, S. Levine, and G. Pfurtscheller, "Visualization of significant erd/ers patterns in multichannel eeg and ecog data," *Clinical Neurophysiology*, vol. 113, p. 43–47, 2002.

[7] G. R. Müller-Putz, R. Scherer, C. Brunner, R. Leeb, and G. Pfurtscheller, "Better than random? a closer look on bci results," *International Journal of Bioelectromagnetism*, vol. 10, pp. 52–55, 2008.

[8] V. Kaiser, A. Kreilinger, G. R. Müller-Putz, and C. Neuper, "First steps toward a motor imagery based stroke bci: New strategy to set up a classifier," *Frontiers in Neuroscience*, vol. 5, p. 86, 2011.

Biomed Tech 2013; 58 (Suppl. 1) © 2013 by Walter de Gruyter · Berlin · Boston. DOI 10.1515/bmt-2013-4451

On the Development of a Test Setup for a Non-Destructive Quality Control of Centifluidic Medical Devices

Thomas Pollack[1], Hermann Seitz[1]

[1]Fluid Technology and Microfluidics, University of Rostock, Germany
thomas.pollack@uni-rostock.de

Abstract: *A non-destructive quality control of centifluidic medical devices is investigated. The medical device is an intravenous infusion filter which is produced a million times per year. This production volume has to be quality controlled. By now the monitoring is done by a destructive random sample. The non-destructive control of 100% of the production volume is the aim of the project. For this purpose a test method will be developed. Therefore the behaviour of the filters using liquid and gas is investigated. To establish comparability between the fluids the Reynolds numbers have to overlap.*

Keywords: *non-destructive, test method, infusion filter, pressure loss; Reynolds number*

Introduction

Infusion filters ensure the purity of an intravenous solution. Intravenous therapy is the infusion of liquid substances like NaCl 0.9% or G5% into a vein to replace liquid, correct electrolyte imbalances or to deliver medicine. These solutions can be contaminated with microorganisms, particles, undissolved drugs or air bubbles which have to be removed, because of their danger to health. Infusion filters remove these risks using ultra- and microfiltration membranes. [1, 2]

Figure 1: infusion filter RPM [3]

Existing integrity monitoring tests for filtering devices are divided into destructive and non-destructive and direct or indirect methods. Direct methods provide instantaneous information about oversized pores or defects in a membrane system. Indirect methods rely on monitoring a surrogate parameter such as turbidity. [4] The direct test method which is typically used by producers of infusion filters is the bubble point test which is non-destructive but contaminates the medical device. For this reason these devices cannot be reused for clinical use and leads to a control by random sample.

A non-destructive and non-contaminating 100% quality control will be developed. Therefore the flow behaviour of liquid and gas in the infusion filters is investigated. The behaviour of air and gas is represented by the characteristic pressure loss. The experiments are performed under low flow velocities to ensure incompressibility. The experimental results show a need for a high accuracy experimental setup, both actuators and sensors. The turbulence behaviour of both fluids is compared using the Reynolds Number (eq. 1).

Methods

Analytic

The Bernoulli equation for a steady flow of an incompressible fluid with constant density is used to calculate the levels of the static and dynamic pressure. The flow behaviour of the infusion filter is described by its characteristic pressure loss (eq. 2). This loss coefficient is not a constant. It depends on the density of the fluid and the flow velocity, which leads to an additional dependency of pressure and temperature. The characteristic pressure loss is represented as the function: $\zeta = f(\mathrm{Re})$. The loss coefficient cannot be described analytically, only with experimental data (pressure loss, flow volume and density). [5] Figure 2 shows the decreasing loss coefficient by increasing flow velocity and density.

$$\mathrm{Re} = \frac{v d \rho}{\eta} \qquad (1)$$

$$\zeta = \frac{2 p_{loss}}{\rho v^2} \qquad (2)$$

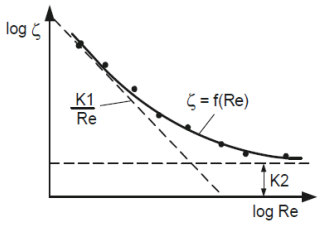

Figure 2: characteristic loss coefficient [5]

The variables used in formula 1 and 2 are the flow velocity v, the inner diameter of the filter entry d, the density ρ, the dynamic viscosity η, the loss coefficient ζ and the pressure loss p_{loss}.

Experimental Setup

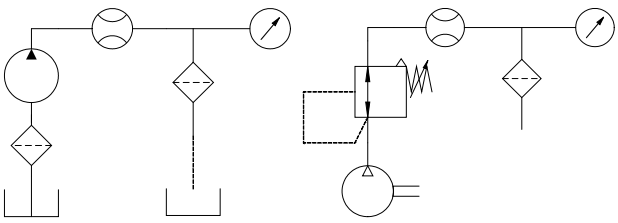

Figure 3: experimental setup water (left) and air (right)

The experimental setup for water consists of a micro gerotor pump (mzr 7205 [6]) with adjustable revolutions per minute, a flow meter, a relative pressure transmitter and an infusion filter. The experimental setup for air consists of a pressure regulator, the same sensors for volume flow and pressure and an infusion filter.

In the case of water the revolutions per minute of the pump are increased, in the case of air the inlet pressure is raised.

The studied infusion filters and their parameters are shown in the following table.

Table 1: parameter of infusion filters [3]

Filter	Pore Size [µm]	Type of Material	Surface Area [cm²]
RF120	0,2	Nylon +	13,5
RF 48	0,2	PET	13,5
RF 24	1,2	PET	13,5
RP	0,2	Nylon +	4
RPM	0,2	Nylon +	2,3

The product spectrum includes infusion filters with three different membrane surface areas, two types of materials and two pore sizes. The experiments were carried out for the RPM type filter (table 1).

Results

The measuring results are shown in the following figures.

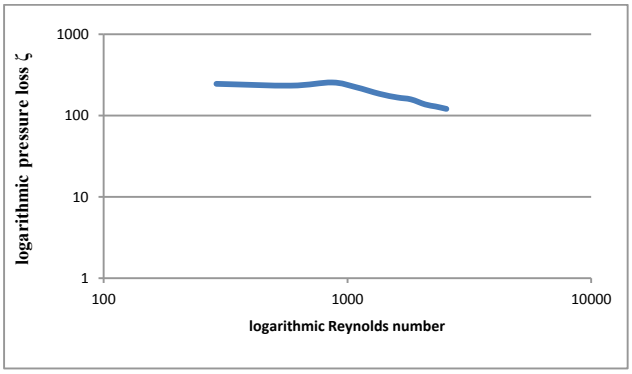

Figure 4: pressure loss over Reynolds, water

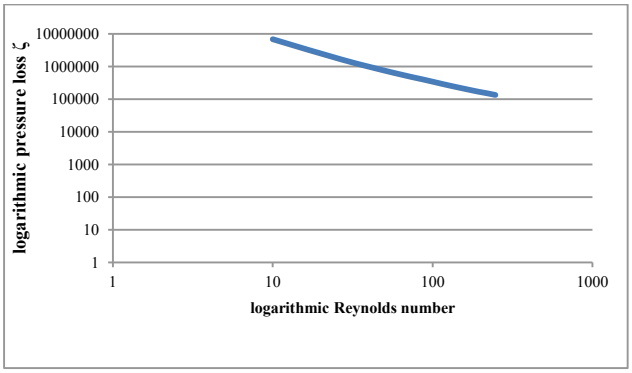

Figure 5: pressure loss over Reynolds, air

The characteristic pressure loss of water and air is calculated assuming a steady and incompressible flow.
For water the Reynolds number is between 300 and 2500. The loss coefficient decreases from 245 to 120. The characteristic pressure loss $\zeta = f(Re)$ shows the above-mentioned behaviour (figure 2).
For air the Reynolds number is between 10 and 250. The loss coefficient decreases from 6.8E6 to 1.4E5. The characteristic pressure loss $\zeta = f(Re)$ shows the above-mentioned behaviour (figure 2).
The experimental setups for water and air differ from each other in terms of the controllable volume flow and flow velocity. The resulting Reynolds numbers do not overlap.

Discussion

Two experimental setups were built to verify the characteristic pressure loss of infusion filters. For water exists a source for volume flow, for air a pressure source. A pressure source for water will be developed to make the both setups more comparable. Both setups will be equipped with a more accurate inlet pressure regulator to approach Reynolds numbers between 0 and 250. This leads to the requirements of high accuracy and resolution of the sensors. Also a temperature sensor will be integrated to measure an occurring change of temperature.
The characteristic pressure loss describes the flow through the filter. It will be used to characterize different types of filters and indicate integrity of membrane and housing. Therefor the Reynolds number is calculated and describes the flow behaviour of water and air and contributes to the comparability.
Further work will investigate the characteristic pressure loss of known and reproducible defects in the filtering membrane or the housing and infusion filters with different parameters like surface area, filter material and pore size (table 1).

Acknowledgement

This project is part of Wachstumskern Centifluidic Technologies (FKZ: 03WKCC 10) and funded from the Bundesministerium für Bildung und Forschung.

Bibliography

[1] Backhouse C. M. et. al.: Particulate contaminants of intravenous medications and infusions, *Journal of Pharmacy and Pharmacology*, vol. 39 (4), pp. 241-245, April 1987
[2] Chee, Stephanie, Tan, William: Reducing infusion phlebitis in Singapore hospitals using extended life end-line filters, *Journal of infusion nursing*, vol. 25 (2), pp. 95-104, March-April 2002
[3] RoweMed AG: *Catalog of products Liquid Management*, Parchim, 2012
[4] Farahbakhsh, K., Adham S. S. et. al.: Monitoring the integrity of low-pressure membranes, *Journal / American Water Works Association*, vol. 95 (6), pp. 95-107, June 2003
[5] D. Will, N. Gebhardt, *Hydraulik: Grundlagen, Komponenten, Schaltungen*, Berlin: Springer, 2011.
[6] HNP Mikrosysteme GmbH: *Produktinformation mzr-7205*, Parchim, September 2011

Biomed Tech 2013; 58 (Suppl. 1) © 2013 by Walter de Gruyter · Berlin · Boston. DOI 10.1515/bmt-2013-4452

Bioelectric impedance of the neonatal heart during normothermic ischemia

Lueck S[1], Reichert D[2], Pliquett U[3], Minor T[4], Preusse CJ[1]

[1]Department of Cardiac Surgery, University of Bonn, Germany
[2]Department of Anaesthesiology, University of Bonn, Germany
[3]Institute for Bioprocessing and Analytical Measurement Techniques, Bad Heiligenstadt, Germany
[4]Surgical Research Division, University of Bonn, Germany

sabrina.lueck@ukb.uni-bonn.de

Abstract: *Ischemia (35°C) induced alterations of the bioelectric impedance were analysed for the first time in neonatal hearts (piglets). The changes of impedance principally did not differ from adult hearts, but great differences could be detected regarding time course and intensity. The reasons for different courses of the bioelectric impedance are most probably related to different metabolic variations of the ischemic neonatal heart.*

Keywords: *neonatal myocardium, bioelectric impedance, ischemia*

Introduction

During myocardial ischemia function, morphology, energetics, and metabolism change in a characteristic manner. Besides the parameters mentioned Gersing and Preusse [1,2] could demonstrate that distinctive organ specific alterations of the bioelectric impedance happen, too. Since it is well known that the neonatal (immature) heart completely differs from the adult one during aerobiosis and anaerobiosis – especially regarding its metabolism – the bioelectric impedance of neonatal hearts under ischemic conditions was analysed to evaluate bioelectric differences between adults and neonates.

Methods

All animal experiments were performed according to the German law of animal protection. Landrace pigs were used for the experiments. The piglets aged between 6 and 10 days had a body weight (bw) of about 3 kg, while the adult pigs weighed 30 kg at an age of 3 months. According to the anaesthesiological protocol all pigs got premedication (midazolam 0.5 mg/kg bw; ketamine 15-20 mg/kg bw) and were intubated and ventilated. Anaesthesia was sustained with midazolam (0.5 mg/kg bw), fentanyl (0.001 mg/kg bw), and pancuronium (0.1 mg/kg bw). After sternotomy, the hearts were excised and immediately put into an incubator at constant humidity (30%) and temperature (35°C). A probe containing four gold plated electrodes (two current injecting electrodes and two voltage sensing electrodes) was placed on the epicardial layer of the left ventricle, parallel to the left anterior descending (LAD). The impedance was measured continuously up to 24 hours with a frequency range from 100 Hz to 1 MHz, using a computer controlled Solartron 1260 Impedance Analyser and ImpDAQ V1.03 iba e.V. Software. The measurements included absolute impedance, its real part (Re) and imaginary part (Im) as well as the resulting phase angle (φ).

Results

Principally, a sigmoid curve of the phase angle could be seen in both neonates and adults. However, the initial plateau phase in the neonates did not last as long as in the adults (neonates 30 min, adults 80 min). Furthermore, the increase of the phase angle was much more rapid and higher in the neonates. After 120 min the phase angle entered a second plateau. In contrast, the plateau phase of the adult hearts was only reached after about 6 hours.
The absolute impedance [Ω] at low frequencies increased up to tenfold in the neonates till reaching the second plateau, while the impedance of the adult hearts only reached a fivefold elevated level.
In order to evaluate the development of an ischemia induced oedema the Extracellular Space Index (ESI) was calculated:

$$ESI = \frac{\text{Re (Z) at 1 MHz [}\Omega\text{]}}{\text{Re (Z) at 300 Hz [}\Omega\text{]}} \quad (1)$$

Directly after excision of the hearts the ESI was 55,3% in the neonates and 50,0% in the adults. Due to a cell swelling the ESI decreased to 11,3% within 120 minutes in the neonates and to 13,0% within 6 hours in the adults.
Measurements lasting for 24 hours showed a rapid re-increase of the ESI in both groups.

Discussion

Electric bioimpedance spectroscopy allows a fast and easily applicable characterization of tissues. Within the frequency range up to 1 MHz, current conduction through tissue is mainly determined by tissue structure, i.e. the extra- and intracellular compartments and the insulating cell membranes [1]. Therefore, early changes in the extra- and intracellular space due to ischemia can be detected.

The sigmoid curve of the phase angle consists of 3 specific parts: 1. the initial plateau phase representing reversible alterations of myocardial structure and function, 2. the increase of the phase angle and 3. a second plateau phase representing irreversible alterations. During the period of increasing phase angle the critical limit of resuscitation is reached.
At low frequencies (< 1 kHz) Re is influenced by the extracellular ion density and/or by the size of the extracellular space. In neonatal hearts the last mentioned parameter plays a major role since it decreases by far faster than in adults. The more intensive alteration of Re in neonates is additionally caused by the higher ischemia induced metabolic turnover compared with adults.
In both groups a re-increase of the ESI up to 99% could be determined indicating a total destruction of cellular structures after 24 hours of normothermic ischemia.
Reasons for the shorter initial plateau phase and for the earlier reaching of the second plateau phase in neonates are discussed and morphological investigations are additionally presented.

Acknowledgement

The German Heart Foundation funded this research project.

Bibliography

[1] Gersing, E: Impedance spectroscopy on living tissue for determination of the state of organs, *Bioelectrochemistry and Bioenergetics*, vol. 45, pp. 145-149, 1998.

[2] Preusse, C.J., Gersing, E., et al.: Intraoperative atraumatic monitoring of myocardial revivability by continuous or intermittent measurement of electrical impedance of the heart, *Thorac Cardiovasc Surg*, vol. 30, special issue 1, p. 18, 1982.